1998

On-line coupling of capillary electrophoresis and liquid chromatography with electrospray ionization mass spectrometry for protein characterization

Liyu Yang
Iowa State University

On-line coupling of capillary electrophoresis and liquid chromatography with electrospray ionization mass spectrometry for protein characterization

by

Liyu Yang

A thesis submitted to the graduate faculty
in partial fulfillment of the requirements for the degree of
DOCTOR OF PHILOSOPHY

Major: Analytical Chemistry
Major Professors: Cheng S. Lee and Robert S. Houk

Iowa State University
Ames, Iowa
1998

Graduate College
Iowa State University

This is to certify that the Doctoral Dissertation of

Liyu Yang

has met the thesis requirement of Iowa State University

Signature was redacted for privacy.

Co-major Professor

Signature was redacted for privacy.

Co-major Professor

Signature was redacted for privacy.

For the Major Program

Signature was redacted for privacy.

For the Graduate College

TABLE OF CONTENTS

GENERAL INTRODUCTION

Dissertation Organization

This dissertation begins with a general introduction of the theory and the literature which provides background and recent progress in this area. Three research papers follow the general introduction with their literature cited. Finally, a general summary presents comments on this work and a list of cited references for the general introduction concludes this dissertation.

Capillary Electrophoresis

The resolving power of capillary electrophoresis (CE) was first demonstrated by Jorgenson and Lukacs[1,2] in 1981. CE is a modern analytical technique which permits rapid and highly efficient separations of analytes in very small sample volumes. Separations are based on the differences in effective mobilities of analytes in electrophoretic media inside the capillary. A basic instrument for CE separation is illustrated in Figure 1, which includes a fused-silica separation capillary, two buffer reservoirs, a high-voltage power supply, and a detector. Different separation modes of CE, such as capillary zone electrophoresis (CZE)[1,2], capillary gel electrophoresis (CGE)[3-6], capillary isotachophoresis (CITP)[7,8], capillary electrochromatography (CEC)[9], capillary isoelectric focusing (CIEF)[10-14], and

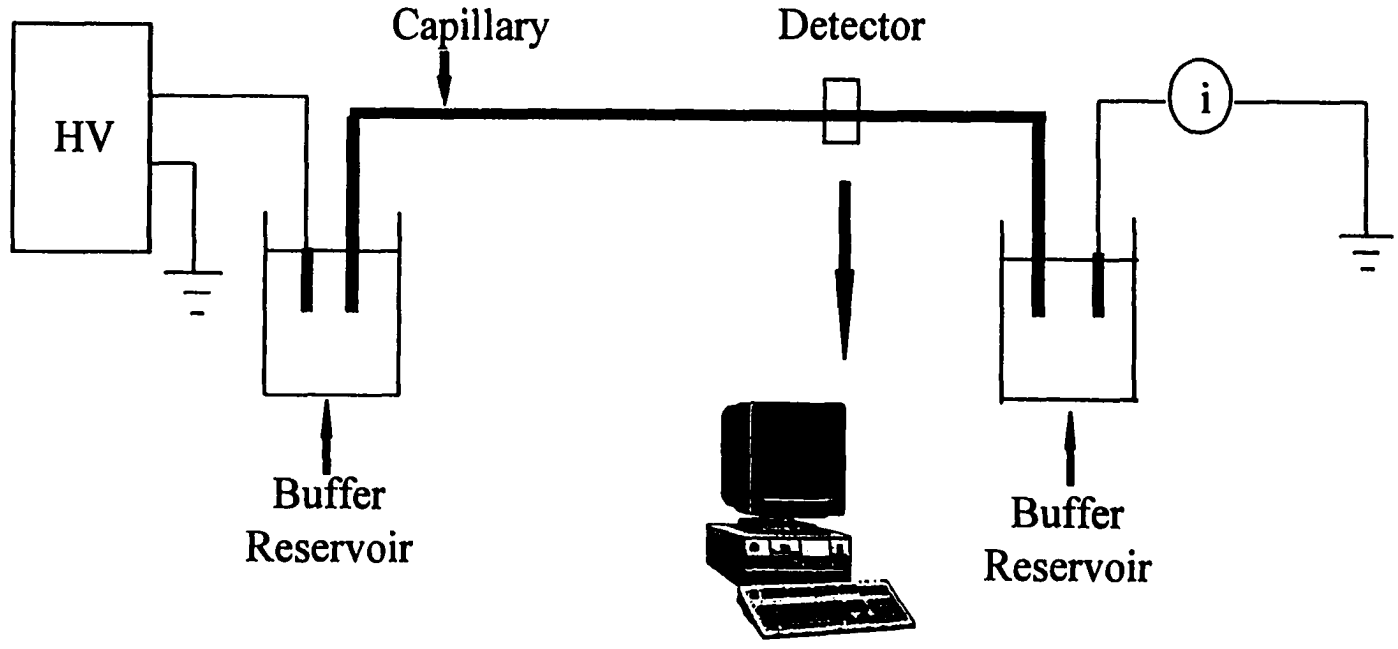

Figure 1

Schematic of a System for Capillary Electrophoresisi

micellar electrokinetic chromatography (MEKC)[15], can be performed using a standard CE instrument. Since the commercial CE instrument became available at the the end of 1980s, CE has increasingly been seen as an alternative or complementary separation method capable of faster analysis and higher efficiency than high performance liquid chromatography (HPLC).

CZE is the most commonly used mode for the separation of ionic compounds in CE. The ionization of surface silanol groups in the fused-silica capillary at pH > 2 results in a negatively charged silica surface and an electrostatic diffuse layer of cations adjacent to the capillary wall. The migration of cations in the diffuse layer induces the electroosmotic flow toward the cathode. Ionic compounds with various charge to mass ratios exhibit different electrophoretic mobilities and are thus separated in CZE. Since the magnitude of the electroosmotic flow is usually greater than the electrophoretic velocities of analytes, both cations and anions can be separated and detected in the same run.

Hjerten and his co-workers were the first to employ polyacrylamide-filled and agarose-filled capillaries for the separation of both small and large molecules[3,4]. Analytes with different sizes migrate through the pores of the gel matrix at different velocities and are thus separated in CGE. Because of the anti-convective media and the minimized solute diffusion, CGE has achieved the highest separation efficiency ever obtained by any analytical separation technique to date. The number of theoretical plates in the range of 10-20 million can be routinely achieved[5,6] for the separation of proteins and DNA fragments.

CITP is performed in a discontinuous buffer system. Sample components stack between the leading and terminating zones, and produce a steady-state migrating configuration

of consecutive sample zones. The leading buffer contains the ions with the highest mobility and the terminating ions are those with the lowest mobility[7,8]. Unlike other CE modes, the migration time of the analyte zone provides no indication of the identity of the analyte and the amount of analyte is proportional to the time between the steps of consecutive analyte zones.

In CEC[9], the capillary is packed with the material which can retain solutes by the partitioning phenomenon similar to that in HPLC. The mobile phase in CEC is driven by electroosmotic flow. The flow profile in CEC is no longer perfect plug-flow as in CZE because of the tortuous nature of the channels resulted from the packing material. CEC, however, still provides a higher efficiency than the pressure-driven system of HPLC.

In MEKC[15], surfactants are added to the electrophoresis buffer at the concentration above the critical micelle concentration to form micelles in equilibrium with the surfactant monomers. Surfactants are amphiphilic species, comprising both hydrophobic and hydrophilic regions. The micelles are spherical in shape with the hydrophobic tails of the surfactant oriented to the interior of the aggregate and the hydrophilic head groups exposed to the aqueous solution. Differential partitioning of solutes between the aqueous and the micellar phases in MEKC results in the separation of neutral and ionic compounds.

CIEF was first described by Hjerten and Zhu in 1985[10] for the separation of proteins based on their differences in isoelectric point (pI). In CIEF, the fused-silica capillary is usually coated with linear polyacrylamide to eliminate the electroosmotic flow and protein adsorption onto the capillary wall. The CIEF capillary is initially filled with a solution

containing the protein analytes and a mixture of carrier ampholytes. These ampholytes are small amphoteric molecules containing both amino and carboxylic groups with different pIs. Under the influence of applied electric field, the negatively charged acidic ampholytes migrate toward the anode and decrease the pH at the anodic section, while the positively charged ampholytes migrate toward the cathode and increase the pH at the cathodic section. These pH changes continue until each ampholyte molecule reaches its pI. Because each ampholyte molecule has its own buffering capacity, a continuous pH gradient is formed in the capillary.

Protein analyte acquires a net negative charge in the region between its pI and cathodic end (where pH > pI) and migrates toward the anode. In contrast, protein analyte exhibits a net positive charge in the region between its pI and anodic end (where pH < pI) and migrates toward the cathode. As a result, protein molecules distributing over the entire capillary at the beginning of the experiment are focused at the regions where pH = pI. To prevent the ampholytes and analytes from migrating into the inlet (anode) and outlet (cathode) reservoirs by diffusion, solutions of 20 mM phosphoric acid and 20 mM sodium hydroxide are typically used as the anolyte and the catholyte, respectively.

Due to the focusing effect, CIEF thus permits analysis of very dilute protein samples with a typical concentration factor of 50-100 times. Furthermore, the analyte molecules leaving the focused zones by diffusion or convection migrate back to their pIs due to the same focusing effect. This zone-sharpening effect makes isoelectric focusing a high resolution tool for the analysis of proteins with a pI difference as small as 0.02 pH units[13].

In CIEF, the focused analyte zones must be mobilized and detected at one end of the capillary. Among various mobilization approaches, the hydrodynamic mobilization described by Hjerten and Zhu[10] involves the connection of a pump to the cathodic end of the capillary via a T-tube. The electric field is maintained during the mobilization step to help minimizing the hydrodynamic band broadening. The so called salt mobilization[12,13] involves the replacement of the anolyte, 20 mM phosphoric acid, with 20 mM sodium hydroxide after the focusing is complete. This replacement under the influence of an electric field results in an increase of solution pH inside the CIEF capillary. The focused ampholytes and protein analytes are no longer neutral and become negatively charged with electrophoretic migration toward the anodic end of the capillary. This is referred to as anodic mobilization. On the contrary, the cathodic mobilization can be achieved by replacing the catholyte, 20 mM sodium hydroxide, with a 20 mM phosphoric acid solution after the focusing is complete.

Alternatively, a small amount of buffer additive such as 0.1% methyl cellulose can be added into the sample solution to suppress the electroosmotic flow in the uncoated capillary[14]. The electroosmotic flow is reduced sufficiently to ensure that the focusing is complete before the analytes migrate past the detection window. The analytes are focused and eluted by electroosmotic flow in one step without an extra mobilization procedure. The buffer need not be changed, nor does the voltage have to be turned off and on. Since a bare silica capillary can be employed, the time consuming coating procedure is eliminated and the potential for instability of a coating, particularly at high pH, is avoided.

Liquid Chromatography

The first commercial HPLC instrument was introduced in 1969. Since then, HPLC has progressed from a difficult "art" into one of the most important separation techniques used to solve a host of problems in the modern laboratory[16, 17]. Figure 2 shows the basic components of an HPLC instrument. The solvent reservoir is employed to store the mobile phase. The pump delivers the mobile phase and is one of the most important components of HPLC since its performance directly affects retention time reproducibility and detector sensitivity. Analytes are introduced through the injector. The separation takes place in the column based on analytes' differential distribution between two phases: the stationary phase packed inside the column and the mobile phase delivered by the pump. As the sample components elute from the column, a suitable detector is used to monitor and transmit the signal to a recording device. The "chromatogram" is a record of the detector response as a function of time and indicates the presence of the analytes as "peaks". There are different forms of liquid chromatography including normal-phase, reversed-phase, size exclusion, ion exchange, and bioaffinity.

In normal-phase chromatography[18,19], the retention is governed by the interaction of the polar parts of the stationary phase and solute. For the retention to occur in normal-phase, the stationary phase must be more polar than the mobile phase. Therefore, the stationary phase is usually alkylamine modified silica or unbonded silica. The mobile phase usually contains organic solvent such as hexane, methylene chloride, chloroform, or diethyl ether.

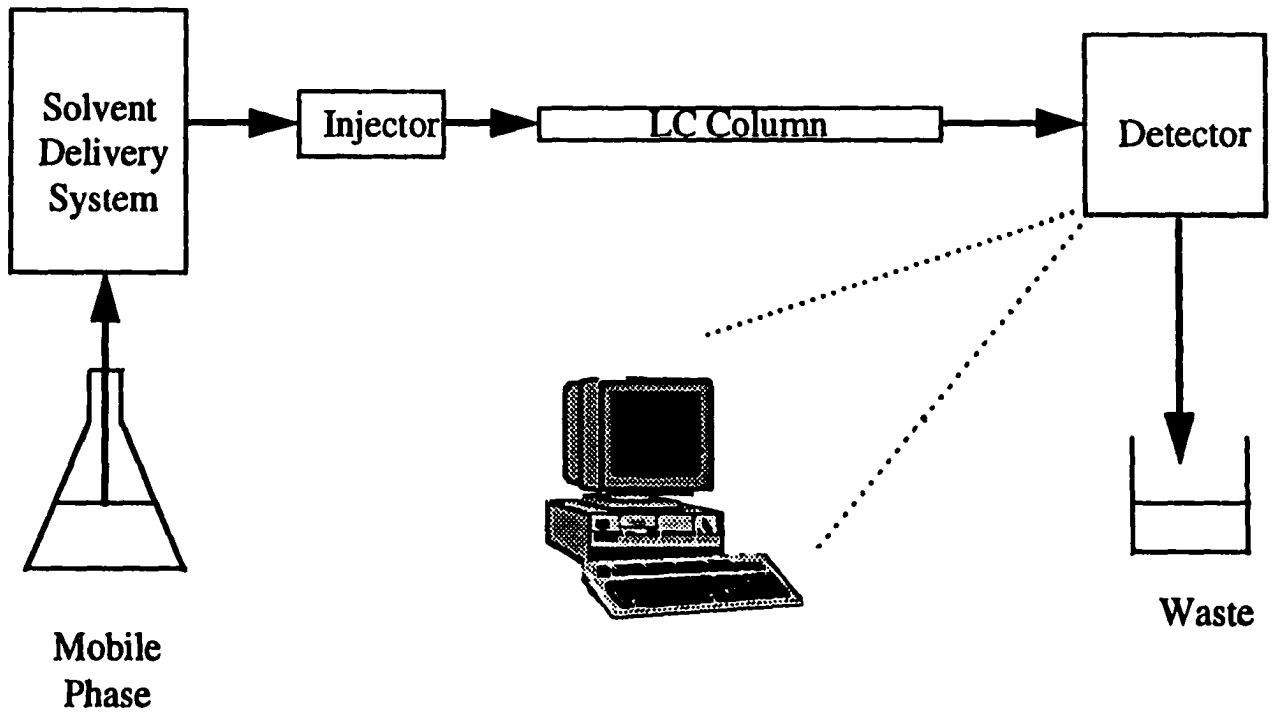

Figure 2

Schematic of a System for Liquid Chromatography

Normal-phase chromatography separates compounds that differ in the number or chemical nature of their polar groups with the nonpolar components emerging from the column first. Mobile phase eluent strength can be increased by adding a more polar solvent.

Size exclusion chromatography is different from all other chromatography methods in that a simple molecule size classification process rather than any interaction phenomena forms the basis of separation. As the sample molecules travel through the column, they penetrate the pores of the packing. The smaller molecules migrate into more of the smaller pores of the cross-linked polymer gel than the larger molecules in the sample. Analyte molecules that are too large to diffuse into any pores are excluded at V_i (interparticle volume or interstitial volume) while the molecules that are small enough to penetrate all the pores are eluted at the breakthrough volume, V_o. All other components elute between V_i and V_o with the larger molecules eluting first.

In ion exchange chromatography, the stationary phase is characterized by the presence of charged centers bearing exchangeable counterions. Retention is based on the attraction between solute ions and charged sites bound to the stationary phase. Typical stationary phases for ion exchange chromatography include polystyrene, cellulose, dextran and controlled-pore glass or porous silica. Mobile phase eluent strength can be enhanced by increasing the solution ionic strength.

The fundamental principle of bioaffinity chromatography consists of the utilization of biologically active substances to form stable, specific, and reversible complexes[20]. The formation of the biologically functioning complexes involves the participation of common

molecular forces such as van der Waal's interaction, electrostatic interaction, dipole-dipole interaction, hydrophobic interaction, and hydrogen bonding. Choice of affinity ligands includes group-specific ligands such as dyes[21], immobilized metals[22], enzyme cofactors[23], and highly specific ligands involving antigen and antibody recognition[24].

Reversed-phase chromatography[16,17] is characterized by a polar mobile phase in conjunction with a nonpolar stationary phase. The most commonly used stationary phase for reversed-phase chromatography is an octadecyl alkyl hydrocarbon chain (C_{18}) which is chemically bonded to the silica substrate. Typical mobile phases are mixtures of methanol/water and acetonitrile/water. Reversed-phase chromatography can be used to separate a broad spectrum of non-ionic, ionizable, and ionic compounds. Retention in reversed-phase chromatography occurs by non-specific hydrophobic interactions of the solutes with the stationary phase. The near universal application of reversed-phase chromatography stems from the fact that virtually all organic molecules have hydrophobic regions in their structures and are capable of interacting with the stationary phase.

The mobile phase is made by choosing one solvent in which the sample is very soluble and another solvent in which the sample is less soluble. One can then prepare a mobile phase by adjusting the amounts of the "strong" and "weak" solvents to a ratio where the attraction of the solutes to stationary phase is in a competitive equilibrium with the attraction (solubility) of the solutes to the mobile phase. The equilibrium of the solutes in the mobile phase relative to that in the stationary phase determines the retention time and effects the separation. The selectivity of reversed-phase chromatography may be

conveniently adjusted by changing the type of organic modifier in the mobile phase. For ionic or ionizable solutes, pH buffers which suppress ionization, or ion-pairing reagents used to form lipophilic complexes, increase the degree of solute transfer to the stationary phase and may be used to control selectivity.

According to the solvophobic theory[25,26], hydrophobic interactions result from repulsive forces between a polar solvent and the nonpolar solute and stationary phase. The solvophobic theory assumes that aqueous mobile phases are highly structured due to the tendency of water molecules to self-associate by hydrogen bonding. As a consequence of the very high cohesive energy of the solvent, the less polar solutes are literally "squeezed out" of the mobile phase and are bound to the hydrocarbon portion of the stationary phase. The driving force in the binding of the solute to the stationary phase is the decrease in the area of the nonpolar segment of the solute molecule exposed to the solvent.

Hydrophobic selectivity in reversed-phase chromatography arises as a consequence of differences in the nonpolar surface areas of different solutes. Reversed-phase chromatography is thus the preferred technique for separating homologous samples. Within a homologous series, the logarithm of the capacity factor is generally a linear function of the carbon number[27]. Branched chain compounds are generally retained to a lesser extent than their straight chain analogs and unsaturated compounds are eluted before the corresponding saturated analogs. Reversed-phase chromatography is also gaining increasing attention as a method for separating biological molecules such as proteins and peptides because the

hydrocarbon-like stationary phases equilibrate rapidly with changes in mobile phase composition and are therefore suitable for use with gradient elution[28,29].

Electrospray Ionization

The researcher who took the first step on the path of electrospray ionization mass spectrometry (ESIMS) is Malcolm Dole[30], for trying to determine molecular weight distribution of some synthetic polymers. After much frustration in trying to develop the so-called Electrohydrodynamic Ionization into an useful ion source for mass spectrometry, most investigators abandoned the technique. It took a long way until the first demonstration of ESI was illustrated by Yamashita and Fenn in 1984[31,32]. ESI soon became one of the most important ionization techniques for the detection and identification of biomolecules in MS.

In ESI, an aqueous solution containing analytes is introduced through a capillary. Under the influence of a positive electric field applied at capillary terminus, the positive ions accumulate on the solution surface. The surface is further drawn out down field such that the so-called Taylor cone[33] forms. At a sufficiently high electric field, the cone is unstable and a liquid filament with a diameter of a few micrometers is emitted from the Taylor cone tip. At some distance downstream, the liquid filament becomes unstable and forms separate droplets. Solvent evaporation and droplet disintegration lead to very small and highly charged droplets capable of producing gas phase ions. The ions formed at atmospheric pressure are then

channeled into the high vacuum of the mass spectrometer through a capillary or a set of differentially pumped skimmers.

Two theoretical models have been proposed to account for the formation of gas phase ions from charged droplets. In Dole's Charged Residue Model (CRM)[30], evaporation of solvent molecules from a charged droplet steadily decreases its size, thereby increasing its surface charge density. The droplet continues to shrink until it reaches the Rayleigh limit[34] at which the Coulomb repulsion overcomes the surface tension. The resulting instability breaks up the parent droplet into a hatch of offspring droplets, each of which continues to evaporate until it too reaches the Rayleigh limit. This sequence continues until the offspring droplets ultimately become so small that they contain only one analyte molecule. The analyte molecule retains some of the droplet charge and becomes a gas phase ion as the last solvent molecule evaporates.

For the Ion Desorption Model (IDM) proposed by Iribarne and Thomson[35,36], the charged droplet commences the same sequence of evaporation and Coulomb fission steps as those in CRM. However, the charged droplets at some intermediate stage are small enough so that the surface charge density is sufficiently intense to overcome solvation forces and to lift an analyte ion from the droplet surface into the ambient bath gas. The exact mechanism for ion formation in ESI remains an active research topic in the literature[37-40].

Several features of ESI have contributed to its great success and significance in various biological and biomedical applications. First, ESI can be employed for the direct interfacing of MS with HPLC or CE separations. Furthermore, the multiple charging phenomenon in

ESI allows the determination of molecular weight of macromolecules over 50 kDa using a mass spectrometer with limited m/z range. When averaged, these multiple-charged ions provide excellent accuracy and precision in the mass determination of macromolecules[41-43]. Finally, ESI is probably the 'softest' of all ionization techniques yet developed, involving only the combination of high electric fields, moderated by an atmospheric pressure bath gas with typically only mild heating to enhance desolvation. Thus, the preservation of non-covalent association is possible in ESI. In fact, the application of ESI permits the measurements of non-covalent interactions between biological macromolecules, such as the heme-protein complex[44], enzyme-inhibitor complex[45], oligonucleotide duplex[46], and receptor-ligand complex[47-49].

Quadrupole Mass Spectrometry

Quadrupole mass analyzers are now widely used in many areas of chemical analysis. For applications where extremely high resolution data or exact mass measurements are not required, quadrupoles offer a number of significant advantages over more traditional mass analyzers[50,51].

First, the short distance between the ion source and detector combined with the strong focusing properties of such devices make the quadrupole mass analyzer useful at comparatively high pressures (~ 10^{-5} torr). Second, quadrupoles resolve ions on the basis of their mass-to-charge ratios. Finally, quadrupole mass analyzer is a mechanically simple

instrument compared to other types of mass analyzers. Quadrupole devices do not rely on the use of magnetic fields for their mass discrimination. Thus, the slow scan speeds commonly associated with magnets are avoided.

Quadrupole analyzers are made up of four rods with circular or, ideally, hyperbolic section. The filtering action of the quadrupole mass analyzer is obtained by the application of combination of the time independent (dc) and a time dependent (ac) potential. The stability of the ion motion within the quadrupole can be described using an a-q stability diagram (Figure 3) with the definitions of a and q given by

$$a = 4eU/\omega^2 r_0^2 m \quad (1)$$

$$q = 2eV/\omega^2 r_0^2 m \quad (2)$$

U is the magnitude of the applied dc potential, V is the magnitude of the applied ac or rf potential, ω is the angular frequency ($2\pi f$) of the applied ac waveform, r_0 is the distance from the center axis (the z axis) to the surface of any electrode, m is the mass of the ion. The stability diagram allows the operation of the quadrupole mass analyzer to be reduced from a six-dimensional issue (involving e, ω, r_0, m, U, and V) to a two-dimensional problem involving only the reduced parameters a and q. This results in a tremendous conceptual simplification that allows one to visualize readily the effects of various physical parameters on the operation of the quadrupole mass analyzer.

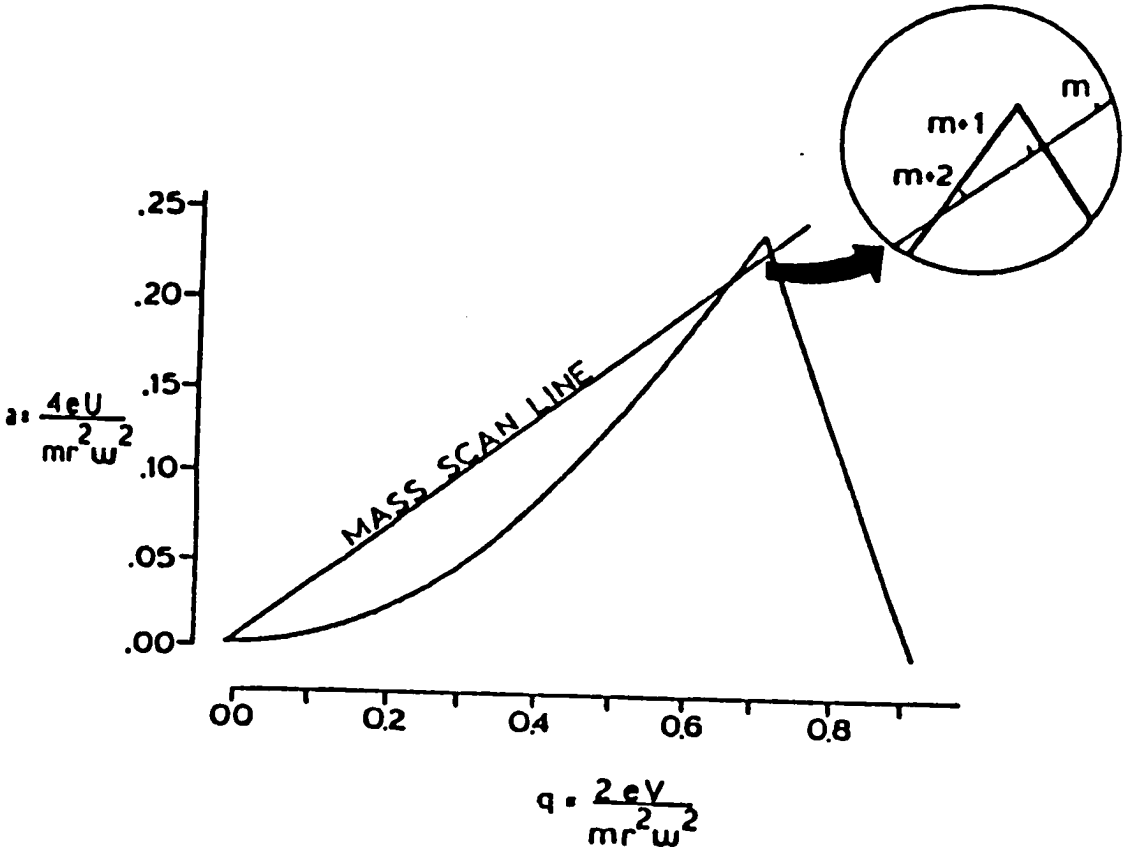

Figure 3. The a-q stability diagram

Fourier Transform Ion Cyclotron Resonance Mass Spectrometry

Marshall and Comisarow[52] built the first fourier transform ion cyclotron resonance mass spectrometry (FTICR/MS) instrument in 1978. Since that time, FTICR/MS has received considerable attention for its ability to make mass measurements with a combination of resolution and accuracy that is higher than any other mass spectrometers[53-56]. All FTICR/MS instruments consist of four main components. First is a magnet, which can be a permanent magnet, an electromagnet, but mostly a superconducting magnet. The performance of the FTICR/MS instrument improves as the magnetic field strength increases and so the trend is to design instruments with stronger fields using superconducting magnets. Recently, FTICR/MS instrument with field strength in excess of 12 Tesla was demonstrated for the high resolution and accuracy measurements for biomolecules with an electrospray ionization source.

The second component common to FTICR/MS instruments is the analyzer cell. The cell is the heart of the instrument, where ions are stored, mass analyzed and detected. The cells can be cubic or cylindrical, consist three pairs of electrodes, a pair of trapping electrodes mounted perpendicular to the magnetic field and two separate pairs of excite electrodes and detection electrodes mounted parallel to the magnetic field. The third feature required of FTICR/MS instruments is an ultrahigh vacuum system. For obtaining ultrahigh resolution, pressures of 10^{-9}-10^{-10} torr are required in the analyzer cell. To achieve these low pressures, cryogenic pumps or turbomolecular pumps are used frequently than diffusion pumps. The

fourth feature that is shared by all FTICR/MS instruments is a sophisticated data system. This includes a frequency synthesizer, delay pulse generator, broadband rf. amplifier and preamplifier, a fast transient digitizer, and a computer to coordinate all of the electronic devices during the data acquisition, as well as to process and analyze the data.

The motion of ions in the FTICR/MS analyzer cell is governed by the magnetic and electric fields that are present. There are three fundamental ion motions in FTICR/MS, cyclotron motion, trapping motion, and magnetron motion. The basis for FTICR/MS is ion cyclotron motion, which arises from the interaction of an ion with the unidirectional magnetic field. The cyclotron frequency, f_c, is in the order of 5 kHz to 5 MHz and is determined only by three physical parameters, the strength of the magnetic field, B, the charge present on the ion, q, and the mass of the ion, m, as shown by equation (3).

$$f_c = qB/2\pi m \qquad (3)$$

The magnetic field is held constant and the mass-to-charge ratio of an ion is determined by measuring its cyclotron frequency. The simplicity of the governing equation for ion motion in FTICR/MS instruments is unique among mass spectrometers. In particular, it should be noted that the cyclotron frequency of an ion is independent of its velocity and therefore its kinetic energy. This is one of the fundamental reasons why the FTICR/MS instrument is able to achieve ultrahigh resolution.

An ion that moves parallel to the magnetic field experiences no force from the magnetic field. Therefore, a small, symmetric voltage is applied to the trapping electrodes to create a potential well to trap ions in the analyzer cell along the magnetic field axis. Positive

voltage is applied to store positive ions while negative voltage is applied to store negative ions. Ions undergo simple harmonic oscillation between the trapping plates.

The combination of the magnetic and electric field together introduces a third fundamental motion of the ions, the magnetron motion. The magnetron frequency f_m, is a function of the magnitude of the trapping potential, V, the magnetic field strength, B, the distance between the trapping plates, a, and the geometry of the analyzer cell, represented by the geometry factor α, as shown in equation (4).

$$f_m = \alpha V/\pi a^2 B \qquad (4)$$

Magnetron frequencies are in the order of 1-100 Hz and are much lower than cyclotron frequency. It should be noted that magnetron motion serves no useful analytical purpose. It is a consequence of the curvature of the trapping electric field due to the finite length of the cell electrodes.

With ESI, ions are formed externally at atmospheric pressure and guided to the analyzer cell through differential pumping stages and quadrupole focusing or electrostatic focusing[57-60]. After ions are formed and trapped ion the analyzer cell, they are excited into coherent motion by applying a sinusoidal voltage to the excitation plates. Ions that are in resonance with the frequency of the applied excitation rf electric field absorb energy and spiral outwards to their resonance orbit. Ions that are not in resonance do not absorb energy and remain at the center of the cell. All ions of the same mass-to-charge ratio are excited coherently, which means that they are grouped as tightly after excitation as they were initially. Ions of the same m/z ratio undergo cyclotron motion as a packet. As they pass the

cell's electrodes, the coherent orbiting ion packet attracts electrons to first one and then the other of the detection plates. This alternating current is called the image current[61]. The frequency of the detected image current is nearly equal to the frequency of the cyclotron frequency. It is exactly equal to the difference between the cyclotron and magnetron frequencies.

The number of ESI/FTICR/MS instruments is growing exponentially[62,63]. There are many reasons for the rapid increase and acceptance in popularity. For example, the typical m/z range of ions generated in ESI is between 500 to 4000 Da/z and coincides with the mass range of FTICR/MS. A second area of compatibility of ESI with FTICR/MS is tandem mass spectrometry. FTICR/MS provides the unambiguous charge state and thus molecular weight information through the isotopically resolved peaks. As a consequence, ESI/FTICR/MS is showing promise in the generating structural information of biomolecules in the 10 to 100 kDa range from a single mass spectrum. Finally, FTICR/MS is the ideal technique to study the reactivity and higher-order structure of electrosprayed biomolecular ions. In contrast with the microsecond to millisecond timescale for most mass analyzers, the trapped ion cell of FTICR/MS provides an attractive environment in which to probe these complex ions from seconds to hours.

Capillary Electrophoresis-Electrospray Ionization Mass Spectrometry

CE is a high efficiency separation method, while ESIMS allows the formation of multiple-charged ions directly from the electrophoresis eluent and the precise mass determination of high molecular weight ions. The combination of CE with ESIMS is very attractive for obtaining higher selectivity and for structural analysis of analytes in a MS/MS mode.

Capillary Electrophoresis-Electrospray Ionization Mass Spectrometry Interface

The principal requirement of a CE-ESIMS interface is to produce the gas phase ions directly from the CE running buffer and transport the gas ions from the atmospheric pressure region into the mass spectrometer as efficiently as possible. The first CE-ESIMS interface was described by Smith and his co-workers[64]. A stainless steel needle was employed to ensure electrical contact with the solution eluting out of the CE capillary, hence terminating the CE circuit and initializing the electrospray process. A less satisfactory method for making the electric contact between the electrophoretic buffer and the electrospray interface was made by depositing a thin metal film on the outer surface of the capillary instead of using a stainless steel needle[65].

Smith and his co-workers[66] also introduced an improved ESIMS interface equipped with a coaxial sheath liquid as shown in Figure 4. In this design, a fused-silica capillary

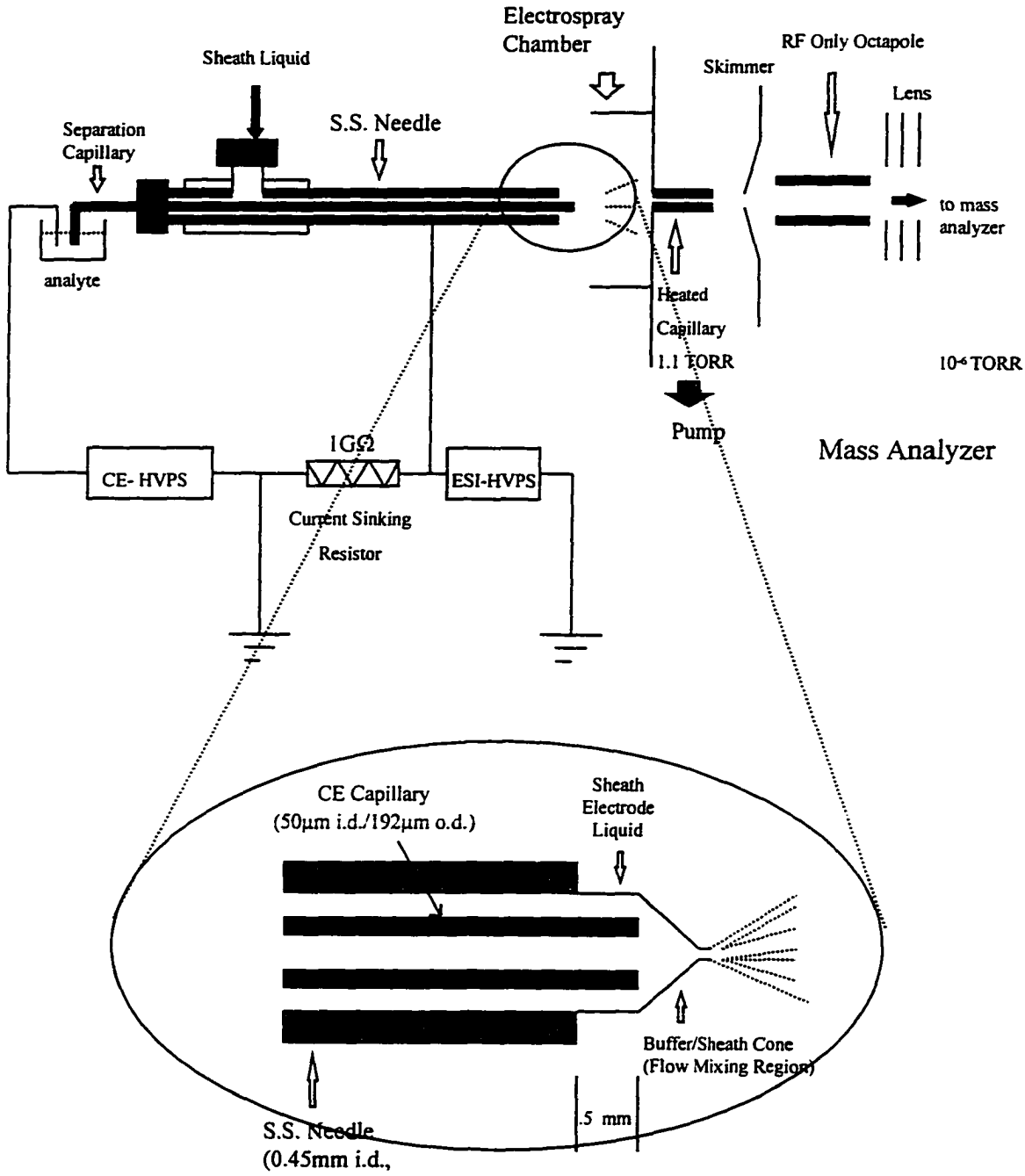

Figure 4

Schematic Diagram of On-line CE-ESIMS

protruded about 0.5 mm from a stainless steel needle. The sheath liquid usually consisted of a mixture of water and volatile organic solvent such as methanol. When the CE buffer was mixed with the sheath liquid at the end of the capillary, the surface tension decreased while the volatility increased, which enhanced the electrospray efficiency. Furthermore, the sheath liquid established electrical contact at the end of the capillary. The sheath potential was controlled around 5 kV (for positive ion mode) and functioned as both the CE cathodic potential and the electrospray voltage. A counter current flow of warm nitrogen gas (up to 80 °C) between the nozzle and the ESI source was used to aid desolvation, although sufficient heating during transport into the mass spectrometer also accomplished effective desolvation.

Lee et al.[67] developed a liquid junction coupling for CZE-ion spray MS (which is the nebulizing gas assisted ESIMS). The liquid junction and coaxial interfaces were compared by Pleasance et al.[68] and the coaxial sheath flow appeared to have several advantages with regard to ruggedness, ease of use, better sensitivity and electrophoretic performance. Gale and Smith[69] described a sheathless ESI source in which a small diameter etched-tip capillary was incorporated. The ability to electrospray aqueous solutions without the use of an ancillary sheath flow was demonstrated with several biopolymers. Tsuji and his co-workers[70] introduced a simple procedure for preparing gold-coated silica capillaries used in ESIMS. The performance characteristics of these durable capillaries as continuous infusion sources were examined, and their utility in on-line CE-ESIMS was demonstrated.

A microdialysis junction was developed by Zhou and Lunte for providing post-run additive to a CZE separation employing electrochemical detection[71]. Recently, Severs and

co-workers reported the use of a microdialysis junction for making the necessary electrical connection across the dialysis membrane for CZE-ESIMS interfacing[72,73]. A microelectrospray emitter produces a stable electrospray at the low flow rates of CZE effluents and avoids both the makeup flow needed by sheath flow interface and the subsequent dilution and reduction in sensitivity.

Applications of Capillary Electrophoresis-Electrospray Ionization Mass Spectrometry

One of the advantages of incorporating ESIMS lies in the multiple charging of the analytes under ESI conditions. The multiple charging phenomenon in ESI makes the detection of biomacromolecules possible using a quadrupole mass spectrometer with limited m/z range. Various applications have been reported for the analysis of peptides and proteins by CE-ESIMS[74-77]. A reduced elution speed method[74] was described for the enhancement of detection sensitivity in CZE-ESIMS. Mass spectra for a set of standard proteins were obtained from 60 femtomole of proteins, while an albumin tryptic digestion was analyzed with the injections of 40 femtomole of proteins. The use of small i.d. capillaries for the detection of protein analytes at the attomole level was demonstrated by Smith and his co-workers[75]. With the proper selection of running buffers and on-line combination of transient CITP with ESIMS, the concentration detection limits for a full scan were improved by a factor of 100 times, in comparison with CZE-ESIMS[77].

In the pharmaceutical area, identification of non-steroidal anti-inflammatory drugs and their metabolites in human urine was demonstrated using CZE-ESIMS[78]. The application of CZE-ESIMS for drug metabolic studies with a particular emphasis on neuroleptic drugs was reported by Tomlinson et al.[79,80] A non-aqueous solution was used as the electrophoretic medium due to the low solubility of drug analytes in aqueous solution. Furthermore, CE-ESIMS has been applied for the analysis of compounds of environmental concern, such as agrochemicals, pesticides, inorganic compounds and dyes[81-84]. For example, Lamoree and his co-workers[83] demonstrated the determination of β-agonists which are used illegally in the cattle industry to increase meat production.

Smith and co-workers developed the first successful CE-FTICR/MS interface and have acquired the first on-line high resolution mass spectra of CE samples[85-88]. In their first demonstration of the feasibility of the CE-FTICR/MS interface, a mixture of six proteins was separated and detected by on-line CE-FTICR/MS[85]. Sufficient mass-spectral resolving power was achieved to observe the individual isotopes in charge states for proteins as large as carbonic anhydrase (MW 28,802 Da). The actual amount of sample consumed per scan was about 20 attomoles. In later work, a tandem mass spectrometry experiment was performed in which electrosprayed CE solute bands were subjected to sustained off-resonance irradiation (SORI) to produce dissociation spectra for proteins as large as equine apomyoglobin with resolving power of 50,000[87]. CE-FTICR/MS was further applied to the challenging task of directly analyzing cellular proteins[88]. They demonstrated the on-line acquisition of high-resolution mass spectra (average resolution 45,000 fwhm) of both α and β chains of

hemoglobin acquired from the injection of 10 human erythrocytes (corresponding to 4.5 femtomole of hemoglobin.

Liquid Chromatography-Electrospray Ionization Mass Spectrometry

The on-line combination of liquid chromatography and mass spectrometry (LC-MS) has been under investigation for over 20 years. Three major difficulties are met in combining the two powerful analytical techniques, including: (i) the apparent flow rate incompatibility as expressed in the need to introduce 1 ml/min of a liquid effluent from a conventional LC column into the high vacuum of the mass spectrometer, (ii) the solvent composition incompatibility as result of the frequent use of non-volatile mobile phase additives in LC separation development, and (iii) the ionization of non-volatile and/or thermally labile analytes.

The ionization of analytes in liquid is no longer considered a problem in LC-MS since the introduction of powerful soft-ionization techniques such as fast-atom bombardment (FAB), thermospray, electrospray and matrix-assisted laser desorption ionization (MALDI). The only general solution in solving the mobile phase incompatibility problem is a change of the phase system in the LC separation, i.e., by the removal of all non-volatile additives from the mobile phase. However, this solution is dictated purely from the MS point of view and sometimes extremely difficult to achieve in LC. There are also some technological solutions should be mentioned, which may be used to solve the problem. First is the on-line

continuous-flow liquid-liquid extraction for LC-MS developed by Karger's group[89,90]. A second approach based on coupled-column and valve-switching techniques, was first demonstrated by Edlund et al.[91] and later simplified by Walhagen[92]. A third approach is based on the application of micromembrane suppressers, initially developed for conductometric detection in ion chromatography. This approach has been demonstrated for the on-line combination of ion-pair LC and MS and LC-MS analysis of oligosaccharides using mobile phases containing a sodium acetate concentration as high as 0.4 M.[93]

Liquid chromatography-Mass Spectrometry Interface

Many efforts have been made in designing different LC-MS interface to solve the flow-rate incompatibility problem. Over the past 20 years, a total of about 25 different LC-MS interfaces have been described in the literature[94,95]. Only the ones that have demonstrated practical potential for real applications are discussed here.

The moving-belt interface[96] consists of an endless continuously moving Kapton ribbon which transports the column effluent from the LC column outlet towards the MS ion source. Desorption of the analyte into the ion source by flash evaporation at the tip of the moving-belt interface provides the analyte in a gaseous state, susceptible to conventional electrochemical ionization (EI) or chemical ionization (CI). Although quite successful for a few years, the moving-belt interface nowadays is hardly used.

In a thermospray interface[97], a jet of vapor and small droplets is generated out of a heated vaporizer tube. The analytes are ionized by means of solvent-mediated CI reactions and ion evaporation processes. The reagent gas for solvent-mediated CI can be generated either in a conventional way using energetic electrons from a filament or discharge electrode, or in a process called thermospray ionization, where the volatile buffer dissolved in the eluent is involved. The thermospray interface for many years has been the interface of choice and continues to solve practical problems in everyday practice.

In a continuous-flow or dynamic fast-atom bombardment interface (CF-FAB)[98] a small liquid stream, typically 5-15 μl/min, mixed with an appropriate FAB matrix solvent, flows through a narrow-bore fused-silica capillary towards either a stainless-steel frit or gold-plated FAB target. Ions are generated by bombardment of the liquid film by fast atoms. The use of CF-FAB is decreasing due to the introduction of especially the electrospray interface. However, continued application of CF-FAB especially at magnetic sector instruments can be expected owing to the ease of implementation of CF-FAB interface.

In a particle-beam interface[99], the column effluent is nebulized either pneumatically or by thermospray nebulization, into a near atmospheric-pressure desolvation chamber, which is connected to a momentum separator. In the separator, the high-mass analytes are preferentially transferred to the MS ion source while the low-mass solvent molecules are efficiently pumped away. The analyte molecules are transferred as small particles to a conventional ion source, where they disintegrate upon collisions at the heated source walls. The released gaseous molecules are ionized by EI or CI.

In an atmospheric-pressure chemical ionization (APCI) interface[100], the column effluent is pneumatically nebulized into a heated stainless-steel tube, where the solvent evaporates almost completely. Atmospheric-pressure chemical ionization is initiated by electrons from a corona discharge needle in the same region. Subsequently, the ions generated are sampled into the high vacuum of the mass spectrometer for mass analysis.

In an electrospray ionization interface[101,102], the column effluent is nebulized into the atmospheric-pressure region as a result of the influence of a high electric field applied at the electrospray capillary tip. The solvent emerging from the capillary tip breaks into highly charged droplets, typically only a few micrometers in diameter. The charged droplets drift in the electric field between the capillary and the mass spectrometer sampling aperture. In transit through the MS interface, the droplets experience conditions that cause evaporation and droplet disintegration, leading ultimately to very small, highly charged droplets capable of producing gas-phase ions, either by ion emission or complete solvent evaporation. In some designs, the electrospray nebulization is assisted by pneumatic nebulization. Such an approach is called an ionspray interface[103].

Applications of Reversed-phase Liquid Chromatography-Electrospray Ionization Mass Spectrometry

It is estimated that somewhere between 75-90% of all HPLC separations are carried out in the reversed-phase mode[17] while electrospray ionization (ESI) has become one of the leading sample introduction/ionization technique for MS.[104] Reversed-phase liquid chromatography (RPLC)-electrospray ionization mass spectrometry (ESIMS) combines the two most popular and powerful techniques together and has had a major impact in many fields especially the bio-related areas of pure and applied science and technique.

RPLC-ESIMS is a well-established method for the identification and characterization of proteins and peptides because of its inherent selectivity, specificity, and sensitivity. This method is particularly valuable for mixture analysis because of the combined strengths of LC to purify, concentrate, and resolve complex mixtures, and ESIMS for mass separation and determination. Typical protocols for protein identification or characterization of modifications begin with the enzymatic digestion of the protein sample, resulting in a complex mixture of peptides. The separation of these mixtures by RPLC facilitates the task of spectra interpretation in ESIMS.

Carr and his co-workers developed mass spectrometric methods of glycopeptide-specific detection in LC-ESIMS[105]. The most specific method involves monitoring of sugar oxonium fragment ions during precursor-ion scan ESIMS/MS. Signals from nonglycosylated peptides are virtually eliminated, resulting in a total-ion current chromatographic trace of only

the glycopeptides present in the digest. The corresponding mass spectra yield molecular weight and glycopeptide microheterogeneity information. An alternative and complementary approach which they termed collisional-excitation scanning also involves fragmentation of glycopeptides to sugar oxonium ion fragments in the source region but does not involve any mass-selection process, permitting the experiment to be performed in a single quadrupole instrument. A selected-ion chromatogram for carbohydrate-specific ions such as the N-acetylhexosamine oxonium ion (*m/z* 204) produces a glycopeptide-specific trace.

RPLC-ESIMS has also been demonstrated as a sensitive and selective method for the analysis of drugs and their metabolites in complex biological matrixes. Crowther et al.[106] applied RPLC-ESIMS to the analysis of a pentapeptide drug (IRI-514) in rabbit and human plasma. The lower limit of quantitation using selected ion monitoring was determined to be 2 ng/ml. Jackson et al.[107] investigated the application of RPLC-ESIMS for drug metabolism studies using S 9788 and various synthesized metabolic products as model compounds to assess the response characteristics with regard to compound lipophilicity and the influence of biological matrix components. The results demonstrated the versatility of the electrospray ionization technique to analyze compounds of widely varying polarity and the power of MS/MS to identify unequivocally metabolic products. Weidolf and co-workers[108] noted that although the limit of detection by LC/MS with selected ion monitoring (SIM) was around 10 pg for standards of sulfoconjugated metabolites of the synthetic steroid boldenone, as compared to 100 pg using selected reaction monitoring (SRM) or multiple reaction monitoring (MRM), MS/MS showed improved selectivity for structure confirmation and quantitation in

biological extracts. Unless rigorous sample clean-up strategies are employed or fortuitous chromatographic conditions can be found, ions originating in the mobile phase or from endogenous substances present in biological extracts can result in considerable background noise even when SIM is used. The effect is most pronounced in the lower m/z values.

CHARACTERIZATION OF MICRODIALYSIS ACIDIFICATION FOR CAPILLARY ISOELECTRIC FOCUSING-MICROELECTROSPRAY IONIZATION MASS SPECTROMETRY

Liyu Yang and Cheng S. Lee

Steven A. Hofstadler and Richard D. Smith

A paper submitted to Anal. Chem.

ABSTRACT

A microdialysis junction, based on a microdialysis membrane connecting both a separation capillary and a short, sharply tapered microelectrospray emitter capillary, is demonstrated for on-line combination of capillary isoelectric focusing (CIEF) with electrospray ionization mass spectrometry (ESIMS). The microdialysis junction provides the necessary electrical connection across the dialysis membrane for defining the electric fields needed for the CIEF separation and the electrospray process. Additionally, post-separation acidification of focused protein zones eluted from the CIEF capillary is achieved using the microdialysis junction while maintaining separation efficiency and resolution. A microelectrospray emitter produces a stable electrospray of protein analytes without the need for a makeup liquid flow and eliminates any subsequent sample dilution and reduction in MS sensitivity. The microdialysis junction is advantageous over the coaxial liquid sheath interface as evidenced by the simplicity in operation procedures, the enhancement in

detection sensitivity, and the linear correlation between protein's migration time and isoelectric point in CIEF-ESIMS.

INTRODUCTION

In capillary isoelectric focusing (CIEF), the coated fused-silica capillary contains not only carrier ampholytes for the creation of a pH gradient but also proteins[1-3]. When an electric potential is applied, the negatively charged acidic ampholytes migrate toward the anode and decrease the pH at the anodic section, while the positively charged basic ampholytes migrate toward the cathode and increase the pH at the cathodic section. These pH changes continue until each ampholyte species reaches its isoelectric point (pI). Protein analytes as amphoteric macromolecules also focus at their pI values in narrow zones in the same way as the individual ampholytes.

Theoretically, there is no movement in the coated capillary when the focusing is completed. Thus, the entire pH gradient, along with the focused protein zones, must be mobilized past the UV detection window or into the mass spectrometer. On-line coupling of CIEF with electrospray ionization mass spectrometry (ESIMS) is very attractive for the direct identification of analytes, selectivity enhancement, and structure confirmation by MS/MS techniques. At the end of the CIEF capillary, the mobilized protein zones are analyzed by ESIMS using a coaxial sheath flow configuration[4-9]. The use of sheath flow establishes the electrical connection at the CIEF capillary terminus, which serves to define the electric field along the CIEF capillary and apply an electric voltage for electrospray ionization[10].

The disadvantage in employing a coaxial liquid sheath flow is the addition of excess electrolyte to the CIEF effluent. The presence of additional sheath liquid decreases analyte sensitivity in ESIMS due to the larger initial drop size and the effective competition for the limited number of charges in the electrospray process. The excess electrolyte results in a smaller fraction of protein analytes in solution being converted to the gas phase ions. The use of smaller diameter and more sharply tapered emitters in ESI improves analyte sensitivity, minimizes sample consumption, and allows ionization of aqueous samples[11-14]. Based on a thin gold coating deposited on the tapered terminus of the capillary, a sheathless capillary zone electrophoresis (CZE)-ESIMS interface has demonstrated all these advantages in conjunction with on-line separation[15-17], even allowing hemoglobin analysis at the single-cell level[16]. However, the limited lifetime and difficulty of production of these capillaries restrict more routine applications of this CZE-ESIMS interface design.

A microdialysis junction was developed by Zhou and Lunte for providing post-run additive to a CZE separation employing electrochemical detection[18]. On-line microdialysis sample cleanup for ESIMS was demonstrated by Liu et al.[19] for oligonucleotide analysis. Concentration and desalting of analytes in small volumes, prior to CZE separations, were achieved by using an array of hollow fibers[20]. Simultaneously with the concentration, the sample can be purified using a fiber with an appropriate molecular weight cutoff value. Recently, Severs and her co-workers reported the use of a microdialysis junction for making the necessary electrical connection across the dialysis membrane for CZE-ESIMS interfacing[21,22]. A microelectrospray emitter produced a stable electrospray at the low flow rates of CZE effluents and avoided both the need for a makeup flow provided by sheath flow interface and the subsequent dilution and reduction in sensitivity.

In this study, the performance and the capabilities of the microdialysis interface are further investigated and illustrated for CIEF-ESIMS. Besides the electrical connection across the microdialysis junction, post-run acidification via the dialysis membrane is demonstrated for enhancing the protonation and the ionization efficiency of focused proteins while maintaining separation efficiency, resolution, and sensitivity in CIEF-ESIMS. Reproducibility studies and comparisons with coaxial liquid sheath flow interface are made with regard to operation procedures, sensitivity, and the correlation between protein's migration time and pI in CIEF-ESIMS. The use of microdialysis junction together with in-probe sequential focusing and mobilization lend themselves to automation.

EXPERIMENTAL SECTION

Materials and Chemicals. Model proteins, including cytochrome *c* (horse heart, pI 9.6), myoglobin (horse heart, pI 7.2 and 6.8), carbonic anhydrase I (human erythrocyte, pI 6.6), and carbonic anhydrase II (bovine erythrocyte, pI 5.9), were acquired from Sigma (St. Louis, MO). Another batch of bovine carbonic anhydrase II obtained from Sigma exhibited a pI of 5.4. Carrier ampholytes, pharmalyte 3-10, were obtained from Pharmacia (Uppsala, Sweden). All other chemicals, including acetic acid, ammonium acetate, ammonium hydroxide, methanol, phosphoric acid, and sodium hydroxide were purchased from Fisher (Fair Lawn, NJ). All background electrolytes and sample solutions were prepared using water purified by a Nanopure II system (Branstead, Dubuque, IA) and further filtered with a 0.22 μm membrane (Millipore, Bedford, MA).

Fused-silica capillaries with 50 μm i.d. and 192 μm o.d. (Polymicro Technologies, Phoenix, AZ) were coated internally with linear polyacrylamide for the elimination of electroosmotic flow and protein adsorption onto the capillary wall[3]. The polyimide coating

on the external capillary surface was removed from the last 2 cm of short lengths of silica capillary, and these portions were then etched in 40% hydrofluoric acid (Aldrich, Milwaukee, WI) for approximately 20 min. A nitrogen flow was introduced into the capillary to prevent hydrofluoric acid from etching the inner capillary wall coated with linear polyacrylamide. The resulting capillary tip was trimmed to produce a sharp ion emitter. The 250 μm i.d. polysulfone dialysis tubing (nominal molecular weight cutoff of 10,000) was obtained from A/G Technology Corp. (Needham, MA).

Microdialysis Interface Design. The CIEF capillary and a 1-cm-long ESI emitter capillary were butted together inside a 0.5 cm length of polysulfone dialysis tubing. Epoxy (Loctite, Cleveland, OH) was then applied around the outside of the dialysis tubing/capillary boundaries. After the epoxy had dried, the capillary was inserted through a 100 μl Eppendorf pipet tip containing the anolyte for the CIEF separation. The pipet tip was mounted on an x-y-z motion manipulator for positioning relative to the heated metal capillary of a TSQ 7000 mass spectrometer (Finnigan MAT, San Jose, CA). A platinum wire was inserted in the pipet tip and connected to a ground or a high-voltage (HV) power supply to provide electrical connection at the microdialysis junction.

Capillary Isoelectric Focusing-Electrospray Ionization Mass Spectrometry. The CIEF apparatus was constructed in-house using a CZE 1000R HV power supply (Spellman High-Voltage Electronics, Plainview, NY). The mass spectrometer was a TSQ 7000 (Finnigan MAT) triple quadrupole equipped with an electrospray ionization source. Two separate electrospray probes, including a home-built microelectrospray ionization source[12] and the standard Finnigan electrospray source, were employed when using the microdialysis junction and a coaxial sheath flow system, respectively.

The first quadrupole was used for the mass scanning of protein ions, while the second and third quadrupoles were operated in the radio frequency-only mode. The electron multiplier was set at 1.4 kV, with the conversion dynode at -15 kV. The heated desolvation capillary in the ESI source was held at 200 °C. The mass spectrometer was tuned and calibrated using an acetic acid solution (methanol/water/acetic acid, 50:49:1 v/v/v) containing myoglobin and the small peptide methionine-arginine-phenylalanine-alanine.

The detailed configuration of CIEF-ESIMS using coaxial liquid sheath flow interface, including sheath liquid and electrical connection, was described elsewhere[4,5,8]. A 30-cm-long coated capillary was mounted within the electrospray probe. The capillary was filled with a solution containing 0.5% pharmalyte 3-10 and model proteins. The outlet reservoir, containing 20 mM sodium hydroxide as the catholyte, was located inside the electrospray housing during the focusing step. The inlet reservoir, containing 20 mM phosphoric acid as the anolyte, was kept outside at the same height as the outlet reservoir. Focusing was performed at a 15 kV constant voltage for approximately 10 min. Once the focusing was complete, the electric potential was turned off, and the outlet reservoir was removed. The capillary tip was fixed about 0.5 mm outside the electrospray needle. A sheath liquid composed of 50% methanol, 49% water, and 1% acetic acid (v/v/v) at pH 2.6 was delivered at a flow rate of 0.3 μl/min using a Harvard Apparatus 22 syringe pump (South Natick, MA). During the cathodic mobilization step, two HV power supplies were used for delivering the electric potentials of 19 kV and 4 kV to the inlet electrode and electrospray needle, respectively. To speed up protein mobilization and minimize the formation of moving ionic boundary inside the CIEF capillary[5,23], gravity mobilization was combined with cathodic mobilization by raising the inlet reservoir 8 cm above the electrospray needle.

For all CIEF-ESIMS measurements using the microdialysis junction, a 10% acetic acid solution was employed as the anolyte and added into the pipet tip. The inlet reservoir, containing 0.3% ammonium hydroxide as the catholyte, was kept at the same height as the microdialysis junction. Focusing was performed by applying a constant voltage of -15 kV at the inlet reservoir for approximately 10 min. A common ground connection was formed between the CIEF system and the microdialysis junction. Immediately after the focusing, pressure mobilization was achieved by applying a 0.2 psi nitrogen pressure at the inlet reservoir. During the pressure mobilization step, two HV power supplies were used for delivering the electric potentials of -13 kV and 2 kV to the inlet electrode and platinum wire connected to the microdialysis junction, respectively. There was no cathodic mobilization of focused protein zones and no need for readjusting capillary position for all CIEF-ESIMS measurements when using the microdialysis junction.

RESULTS AND DISCUSSION

Effects of Solution Conditions on Positive Electrospray Protein Mass Spectra in the Presence of Carrier Ampholytes. The effects of carrier ampholyte concentration on the average charge states and the ion signals for protein analytes in ESIMS were studied in our previous work[4]. To investigate the effects of solution compositions typically employed in the coaxial liquid sheath flow, 0.1 mg/ml myoglobin and 0.5% pharmalyte 3-10 were prepared in various solution conditions and were infused at 0.3 μl/min through a home-built microelectrospray ionization source[12]. Due to the application of the microelectrospray ionization source, a smaller electric voltage of 2 kV, in comparison with 4 kV when using the standard Finnigan electrospray needle, was employed in the direct infusion experiments. The

positive ESI mass spectra of myoglobin and pharmalyte 3-10 at various solution conditions are summarized in Fig. 1 for comparison.

The ions of pharmalyte 3-10 were observed in the low *m/z* range up to *m/z* 1,000. For solutions containing either deionized water or a mixture of methanol and water (Fig. 1A-B), the pharmalyte ions successfully competed against the formation of myoglobin ions in the electrospray process. Thus, the pharmalyte ions similar to simple electrolyte ions led to higher solution conductivity and contributed to the establishment of the charge excess known to exist in droplets formed during the electrospray process. The suppression of protein ion intensity due to the addition of pharmalyte ions could be qualitatively accounted for by the ion competition theories of Tang and Kebarle[24,25] and Wang and Cole[26].

Immediately after the addition of 1% acetic acid, the mass spectrum of myoglobin exhibited twelve peaks, each one corresponding to a different protonation state of myoglobin (Fig. 1C). These protonation states ranged from +9 to +20 with +15 being the most intense. There was no significant difference in the protein ion intensity before and after the addition of methanol into acetic acid solution (Fig. 1C-D). By comparing the results shown in Fig. 1A-D, solution acidity played the most important role in protein protonation and favored protein analytes in competition with carrier ampholytes for the formation of gas phase ions in the electrospray process. No significant difference in the protein ion intensity was observed by raising the acetic acid concentration from 1 to 10% (data not shown).

Effects of Sheath Liquid Flow Rate on Positive Electrospray Protein Mass Spectra in the Presence of Carrier Ampholytes. Achieving stable electrospray operation with a liquid sheath flow interface involves simultaneous optimization of multiple parameters including capillary dimensions, capillary position, sheath liquid flow rate and composition,

gas sheath flow rate, and ESI conditions[9,11,12,27-30]. To study the effects of flow rates typically employed in the coaxial liquid sheath interface for CIEF-ESIMS, 0.1 mg/ml myoglobin and 0.5% pharmalyte 3-10 were prepared in deionized water and were infused at 50 nl/min through a 50 μm i.d./192 μm o.d. fused-silica capillary in a standard Finnigan electrospray source. The infusion rate was nearly the same as the flow rate through the CIEF capillary during the mobilization step. A sheath liquid composed of 50% methanol, 49% water, and 1% acetic acid (v/v/v) at pH 2.6 was delivered at various flow rates using a syringe pump.

The positive ESI mass spectra of myoglobin and pharmalyte 3-10 at various sheath liquid flow rates are summarized in Fig. 2 for comparison. The results shown in Fig. 2 demonstrated that the coaxial liquid sheath interface was effective in establishing a consistent electrospray over a 17-fold change of sheath liquid flow rate (5 - 0.3 μl/min). In fact, Kirby et al.[9] combined optimal component sizes, tapered capillary tips, and adjustment of the capillary with respect to the liquid sheath tube to establish a rugged, stable liquid sheath interfacing procedure. The interface was particularly effective at low flow rates and allowed stable operation with a sheath liquid flow rate as low as 250 nl/min.

In this study, the protein ion intensity decreased with increasing sheath liquid flow rate, indicating the effect of sample dilution. Additionally, protein analytes competed favorably with carrier ampholytes for the formation of gas phase ions in the electrospray process at low sheath liquid flow rates. Based on the results shown in Figs. 1 and 2, a sheath liquid composed of 50% methanol, 49% water, and 1% acetic acid (v/v/v) at pH 2.6 was delivered at a flow rate of 0.3 μl/min for all CIEF-ESIMS measurements using the coaxial liquid sheath interface.

Capillary Isoelectric Focusing-Electrospray Ionization Mass Spectrometry Using Coaxial Liquid Sheath Interface. Due to cathodic mobilization, the acetate ions used in the sheath liquid competed with hydroxide ions for electromigration into the capillary. Since fewer hydroxide ions entered the capillary, the pH gradient drifted downward. Protein analytes previously focused at their pI values became positively charged and migrated toward the cathodic end. Thus, the basic protein cytochrome c migrated ahead of acidic proteins such as carbonic anhydrase I and II. The reconstructed ion electropherogram of the protein mixture with a final concentration of 0.1 mg/ml for each protein analyte is shown in Fig. 3A. The reconstructed ion electropherogram was obtained from mass scans between *m/z* 600 and *m/z* 2000 at a scan rate of 2 s/scan. All protein peaks were directly identified on the basis of mass spectra of protein analytes taken from the average scans under the peaks. No significant difference in the protein ion intensity was observed by raising the acetic acid concentration from 1 to 10% in the sheath liquid (data not shown).

Poor linear correlation was observed between the migration times for the model proteins during the cathodic mobilization step in CIEF-ESIMS and their known pI values (Fig. 4A). It is known that progressive flow of non-hydroxyl anions (acetate ions in this study) in cathodic mobilization causes a progressive pH shift down the capillary, resulting in mobilization of proteins in sequence[31]. The rate of pH change depends on the amount of anion moving into the capillary, the mobility of the anion, and the buffering capacity of carrier ampholytes. Basic and neutral proteins are therefore more efficiently mobilized toward the cathode, the end of the capillary for all ESIMS measurements. However, acidic proteins at the far end of the capillary are mobilized with low efficiency and may exhibit additional zone broadening.

Capillary Isoelectric Focusing-Electrospray Ionization Mass Spectrometry Using Microdialysis Junction. The microdialysis junction provides the necessary electrical connection across the dialysis membrane for defining the electric fields needed for the CIEF separation and the electrospray process. Additionally, the microdialysis junction containing 10% acetic acid solution acidified protein analytes eluted from the CIEF capillary during the pressure mobilization step. Excess acetic acid used in the microdialysis junction facilitated and enhanced buffer exchange for solution acidification and protein protonation.

The reconstructed ion electropherogram of the protein mixture with a final concentration of 0.01 mg/ml for each protein analyte is shown in Fig. 3B. The reconstructed ion electropherogram was obtained from the mass scan between *m/z* 600 and *m/z* 2000 at a scan rate of 2 s/scan. Due to the use of pressure mobilization and the location of anodic end at the end of the CIEF capillary, acidic proteins such as carbonic anhydrase I and II were eluted ahead of basic protein of cytochrome *c*. All protein peaks were directly identified on the basis of mass spectra of protein analytes taken from the average scans under the peaks.

A major factor for causing reduced sensitivity in the coaxial liquid sheath interface was the large dilution factor and background ion production due to the introduction of makeup liquid. The flow rate at the ESI emitter with the microdialysis junction was nearly the same as the flow rate through the CIEF capillary. There was no significant fluid addition through the dialysis membrane, only ionic transfer and buffer exchange. By comparing the results shown in Fig. 3A-B, there was a substantial gain in both signal intensity and signal/noise ratio using the microdialysis junction interface even though the protein analytes were diluted by 10-fold. The results indicated that at least an order of magnitude improvement in detection limits for the CIEF-ESIMS measurements could be achieved using the microdialysis junction.

The CIEF separation capillary and the short (1 cm), sharply tapered ESI emitter capillary were butted together without leaving any intentional gap inside the microdialysis tubing. The design of the microdialysis junction minimized any additional analyte band broadening while migrating through the junction and the ESI emitter capillary. The design allowed high-efficiency CIEF separation to be maintained through the interface (Fig. 3B). In fact, two isoforms of cytochrome *c* were resolved in CIEF-ESIMS using the microdialysis junction with pressure mobilization.

During pressure mobilization, it was necessary to apply an electric field across the capillary in order to maintain focused protein zones. In the presence of an electric field, the zone-sharpening effect, the characteristic of isoelectric focusing, minimized any additional band broadening contributed by the parabolic shape of the hydrodynamic flow. In comparison with cathodic mobilization, pressure mobilization maintained the relative position of protein analytes during mobilization. As a result, better separation resolution among acidic proteins of two carbonic anhydrase II (pI 5.4 and pI 5.9) was obtained using pressure mobilization (Fig. 3B) than applying the combination of cathodic and gravity mobilization (Fig. 3A). Additionally, the linear correlation coefficients of 0.99 and 0.97 between the migration time and protein's pI were obtained in the pH ranges of 5-8 and 5-10, respectively (Fig. 4B).

Lamoree et al. introduced a coupled-capillary setup, which incorporated a microdialysis device between a CIEF separation capillary and a transfer capillary, for on-line coupling of CIEF with ESIMS[32]. In their setup, carrier ampholytes eluted from the CIEF capillary were removed in a dialysis tubing and the protein analytes were subsequently delivered into ESIMS through a 40-cm-long transfer capillary. At the end of the transfer

capillary, a sheath liquid composed of methanol, water, and acetic acid was employed in the coaxial liquid sheath interface for establishing necessary electrical connection. Again, there was no apparent loss in separation efficiency and resolution of focused protein zones across the microdialysis junction. However, significant reduction in separation resolution was observed in the reconstructed ion electropherogram due to analyte diffusion and the absence of a pH gradient for maintaining the focused protein zones in the transfer capillary.

The infusion of the catholyte (0.3% ammonium hydroxide) into the CIEF capillary occurred during the pressure mobilization step. Thus, the reproducibility of migration time and peak area in CIEF-ESIMS was investigated by performing consecutive runs in the same CIEF capillary. In general, at least 10 consecutive runs with the average coefficients of variation (% CV), which ranged from 5% for migration time to 12% for peak area, were obtained using the polyacrylamide coated capillary. The reproducibility and the lifetime of coated capillary employed in the microdialysis junction were comparable to those observed in CIEF-ESIMS using the coaxial liquid sheath interface.

The mass spectra taken from the average scans under the peaks of cytochrome *c* (Fig. 3A-B) are shown in Fig. 5A-B for comparison. The mass spectrum of cytochrome *c* obtained from CIEF-ESIMS using the coaxial liquid sheath interface displayed two separate electrospray ionization envelopes (Fig. 5A). The charge states of these two envelopes centered at +14 and +8, corresponding to the denatured and intermediate conformation states of cytochrome *c*[33]. The mass spectrum of native cytochrome *c* in deionized water ranged from +7 to +12 with +10 being the most intense (data not shown). The intermediate state of cytochrome *c* exhibited a relatively tight conformation and accepted far fewer protons than the native state[33]. On the other hand, the mass spectrum obtained from CIEF-ESIMS using

the microdialysis junction was mainly contributed by the denatured cytochrome *c* (Fig. 5B). The observation of three conformational states is in concert with the earlier results of acid unfolding of cytochrome *c* studied by acid-base titrations, spectrophotometry, circular dichroism, fluorescence, viscometry, and ESIMS[33-36].

ACKNOWLEDGEMENT

The authors wish to thank Dr. Scott Shaffer for helpful discussion. The authors also acknowledge the Microanalytical Instrumentation Center of the Institute for Physical Research and Technology at Iowa State University, the U.S. Department of Energy, and Laboratory Directed Research and Development of Pacific Northwest Laboratory for support of this research. Pacific Northwest Laboratory is operated by Battelle Memorial Institute for the U.S. Department of Energy, through Contract No. DE-AC06-76RLO 1830. C.S.L. is a National Science Foundation Young Investigator (BCS-9258652).

REFERENCES

1. Hjerten, S.; Zhu, M. D. *J. Chromatogr.* **1985,** 346, 265-270.
2. Hjerten, S.; Liao, J. L.; Yao, J. *J. Chromatogr.* **1987,** 387, 127-138.
3 Kilar, F.; Hjerten, S. *Electrophoresis* **1989,** 10, 23-29.
4. Tang, Q.; Harrata, A. K.; Lee, C. S. *Anal. Chem.* **1995,** 67, 3515-3519.
5. Tang, Q.; Harrata, A. K.; Lee, C. S. *Anal. Chem.* **1996,** 68, 2482-2487.
6. Tang, Q.; Harrata, A. K.; Lee, C. S. *J. Mass Spectrom.* **1996,** 31, 1284-1290.
7. Yang, L.; Tang, Q.; Harrata, A. K.; Lee, C. S. *Anal. Biochem.* **1996,** 243, 140-149.
8. Tang, Q.; Harrata, A. K.; Lee, C. S. *Anal. Chem.* **1997,** 69, 3177-3182.

9. Kirby, D. P.; Thorne, J. M.; Gotzinger, W. K.; Karger, B. L. *Anal. Chem.* **1996,** 68, 4451-4457.

10. Smith, R. D.; Wahl, J. H.; Goodlett, D. R.; Hofstadler, S. A. *Anal. Chem.* **1993,** 65, 574A-584A.

11. Chowdhury, S. K.; Chait, B. T. *Anal. Chem.* **1991,** 63, 1660-1664.

12. Gale, D. C.; Smith, R. D. *Rapid Commun. Mass Spectrom.* **1993,** 7, 1017-1021.

13. Emmett, M. R.; Caprioli, M. R. *J. Am. Soc. Mass Spectrom.* **1994,** 5, 605-613.

14. Wilm, M.; Mann, M. *Anal. Chem.* **1996,** 68, 1-8.

15. Wahl, J. H.; Gale, D. C.; Smith, R. D. *J. Chromatogr. A* **1994,** 659, 217-222.

16. Hofstadler, S. A.; Severs, J. C.; Swanek, F. K.; Ewing, A. G.; Smith, R. D. *Rapid Commun. Mass Spectrom.* **1996,** 10, 919-923.

17. Ramsey, R. S.; McLuckey, S. A. *J. Microcolumn Sep.* **1995,** 7, 461-469.

18. Zhou, J.; Lunte, S. M. *Anal. Chem.* **1995,** 67, 13-18.

19. Liu, C.; Wu, Q.; Harms, A. C.; Smith, R. D. *Anal. Chem.* **1996,** 68, 3295-3299.

20. Zhang, R.; S. Hjerten *Anal. Chem.* **1997,** 69, 1585-1592.

21. Severs, J. C.; Harms, A. C.; Smith, R. D. *Rapid Commun. Mass Spectrom.* **1996,** 10, 1175-1178.

22. Severs, J. C.; Smith, R. D. *Anal. Chem.* **1997,** 69, 2154-2158.

23. Foret, F.; Thompson, T. J.; Vouros, P.; Karger, B. L.; Gebauer, P.; Bocek, P. *Anal. Chem.* **1994,** 66, 4450-4458.

24. Tang, L.; Kebarle, P. *Anal. Chem.* **1991,** 63, 2709-2715.

25. Tang, L.; Kebarle, P. *Anal. Chem.* **1993,** 65, 3654-3668.

26. Wang, G.; Cole, R. B. *Anal. Chem.* **1994,** 66, 3702-3708.

27. Varghese, J.; Cole, R. B. *J. Chromatogr.* **1993,** 639, 303-316.

28. Tetler, L. W.; Cooper, P. A.; Powell, B. *J. Chromatogr. A* **1995,** 700, 21-26.

29. Banks, J. F., Jr. *J. Chromatogr. A* **1995,** 712, 245-252.

30. Tomlinson, A. J.; Benson, I. M.; Naylor, S. *J. Capillary Electrophor.* **1994,** 1, 127-135.

31. Rodriguez-Diaz, R.; Wehr, T.; Zhu, M.; Levi, V. *Handbook of Capillary Electrophoresis;* Second Edition; Landers, J. P. Ed.; CRC Press: Boca Raton, 1997; Chapter 4.

32. Lamoree, M. H.; Tjaden, U. R.; van der Greef, J. *J. Chromatogr. A* **1997,** 777, 31-39.

33. Chowdhury, S. K.; Katta, V.; Chait, B. T. *J. Am. Chem. Soc.* **1990,** 112, 9012-9013.

34. Theorell, H.; Akesson, A. *J. Am. Chem. Soc.* **1941,** 63, 1804-1820.

35. Drew, H. R.; Dickerson, R. E. *J. Biol. Chem.* **1978,** 253, 8420-8427.

36. Goto, Y.; Calciano, L. J.; Fink, A. L. *Proc. Natl. Acad. Sci.* **1990,** 87, 573-577.

FIGURE LEGENDS

Fig. 1 Positive ESI mass spectra of myoglobin and pharmalyte 3-10 obtained at various solution conditions: (A) deionized water, (B) 50% methanol and 50% water (v/v), (C) 50% methanol, 49% water, and 1% acetic acid (v/v/v), and (D) 1% acetic acid.

Fig. 2 Positive ESI mass spectra of myoglobin and pharmalyte 3-10 obtained at various sheath liquid flow rates: (A) 5 μl/min, (B) 3 μl/min, (C) 1 μl/min, (D) 0.5 μl/min, (E) 0.3 μl/min.

Fig. 3 CIEF-ESIMS separations of model proteins using (A) the coaxial liquid sheath interface with a concentration of 0.1 mg/ml for each protein, and (B) the

microdialysis junction with a concentration of 0.01 mg/ml for each protein. Model proteins included: (1) carbonic anhydrase II (pI 5.4); (2) carbonic anhydrase II (pI 5.9); (3) and (4), carbonic anhydrase I (pI 6.6); (5) and (6), myoglobin (pI 6.8 and 7.2); and (7) and (8) cytochrom *c* (pI 9.6).

Fig. 4 Calibration curves of migration time versus protein's pI in CIEF-ESIMS using (A) the coaxial liquid sheath interface and (B) the microdialysis junction.

Fig. 5 Positive ESI mass spectra taken from the average scans under the peaks of cytochrome c in CIEF-ESIMS using (A) the coaxial liquid sheath interface (from Fig. 3A) and (B) the microdialysis junction (from Fig. 3B).

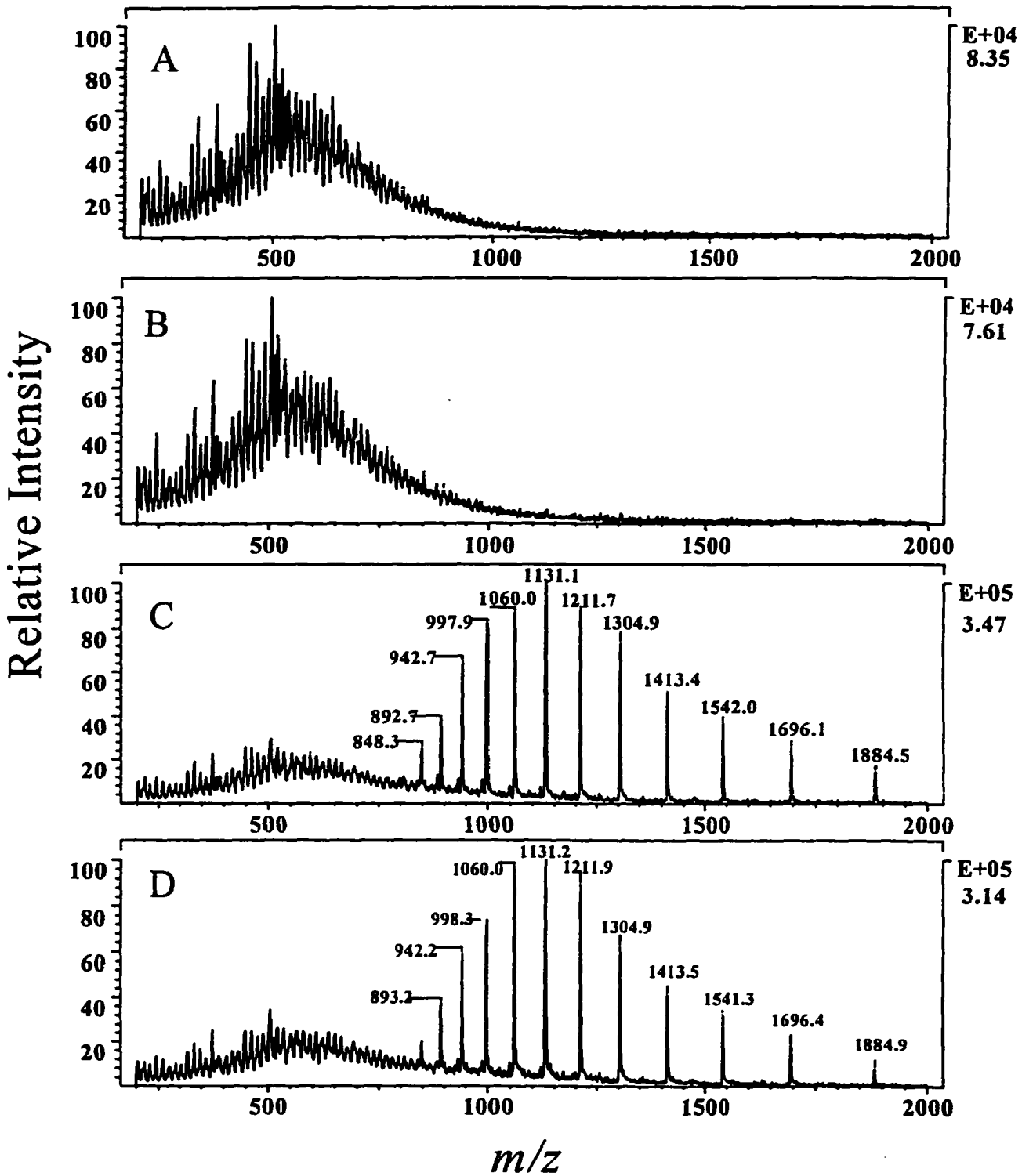
A
B
C
D
Relative Intensity
m/z
E+04
8.35
E+04
7.61
E+05
3.47
E+05
3.14
1131.1
1060.0
1211.7
997.9
1304.9
942.7
1413.4
1542.0
892.7
1696.1
848.3
1884.5
1131.2
1060.0
1211.9
998.3
1304.9
942.2
1413.5
893.2
1541.3
1696.4
1884.9

Figure 1

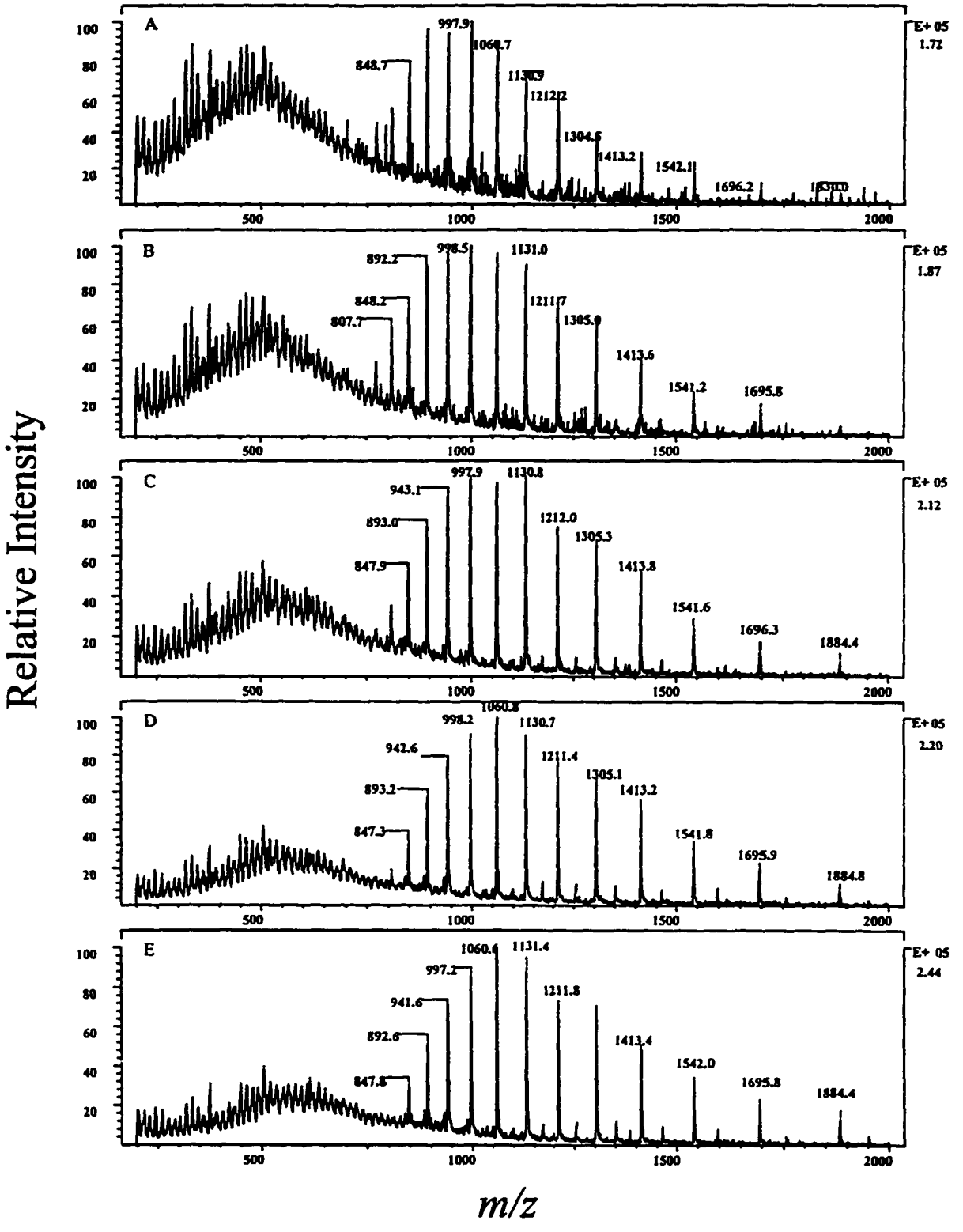
A
B
C
D
E
Relative Intensity
m/z
E+05
1.72
1.87
2.12
2.20
2.44
848.7
997.9
1060.7
1130.9
1212.2
1304.6
1413.2
1542.1
1696.2
892.2
998.5
1131.0
848.2
807.7
1211.7
1305.0
1413.6
1541.2
1695.8
943.1
997.9
1130.8
893.0
847.9
1212.0
1305.3
1413.8
1541.6
1696.3
1884.4
998.2
1060.8
1130.7
942.6
1211.4
893.2
847.3
1305.1
1413.2
1541.8
1695.9
1884.8
997.2
1060.6
1131.4
941.6
1211.8
892.6
847.5
1413.4
1542.0
1695.8
1884.4

Figure 2

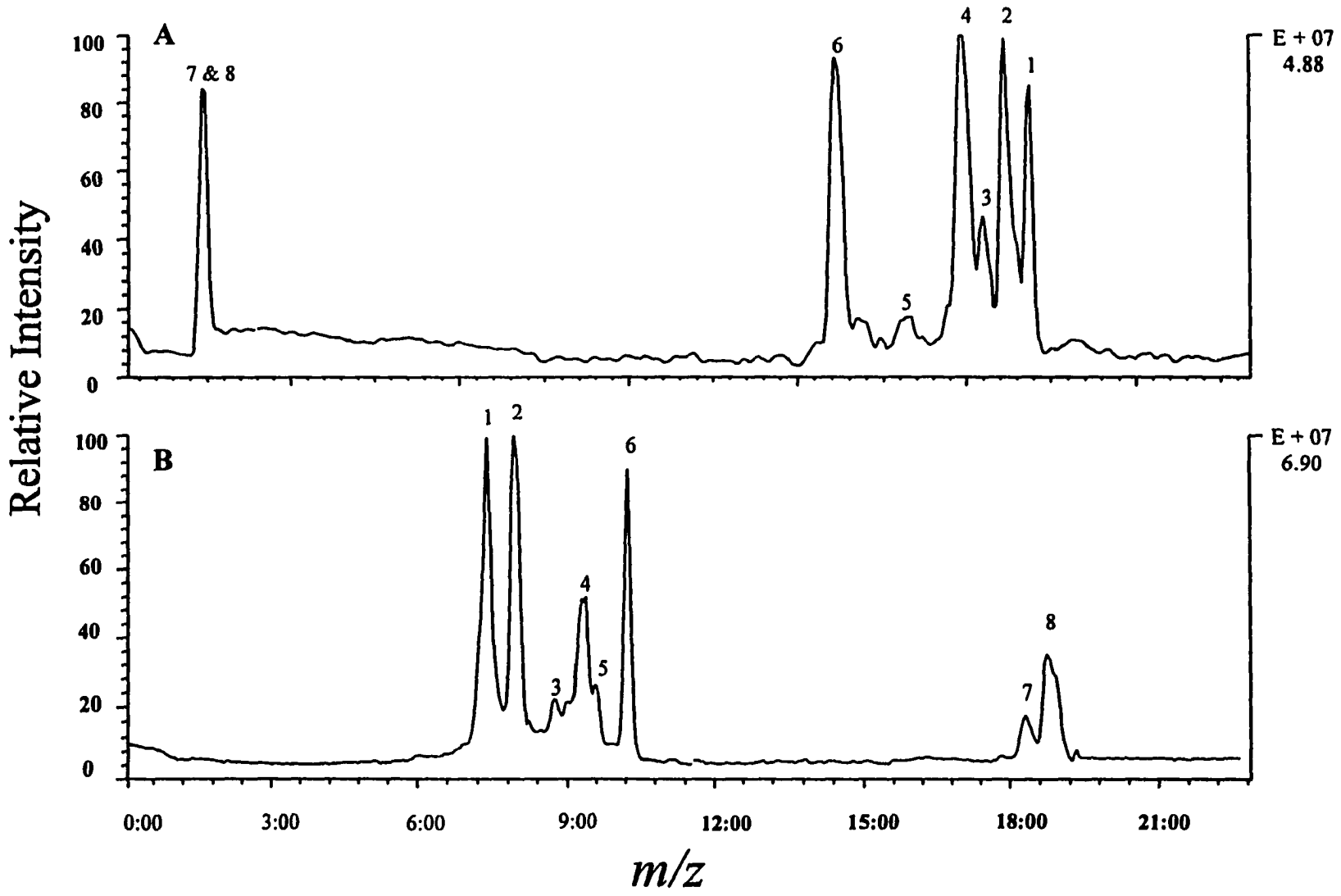
A
B
Relative Intensity
100
80
60
40
20
0
7 & 8
6
4
2
1
3
5
E + 07
4.88
E + 07
6.90
0:00
3:00
6:00
9:00
12:00
15:00
18:00
21:00
m/z

Figure 3

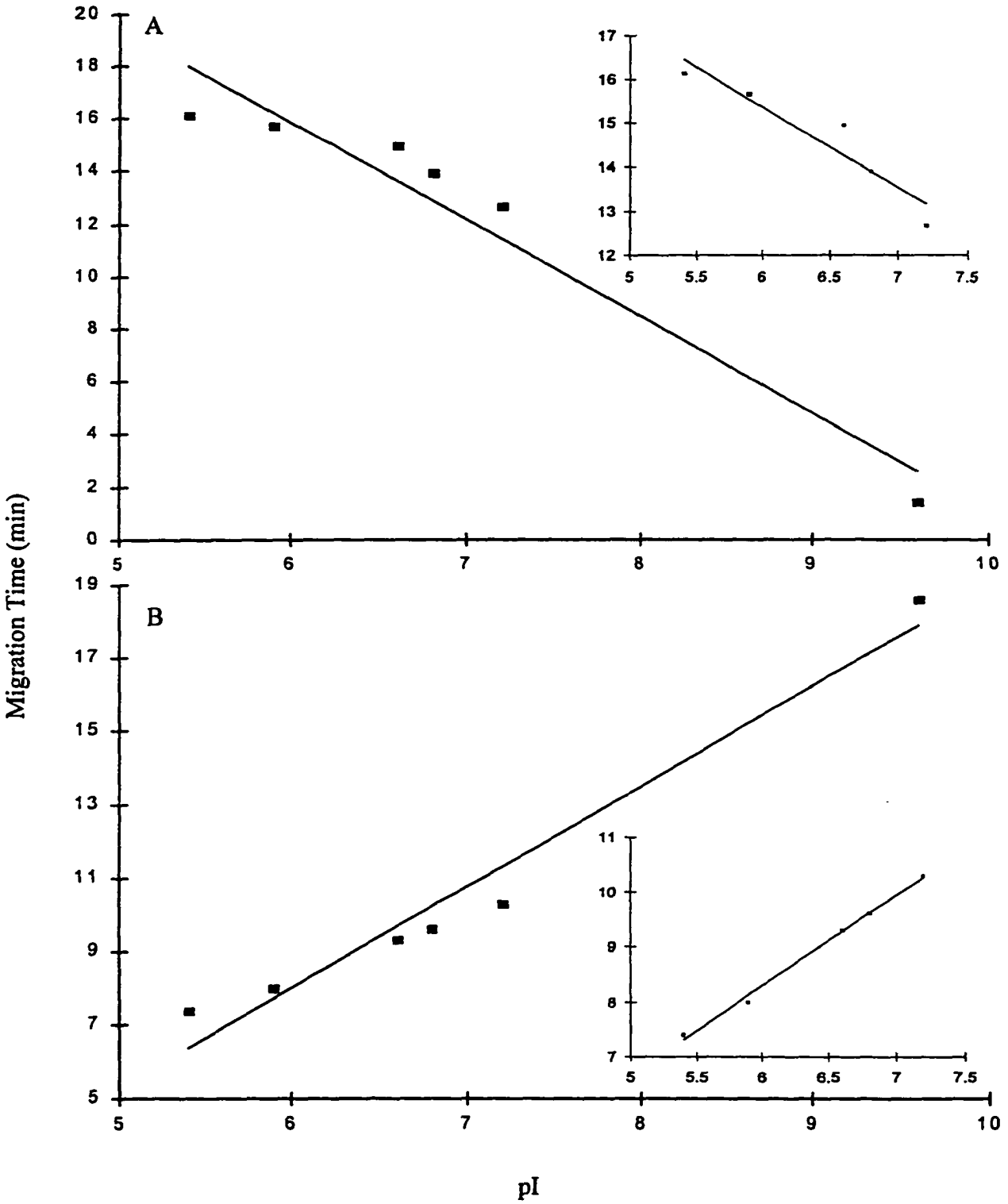
A
B
Migration Time (min)
pI
20
18
16
14
12
10
8
6
4
2
0
19
17
15
13
11
9
7
5
5
6
7
8
9
10
17
16
15
14
13
12
5
5.5
6
6.5
7
7.5
11
10
9
8
7
5
5.5
6
6.5
7
7.5

Figure 4

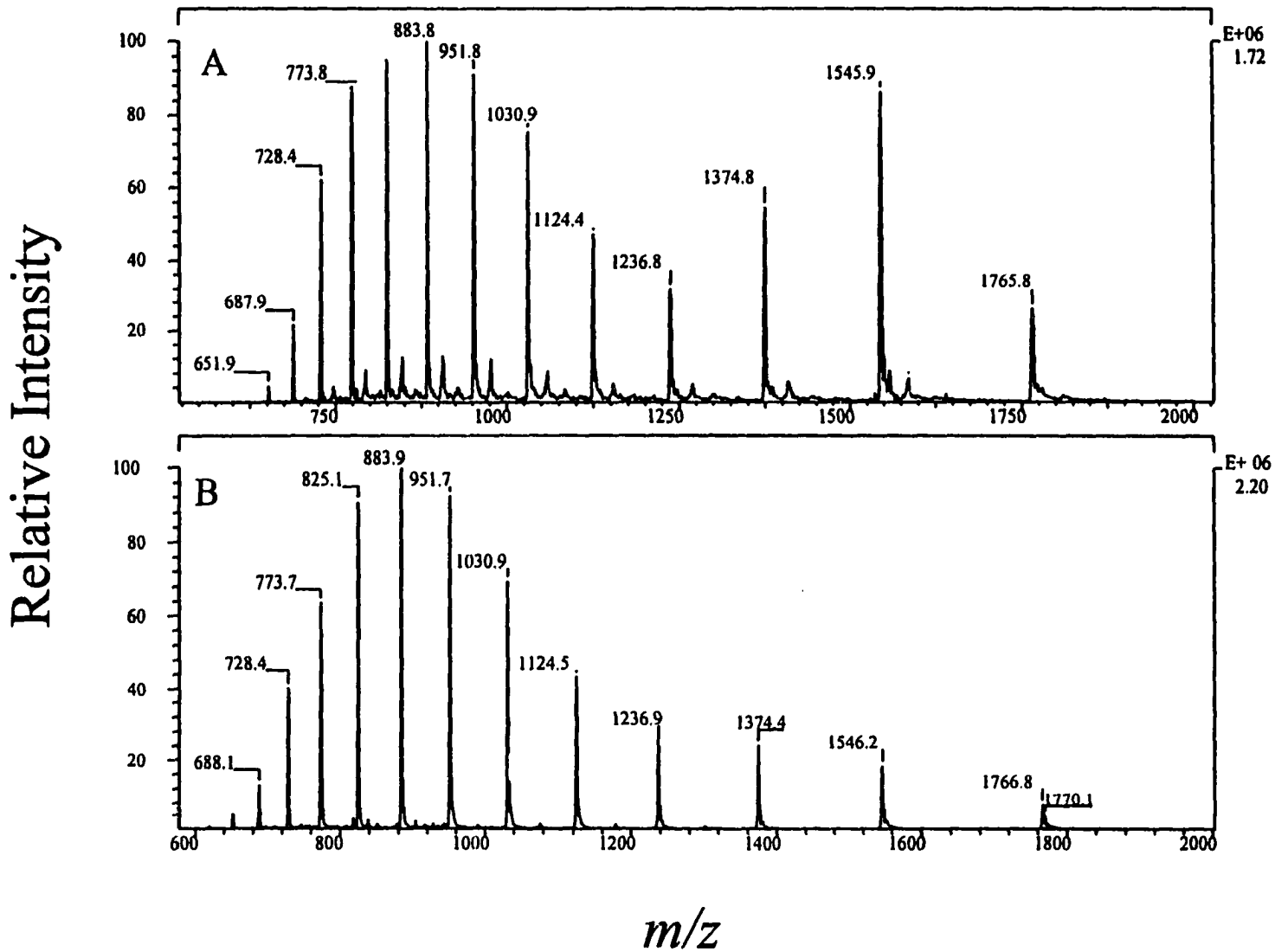
Relative Intensity
A
100
80
60
40
20
883.8
951.8
773.8
1030.9
728.4
1545.9
1374.8
1124.4
1236.8
687.9
1765.8
651.9
E+06
1.72
750
1000
1250
1500
1750
2000
B
100
80
60
40
20
883.9
825.1
951.7
1030.9
773.7
728.4
1124.5
1236.9
1374.4
1546.2
688.1
1766.8
1770.1
E+ 06
2.20
600
800
1000
1200
1400
1600
1800
2000
m/z

Figure 5

CAPILLARY ISOELECTRIC FOCUSING-ELECTROSPRAY IONIZATION FOURIER TRANSFORM ION CYCLOTRON RESONANCE MASS SPECTROMETRY FOR PROTEIN CHARACTERIZATION

Liyu Yang and Cheng S. Lee

Steven A. Hofstadler, Ljijana P. Tolic, and Richard D. Smith

A paper submitted to Anal. Chem.

ABSTRACT

On-line combination of capillary isoelectric focusing (CIEF) with electrospray ionization Fourier transform ion cyclotron resonance mass spectrometry (ESI-FTICRMS) is demonstrated for high resolution analysis of model proteins, human hemoglobin variants, and *Escherichia coli* proteins. The acquisition of high-resolution mass spectra of hemoglobin β chains allows direct identification of hemoglobin variants A and C, which differ in molecular mass by only 1 dalton. The masses of cellular proteins separated in the CIEF capillary are detected using their isotopic envelopes obtained from ESI-FTICRMS. The factors which dictate overall performance of CIEF-ESI-FTICRMS, including duty cycle, mass resolution, scan rate, and sensitivity, are discussed in the context of protein variants and cell lysates analyzed in this study.

INTRODUCTION

Significant advances in Fourier transform ion cyclotron resonance mass spectrometry (FTICRMS) over recent years involved improved interface with external ion sources[1-4], novel ion-manipulation techniques within the trapped ion cell[5-7], and enhanced data processing approaches[8,9]. The advantages of FTICRMS include the ability to simultaneously realize ultrahigh MS resolution, mass measurement accuracy, and high sensitivity. Additionally, FTICRMS provides the capability for high order tandem MS analyses for structural studies due to its nondestructive detection method[10-12].

The combination of electrospray ionization (ESI) with FTICRMS was pioneered by McLafferty and co-workers[13]. The use of ESI-FTICRMS demonstrated extensive potential for the characterization of biopolymers[14] with part-per-million mass accuracy and mass resolving power exceeding 10^6. The ESI-FTICR mass spectra provide the ability to distinguish species with similar masses, and identify adducts, post-translational modifications, and substitutions. Resolution of the 1-dalton spacing of peaks (primarily due to ^{13}C isotopic distributions) allows unambiguous determination of charge (and thus mass) from a single charge state.

The coupling of ESI with FTICRMS requires the transport of the ions between the ion source at atmospheric pressure and the trapped ion cell at pressure below 10^{-9} torr. The ESI-FTICR instrumentation developed by Winger et al.[15] allows rapid manipulation of pressures in the FTICR cell between those that appear optimum for ion trapping and cooling (i.e., $> 10^{-5}$ torr) and those for high resolution detection ($< 10^{-9}$ torr). The features of this instrumentation include five differentially pumped regions, two high-speed shutters to enhance differential pumping in regions close to the ESI source, and an integral cryopump

that extends into the bore of the 7-Tesla superconducting magnet, providing effective pumping speeds of > 10^5 L/s in close proximity to the trapped ion cell.

The off-line combination of capillary zone electrophoresis (CZE) with FTICRMS using matrix-assisted laser desorption/ionization was demonstrated by Wilkins and co-workers[16]. However, the mass resolution was insufficient to resolve the 1-dalton spacing of isotopic constituents within the singly and doubly charged species. In comparison with the ESI process, the multiple charging phenomenon inherent in ESI is particularly advantageous to the FTICRMS detection scheme as resolving power is inversely proportional to *m/z*. Additionally, the use of the ESI process facilitates on-line interfacing of FTICRMS with separation methodologies of HPLC and CZE. Thus, the high pumping speed afforded by the cryopumping arrangement[15] provides the relatively rapid mass spectral acquisition rates and is crucial to on-line integration of ESI-FTICRMS with high speed separation technique such as CZE[17].

Immediately after the first demonstration of on-line CZE-ESI-FTICRMS[17], recent results have suggested that the combination may provide a near ideal approach for microsample analyses owing to the inherent sensitivity of the technique and the enhanced information content available from high-resolution and high-precision mass measurements[18-20]. High-resolution mass spectra (average resolution > 45,000 full width at half-maximum, fwhm) of both the a and b chains of hemoglobin were acquired from the injection of 10 human erythrocytes, which corresponded to 4.5 fmole of hemoglobin[19]. By employing multiple frequency sustained off-resonance irradiation for collisional dissociation of ions in the trapped ion cell[18], a partial amino acid sequence for the a chain of human hemoglobin was obtained from the injection of a population of 75 erythrocytes[20]. High order tandem MS

measurements offered the potential for sensitive peptide finger-printing and the ability to distinguish relatively small variations in biopolymer composition[18].

In this study, on-line combination of capillary isoelectric focusing (CIEF) with ESI-FTICRMS is presented for the characterization of model proteins, human hemoglobin variants, and *Escherichia coli (E. coli)* proteins. In addition to high resolution separation of CIEF, FTICRMS affords high-resolution and high-precision mass measurements for protein analytes. The focusing effect of CIEF further permits analysis of dilute protein samples with a typical concentration factor of 50-100 times. With the full genome of several microorganisms having been sequenced and that of the human genome well underway, the analysis of the corresponding proteomes begins to come into sight[21]. Two-dimensional analysis of cellular proteins using CIEF-ESI-FTICRMS provides a major step towards the comprehensive characterization of complex biological processes such as development, differentiation, and signal transduction in the field of cellular biochemistry.

EXPERIMENTAL SECTION

Materials and Chemicals. Model proteins, including cytochrome *c* (horse heart, pI 9.6), myoglobin (horse heart, pI 7.2 and 6.8), carbonic anhydrase I (human erythrocyte, pI 6.6), and carbonic anhydrase II (bovine erythrocyte, pI 5.9), were purchased from Sigma (St. Louis, MO). Another batch of bovine carbonic anhydrase II obtained from Sigma exhibited a pI of 5.4. Human hemoglobin variants A (pI 7.10), C (pI 7.50), S (pI 7.25), and F (pI 7.15) were acquired from Isolab (Akron, OH).

The *E. coli* cells were suspended in a buffer which consisted of 10 mM Tris-HCl (pH 7.0), 5 mM magnesium chloride, 0.1 mM dithiothreitol, and 10% glycerol. The cells were disrupted by sonication for the release of cellular proteins[22]. After sonication, DNase (Sigma)

was added with a final concentration of 50 μg/ml for the digestion and removal of nucleic acids. The cellular proteins were collected in the supernatant by centrifugation at 2000g for 10 min. The protein solution was then desalted using a microdialysis setup[23]. The total protein concentration of the resulting solution determined by the Bradford method (Bio-Rad kit, Richmond, CA) was around 12 mg/ml.

Fused-silica capillaries with 50 μm i.d. and 192 μm o.d. (Polymicro Technologies, Phoenix, AZ) were coated internally with linear polyacrylamide for the elimination of electroosmotic flow and protein adsorption onto the capillary wall[24]. Carrier ampholytes, pharmalyte 3-10 and 5-8, were obtained from Pharmacia (Uppsala, Sweden). All chemicals, including acetic acid, ammonium acetate, ammonium hydroxide, dithiothreitol, glycerol, magnesium chloride, methanol, phosphoric acid, sodium hydroxide, Tris-HCl were acquired from Fisher (Fair Lawn, NJ). All background electrolytes and sample solutions were prepared using water purified by a Nanopure II system (Branstead, Dubuque, IA) and further filtered with a 0.22 μm membrane (Millipore, Bedford, MA).

Electrospray Ionization-Fourier Transform Ion Cyclotron Resonance Mass Spectrometry. The 7-Tesla ESI-FTICR mass spectrometer utilized in this study was described in detail elsewhere[15]. Briefly, ions were transferred from the ESI source, through a heated metal capillary, to the trapped ion cell by two sets of radio frequency (rf)-only quadrupoles. Background pressure in the trapped ion cell was maintained at 10^{-9} - 10^{-10} torr by a custom cryopumping assembly consisting of two sets of cryobaffels with radiation shields which were maintained at 77 and 14 K, respectively, by closed cycle cryogenic compressors.

The large surface area of the cryobaffels provided pumping speeds in excess of 10^5 L/s, permitting rapid transitions between the high-efficiency, high-pressure ion accumulation (> 10^{-5} torr) and the low-pressure detection events (< 10^{-9} torr). The spectrometer vacuum system was also equipped with a pair of electromechanical shutters which blocked the conductance limits during non-injection events, aiding differential pumping and improving the vacuum quality. The heated desolvation capillary in the ESI source was held at 180 ^{0}C. Tuning and calibration of the mass spectrometer were established using an acetic acid solution (methanol/water/acetic acid, 50:49:1 v/v/v) containing myoglobin and a small peptide of methionine-arginine-phenylalanine-alanine.

Capillary Isoelectric Focusing-Electrospray Ionization-Fourier Transform Ion Cyclotron Resonance Mass Spectrometry. The CIEF apparatus was constructed in-house using a CZE 1000R high-voltage (HV) power supply (Spellman High-Voltage Electronics, Plainview, NY). All on-line CIEF-ESI-FTICR measurements were performed using a coaxial liquid sheath flow configuration[25] in a standard Finnigan (San Jose, CA) MAT ESI source. A 30-cm-long coated capillary was mounted within the electrospray probe. The capillary was filled with a solution containing 0.5% pharmalyte and protein sample. The outlet reservoir, containing 20 mM sodium hydroxide as the catholyte, was located inside the electrospray housing during the focusing step. The inlet reservoir, containing 20 mM phosphoric acid as the anolyte, was kept outside at the same height as the outlet reservoir. Focusing was performed at a 15 kV constant voltage for approximately 10 min.

Once the focusing was complete, the electric potential was turned off, and the outlet reservoir was removed. The capillary tip was fixed about 0.5 mm outside the electrospray needle. A sheath liquid composed of 50% methanol, 49% water, and 1% acetic acid (v/v/v) at

pH 2.6 was delivered at a flow rate of 1 μl/min using a Harvard Apparatus 22 syringe pump (South Natick, MA). During the cathodic mobilization step, two HV power supplies were used for delivering the electric potentials of 19 kV and 4 kV to the inlet electrode and electrospray needle, respectively. To speed up protein mobilization and minimize the formation of moving ionic boundary inside the CIEF capillary[26,27], gravity mobilization was combined with cathodic mobilization by raising the inlet reservoir 8 cm above the electrospray needle.

A typical CIEF-ESI-FTICRMS pulse sequence consisted of four events[20]: 0.4 s ion injection/accumulation, 1 s ion cooling/pumpdown, 835 ms rf excitation and ion detection, and 5 ms quench, resulting in a total scan duration of 2.24 s. A "quench" event was employed at the end of the pulse sequence to eject ions from the cell prior to the next measurement. Broad-band swept excitation over a 500 kHz bandwidth with a 85 Hz/ms sweep rate was followed by detection of 256K data points at 313 kHz (low m/z = 700), resulting in a 835 ms time domain signal. Trap potentials of 4 and 5 V were applied during ion injection and accumulation, respectively. Trap potentials were maintained at 5 and 0.5 V during pump down and ion excitation/detection, respectively. Electronics and all aspects of data acquisition and processing were controlled by an Odyssey (Extrel FTMS, Madison, WI) data station running Odyssey version 2.0 software.

RESULTS AND DISCUSSION

In CIEF, the coated fused-silica capillary contained not only carrier ampholytes for the creation of a pH gradient but also proteins[24,28,29]. When an electric potential was applied, the negatively charged acidic ampholytes migrated toward the anode and decreased the pH at the anodic section, while the positively charged basic ampholytes migrated toward the cathode

and increased the pH at the cathodic section. Protein analytes as amphoteric macromolecules also focused at their isoelectric points (pIs) in narrow zones in the same way as the individual ampholytes.

Theoretically, there was no movement in the coated capillary when the focusing was complete. Thus, the entire pH gradient, along with the focused protein zones, had to be mobilized into the mass spectrometer. To initiate cathodic mobilization, the acetate ions used in the sheath liquid competed with hydroxide ions for electromigration into the capillary. Since fewer hydroxide ions entered the capillary, the pH gradient drifted downward. Protein analytes previously focused at their pI values became positively charged and migrated toward the cathodic end. Additionally, a gravity-induced hydrodynamic flow was introduced by raising the inlet reservoir.

Thus, basic protein of cytochrome *c* migrated ahead of acidic proteins such as carbonic anhydrase I and II in a 0.5% pharmalyte 3-10 solution during the CIEF-ESI-FTICRMS analysis (Fig. 1). The reconstructed ion electropherogram of the protein mixture with a final concentration of 0.1 mg/ml for each protein analyte was obtained from the ions between *m/z* 700 and *m/z* 3000 at a scan rate of 2.24 s/scan. All protein peaks were directly identified on the basis of mass spectra of protein analytes taken from the average scans under the peaks. High-resolution mass spectra of cytochrome c, myoglobin, and carbonic anhydrase II are presented in Fig. 2. This acquisition rate compares favorably with that employed for quadrupole systems over a similar *m/z* range, but provides mass spectrometric resolution for each species, in excess of 45,000 (fwhm), much higher than possible with any alternative analyzer.

The pumping system used in this study facilitated rapid pressure changes, covering the pressure range required in about 1 s. Still, the "pumpdown" event accounted for 45% of the experimental duration while the ion injection interval accounted for less than 18% of the experimental time. Thus, the ionization duty cycle was relatively poor with the single cell configuration. To provide both improved ionization duty cycle and more rapid scan speed, alternative configurations include the incorporation of two trapped ion cells, one for high pressure ion accumulation and one for low pressure ion detection. Similarly, accumulation of ions in an external multipole (e.g., quadrupole) prior to injection into the trap and avoiding the need for introduction of a gas and thus pumpdown, has recently been demonstrated and may be useful for interfacing with on-line separations[30,31].

To investigate the resolving power of CIEF-ESI-FTICRMS, a mixture of human hemoglobin variants A, C, S, and F was prepared in a 0.5% pharmalyte 5-8 solution with a total concentration of 0.1 mg/ml. The reconstructed ion electropherogram of hemoglobin variants was obtained from the ions between *m/z* 700 and *m/z* 3000 at a scan rate of 2.24 s/scan (Fig. 3). Hemoglobin variants F and A, the wild type fetal and adult hemoglobins, were baseline separated and resolved in CIEF-ESI-FTICRMS with a pI difference of 0.05 pH units.

Hemoglobin A is a tetramer of two α globin and two β globin chains, each carrying a heme moiety. An example of the mass spectra obtained from the average scans under the peaks of Fig. 3 is presented in Fig. 4A for hemoglobin A. Two separate ESI envelopes with different ion intensities were observed for the α and β chains. The presence of two separate electrospray envelopes indicated the dissociation of hemoglobin A tetramer due to the heating and/or collisional excitation in the interface region. On the other hand, intact heterodimeric

and tetrameric forms of hemoglobin A could be obtained in the electrospray process by adjusting the atmosphere-vacuum interface conditions[32]. Differences in the relative stabilities of tetrameric proteins, including concanavalin A and hemoglobin formed from the know solution structures, were qualitatively consistent with the gas-phase stability observed in the electrospray process.

In comparison with normal hemoglobin A, the substitution of glutamic acid in position 6 by valine in the β chain of hemoglobin S results in sickle-cell anemia. The substitution of glutamic acid in position 6 by lysine in the β chain of hemoglobin C changes the pI by 0.5 pH units (Fig. 3). At the same time, the change in molecular mass is less than 1 dalton. In our previous study of human hemoglobins[27], the elution of hemoglobin variants C and A was monitored using the same *m/z* ion of 1133 in the selected ion monitoring mode due to the limited mass resolution in a triple quadrupole mass spectrometer. The identification of hemoglobin variants C and A, however, was established by their elution order in the CIEF separation. In contrast, the high mass resolution of ESI-FTICRMS was illustrated using the resolution of the isotopes within the +15 charge state of the β chains (Fig. 5) and provided unambiguous identification of hemoglobin variants C and A.

In this study, the mass accuracy of 1-5 ppm between the expected and the measured molecular masses was routinely obtained for all CIEF-ESI-FTICRMS measurements. The FTICRMS technique has long been recognized for high mass-precision mass measurement even in the absence of calibrant ions. Early experiments by Henry et al.[13] demonstrated that the isotopically resolved peaks of myoglobin exhibited an error of only 1 ppm. In later work with an improved data system, the isotopically resolved peaks yielded mass accuracies with

subpart per million errors[33]. Still later, ESI/FTICR mass accuracies were reduced below the 100 ppb level in the assignment of fragment ions of ubiquitin[34].

A solution containing 0.5% carrier ampholytes (pharmalyte 5-8 and pharmalyte 3-10 at a ratio of 3:1) and *E. coli* proteins was used for all CIEF-ESI-FTICR measurements. The blending of pharmalyte not only gave an effective separation range between pH 3.5 and 9.5, but also enhanced separation resolution and pH gradient in the range of 5-8. A total of 7 mg (12 mg/ml x 0.59 μl of capillary volume) of *E. coli* proteins was loaded in the CIEF capillary. The reconstructed ion electropherogram is shown in Fig. 6A and reveals various protein zones with different pI values. The mass spectra obtained from the average scans under the peaks 2, 9, and 12 are summarized in Fig. 6B-D, respectively.

Resolution of ^{13}C isotopic distributions obtained from ESI-FTICRMS allowed unambiguous determination of charge and protein mass from a single charge state (Fig. 6B-D). Due to the limitation in the size of data file for the analysis of *E. coli* proteins, the number of data points in each scan and the detection interval were decreased to 128K and 400 ms, respectively. Thus, the mass resolution was reduced to 22,000 (fwhm) and provided the isotopic resolution for proteins up to 16,000 daltons. The isotopic resolution facilitated the direct and rapid mass determination without reliance upon a distribution of charge states and the need for a deconvolution program. In fact, the limitations of various computer softwares for the deconvolution of protein masses in the complex ESI mass spectra remain to be investigated. For example, the upper limit for the number of protein electrospray envelopes which can be reliably and confidently deconvoluted has to be addressed.

The advantages of ESI-FTICRMS in mass resolution and detection sensitivity for the analysis of complex protein mixtures were illustrated using a mass spectrum taken from the

average scans under the peak 6 (Fig. 7). The mass spectrum displayed a major protein electrospray envelope with a deconvoluted mass of 28,825 daltons. Additionally, one minor protein with molecular mass of 9,129 daltons was directly identified on the basis of its isotopic distribution. In the absence of high-mass resolution routinely obtained from ESI-FTICRMS, this minor protein would be easily missed by quadrupole analyzers equipped with any electrospray deconvolution software. It is known that the potential ion suppression effect of highly charged or dominant proteins against other protein analytes coeluted from the CIEF capillary affects the qualitative and quantitative determination of protein molecules in ESIMS.

By analyzing all protein zones in the reconstructed ion electropherogram, a total of 112 protein molecules with molecular mass less than 16,000 daltons were measured using their isotopic distributions. As mass resolving power is directly proportional to the length of the detection interval and inversely proportional to *m/z*, achieving high resolution, at very high *m/z* in particular, may require acquisition of a relatively long transient signal during the detection period. For example, Lamoree et al.[35] has produced the FTICR mass spectra of small proteins with resolving power in excess of 2.8×10^6. However, this resolving power is not without a price as long detection intervals (> 2 min), very large data files (> 8 million data points), and substantially increased processing times are required.

The reduction elution speed method introduced by Goodlett et al.[31] provides an approach toward circumventing what at first glance appears to be an inherent incompatibility between high resolution CIEF separation and high resolution FTICRMS detection. As demonstrated in CZE-ESIMS, the method involves only stepwise changes in the electric field strength and is thus readily implemented. Prior to elution of the first analyte peak, the

electric field strength is decreased, resulting in slower migration velocities and wider elution profiles. The reduction elution speed method thus facilitates the acquisition of more, or longer, MS scans.

Additionally, the mass resolving power is directly proportional to magnetic field strength. For example, the 7-Tesla instrument employed in this study yielded a mass resolving power of 45,000 from an 835 ms transient. A 12-Tesla instrument is expected to yield a resolution of 77,000 from an 835 ms transient of the same protein species. Furthermore, FTICR spectrometers based on higher magnetic field strengths will require shorter detection intervals for achieving the same mass resolution. A 12-Tesla instrument should require only 487 ms to obtain a resolution of 45,000 for the same protein species.

Future work in the application of CIEF-ESI-FTICRMS for the analysis of cell lysates is based on the development of a 12-Tesla FTICR system. Ultrahigh mass resolution for large biopolymers is particularly attractive for applications involving the identification of protein variants, post-translational modifications, and unambiguous detection of adducts. Resolution of the isotopic envelope is essential for collisionally activated dissociation (CAD) studies of large mutiply-charged molecules, providing the only broadly applicable method of charge state determination for the CAD products. The great potentials of combining high resolution/preconcentration CIEF separation with ultrahigh resolution, mass measurement accuracy, and high sensitivity of ESI-FTICRMS are waiting to be explored and employed for various biomedical, biopharmaceutical, and environmental applications.

ACKNOWLEDGEMENT

The authors wish to thank The authors wish to thank Ms. Leila Mosavi and Dr. James Bruce for providing *E. coli* cells and helpful discussion in FTICRMS, respectively. The authors also wish to acknowledge the Microanalytical Instrumentation Center of the Institute for Physical Research and Technology at Iowa State University, the U.S. Department of Energy, and Laboratory Directed Research and Development of Pacific Northwest Laboratory for support of this research. Pacific Northwest Laboratory is operated by Battelle Memorial Institute for the U.S. Department of Energy, through Contract No. DE-AC06-76RLO 1830. C.S.L. is a National Science Foundation Young Investigator (BCS-9258652).

REFERENCES

1. Lebrilla, C. B.; Amster, I. J.; McIver, R. T. *Int. J. Mass Spectrom. Ion Proc.* **1989,** 87, R7.
2. Kofel, P.; McMahon, T. B. *Int. J. Mass Spectrom. Ion Proc.* **1990,** 98, 1.
3. Beu, S. C.; Laude, D. A. *Int. J. Mass Spectrom. Ion Proc.* **1991,** 104, 109.
4. Hofstadler, S. A.; Schmidt, E.; Guan, Z.; Laude, D. A. *J. Am. Soc. Mass Spectrom.* **1993,** 4, 168.
5. Gauthier, J. W.; Trautman, T. R.; Jacobson, D. B. *Anal. Chim. Acta* **1991,** 246, 211.
6. Guan, S. H.; Kim, H. S.; Marshall, A. G.; Wahl, M. C.; Wood, T. D.; Xiang, X. Z. *Chem. Revs.* **1994,** 94, 2161.
7. Bruce, J. E.; Anderson, G. A.; Smith, R. D. *Anal. Chem.* **1996,** 68, 534.

8. Bruce, J. E.; Anderson, G. A.; Hofstadler, S. A.; Winger, B. E.; Smith, R. D. *Rapid Comm. Mass Spectrom.* **1993,** 7, 700.

9. Guan, S. H.; Wahl, M. C.; Marshall, A. G. *Anal. Chem.* **1993,** 65, 3647.

10. Marshall, A. G.; Grosshans, P. B. *Anal. Chem.* **1991,** 63, A215.

11. Koster, C.; Kahr, M. S.; Castoro, J. A.; Wilkins, C. L. *Mass Spectrom. Rev.* **1992,** 11, 495.

12. Buchanan, M. V.; Hettjch, R. L. *Anal. Chem.* **1993,** 65, A245.

13. Henry, K. D.; Quinn, J. P.; McLafferty, F. W. *J. Am. Chem. Soc.* **1991,** 113, 5447.

14. Bue, S. C.; Senko, M. W.; Quinn, J. P.; McLafferty, F. W. *J. Am. Soc. Mass Spectrom.* **1993,** 4, 190.

15. Winger, B. E.; Hofstadler, S. A.; Bruce, J. E.; Udseth, S. R.; Smith, R. D. *J. Am. Soc. Mass Spectrom.* **1993,** 4, 566.

16. Castoro, J. A.; Chiu, R. W.; Monnig, C. A.; Wilkins, C. L. *J. Am. Chem. Soc.* **1992,** 114, 7571.

17. Hofstadler, S. A.; Wahl, J. H.; Bruce, J. E.; Smith, R. D. *J. Am. Chem. Soc.* **1993,** 115, 6983.

18. Hofstadler, S. A.; Wahl, J. H.; Bakhtiar, R.; Anderson, G. A.; Bruce, J. E.; Smith, R. D. *J. Am. Soc. Mass Spectrom.* **1994,** 5, 894.

19. Hofstadler, S. A.; Swanek, F. D.; Gale, D. C.; Ewing, A. G.; Smith, R. D. *Anal. Chem.* **1995,** 67, 1477.

20. Hofstadler, S. A.; Severs, J. C.; Smith, R. D.; Swanek, F. D.; Ewing, A. G. *J. High Resol. Chromatogr.* **1996,** 19, 617.

21. Kahn, P. *Science* **1995,** 270, 369.

22. Schleif, R. F.; Wensink, P. C. *Practical Methods in Molecular Biology;* Springer-Verlag: New York, 1981; Chapter 1.

23. Liu, C.; Wu, Q.; Harms, A. C.; Smith, R. D. *Anal. Chem.* **1996,** 68, 3295.

24. Kilar, F.; Hjerten, S. *Electrophoresis* **1989,** 10, 23.

25. Smith, R. D.; Wahl, J. H.; Goodlett, D. R.; Hofstadler, S. A. *Anal. Chem.* **1993,** 65, 574A.

26. Foret, F.; Thompson, T. J.; Vouros, P.; Karger, B. L.; Gebauer, P.; Bocek, P. *Anal. Chem.* **1994,** 66, 4450.

27. Tang, Q.; Harrata, A. K.; Lee, C. S. *Anal. Chem.* **1996,** 68, 2482.

28. Hjerten, S.; Zhu, M. D. *J. Chromatogr.* **1985,** 346, 265.

29. Hjerten, S.; Liao, J. L.; Yao, J. *J. Chromatogr.* **1987,** 387, 127.

30. Burnier, R. C.; Cody, R. B.; Freiser, B. S. *J. Am. Chem. Soc.* **1982,** 104, 7436.

31. Goodlett, D. R.; Wahl, J. H.; Udseth, H. R.; Smith, R. D. *J. Microcol. Sep.* **1993,** 5, 57.

32. Light-Wahl, K. J.; Schwartz, B. L.; Smith, R. D. *J. Am. Chem. Soc.* **1994,** 116, 5271.

33. Beu, S. C.; Senko, M. W.; Quinn, J. P.; Wampler, F. M.; McLafferty, F. W. *J. Am. Soc. Mass Spectrom.* **1993,** 4, 557.

34. Senko, M. W.; Speir, J. P.; McLafferty, F. W. *Anal. Chem.* **1994,** 66, 2801.

35. Lamoree, M. H.; Reinhoud, N. J.; Tjaden, U. R.; Nissen, W. M. A.; van der Greef, J. *J. Biol. Mass Spectrom.* **1994,** 23, 339.

FIGURE LEGENDS

Fig. 1 CIEF-ESI-FTICRMS electropherogram of a mixture of model proteins: (1) cytochrome *c* (pI 9.6); (2) and (3), myoglobin (pI 6.8 and 7.2); (4) and (5), carbonic anhydrase I (pI 6.6); (6) carbonic anhydrase II (pI 5.9); (7) carbonic anhydrase II (pI 5.4).

Fig. 2 Positive ESI mass spectra of (A) cytochrome c, (B) myoglobin, and (C) carbonic anhydrase II (pI 5.4) taken from the average scans under the peaks shown in Fig. 1.

Fig. 3 CIEF-ESI-FTICRMS electropherogram of a mixture of human hemoglobin variants C, S, F, and A.

Fig. 4 Positive ESI mass spectra of (A) hemoglobin A and (B) hemoglobin S taken from the average scans under the peaks shown in Fig. 3.

Fig. 5 High resolution FTICR spectra of the +15 charge state of the β chains in (A) hemoglobin A and (B) hemoglobin C. The spectra were taken from the average scans under the peaks shown in Fig. 3.

Fig. 6 (A) CIEF-ESI-FTICRMS electropherogram of *E. coli* proteins. The positive ESI mass spectra were taken from the average scans under the peaks 2 (B), 9 (C), and 12 (D).

Fig. 7 The positive ESI mass spectrum taken from the average scans under the peaks show in Fig. 6A.

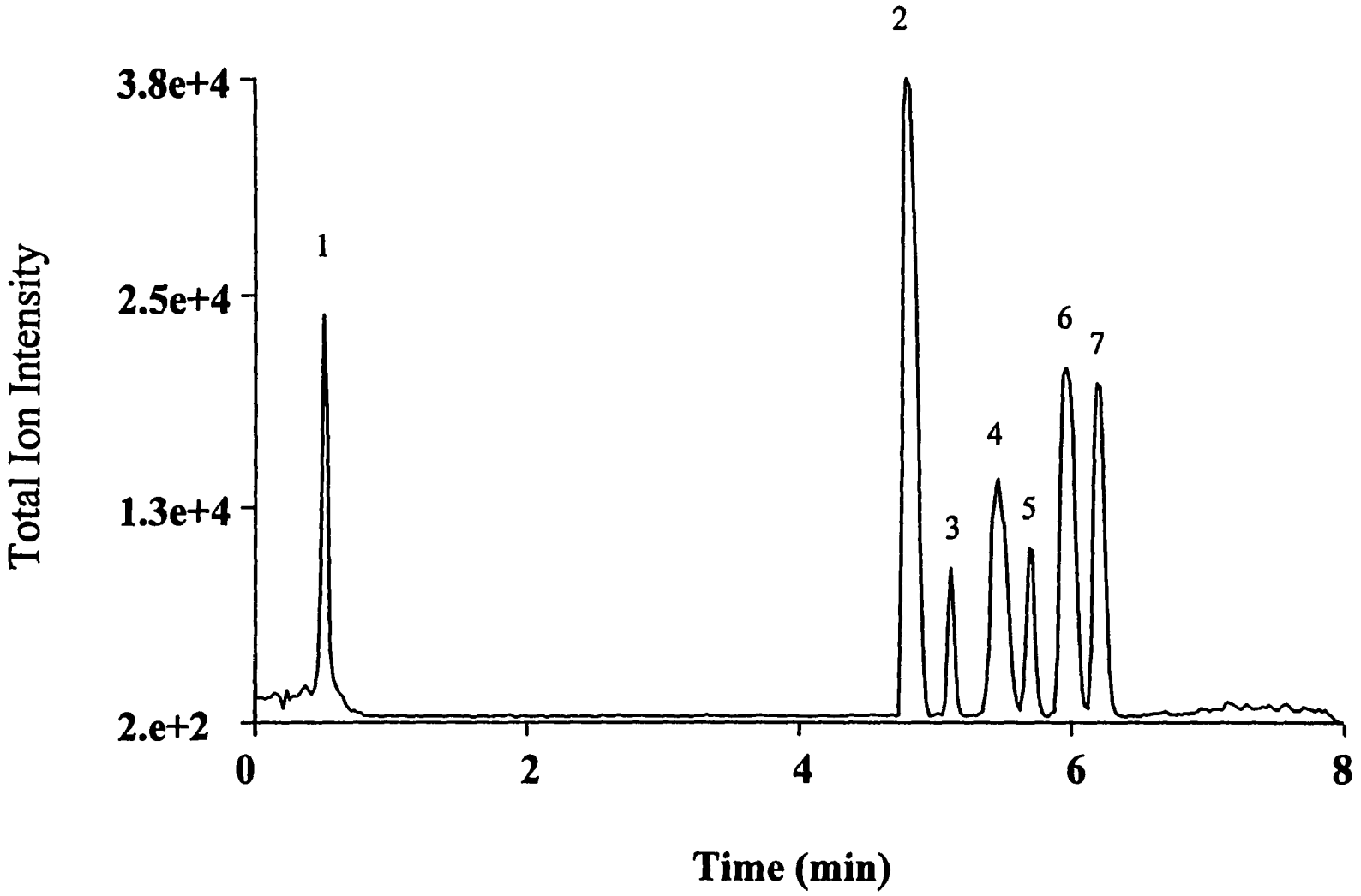
Total Ion Intensity
3.8e+4
2.5e+4
1.3e+4
2.e+2
0
2
4
6
8
Time (min)
1
2
3
4
5
6
7

Figure 1

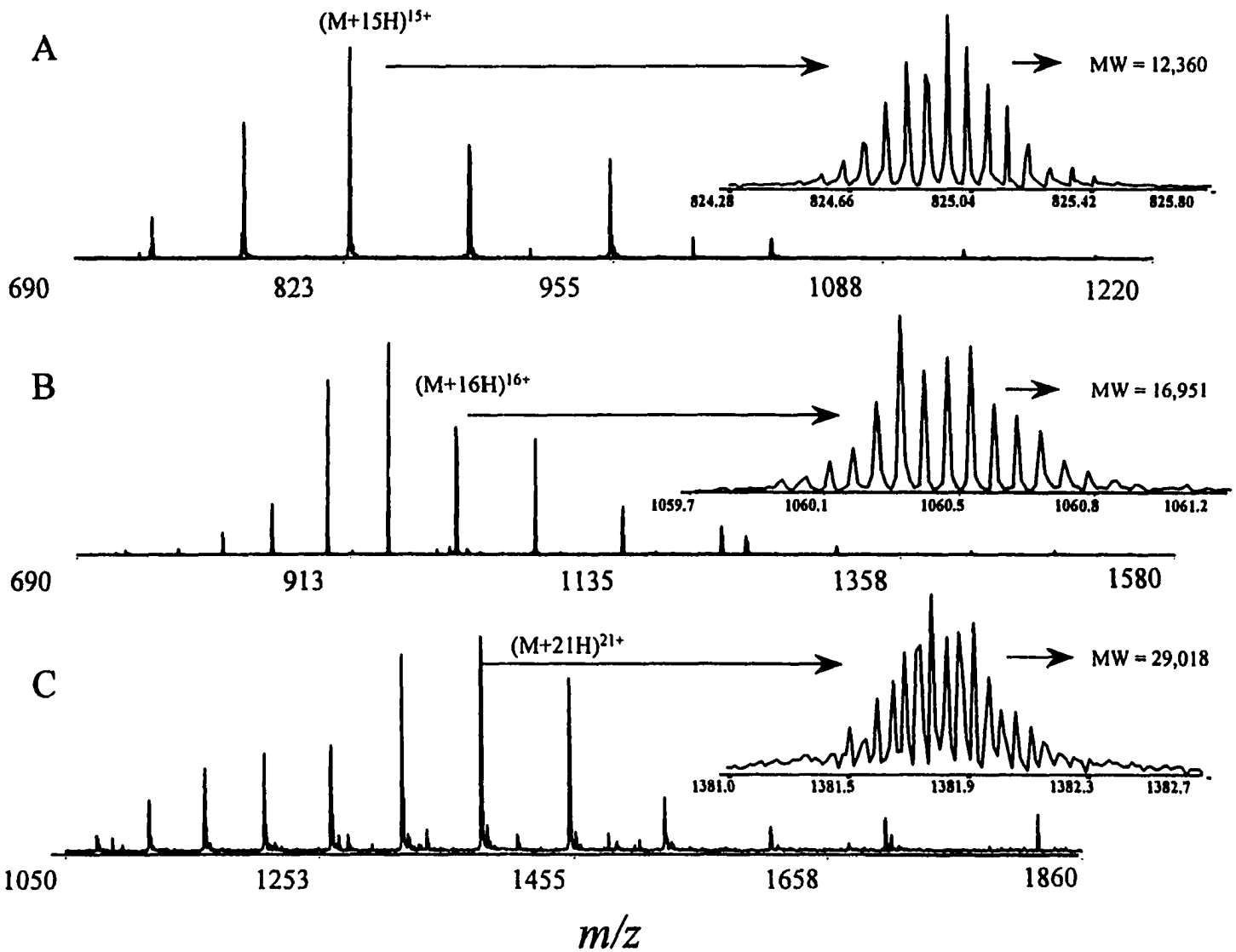
A
(M+15H)15+
MW = 12,360
824.28
824.66
825.04
825.42
825.80
690
823
955
1088
1220
B
(M+16H)16+
MW = 16,951
1059.7
1060.1
1060.5
1060.8
1061.2
690
913
1135
1358
1580
C
(M+21H)21+
MW = 29,018
1381.0
1381.5
1381.9
1382.3
1382.7
1050
1253
1455
1658
1860
m/z

Figure 2

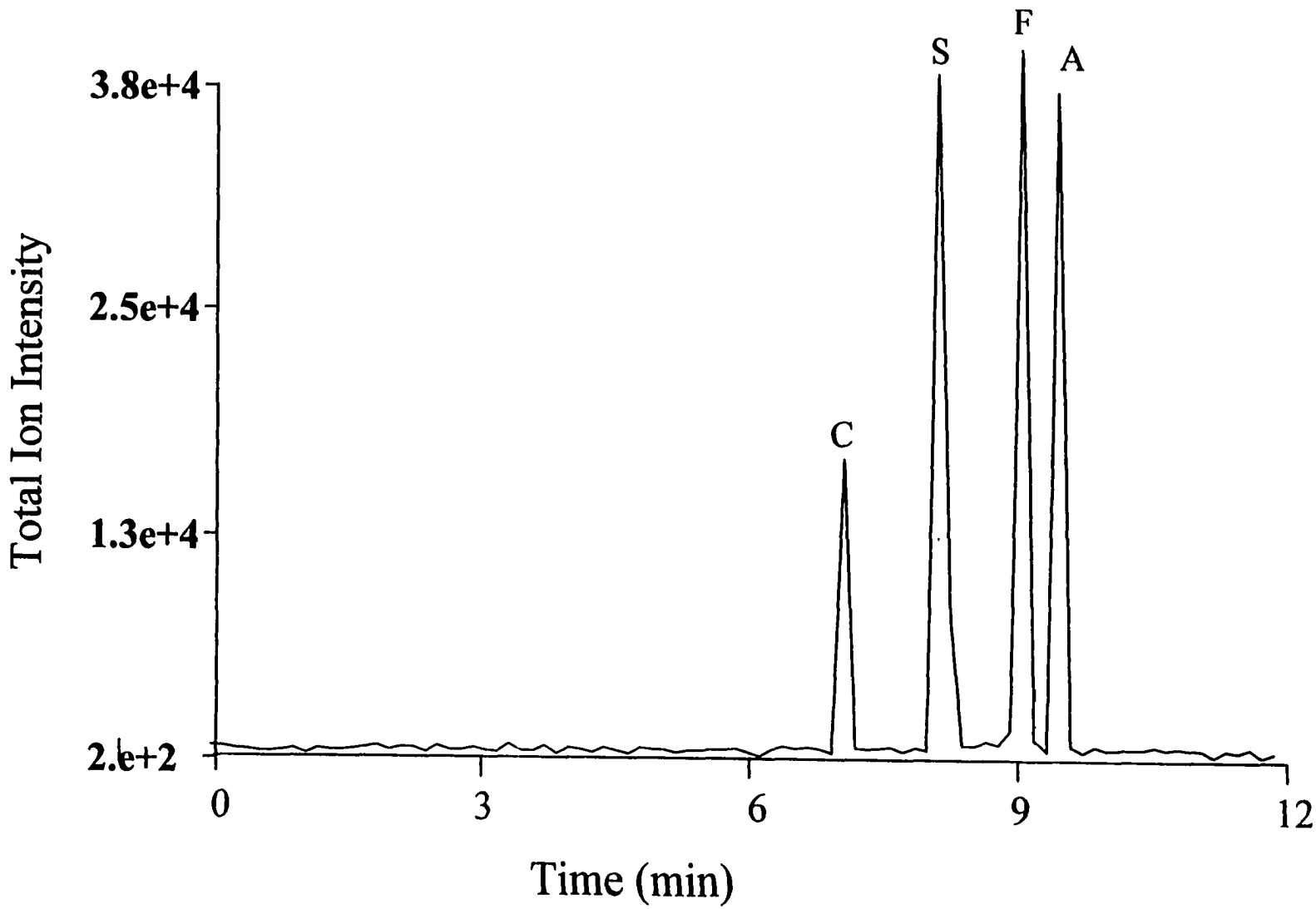

Figure 3

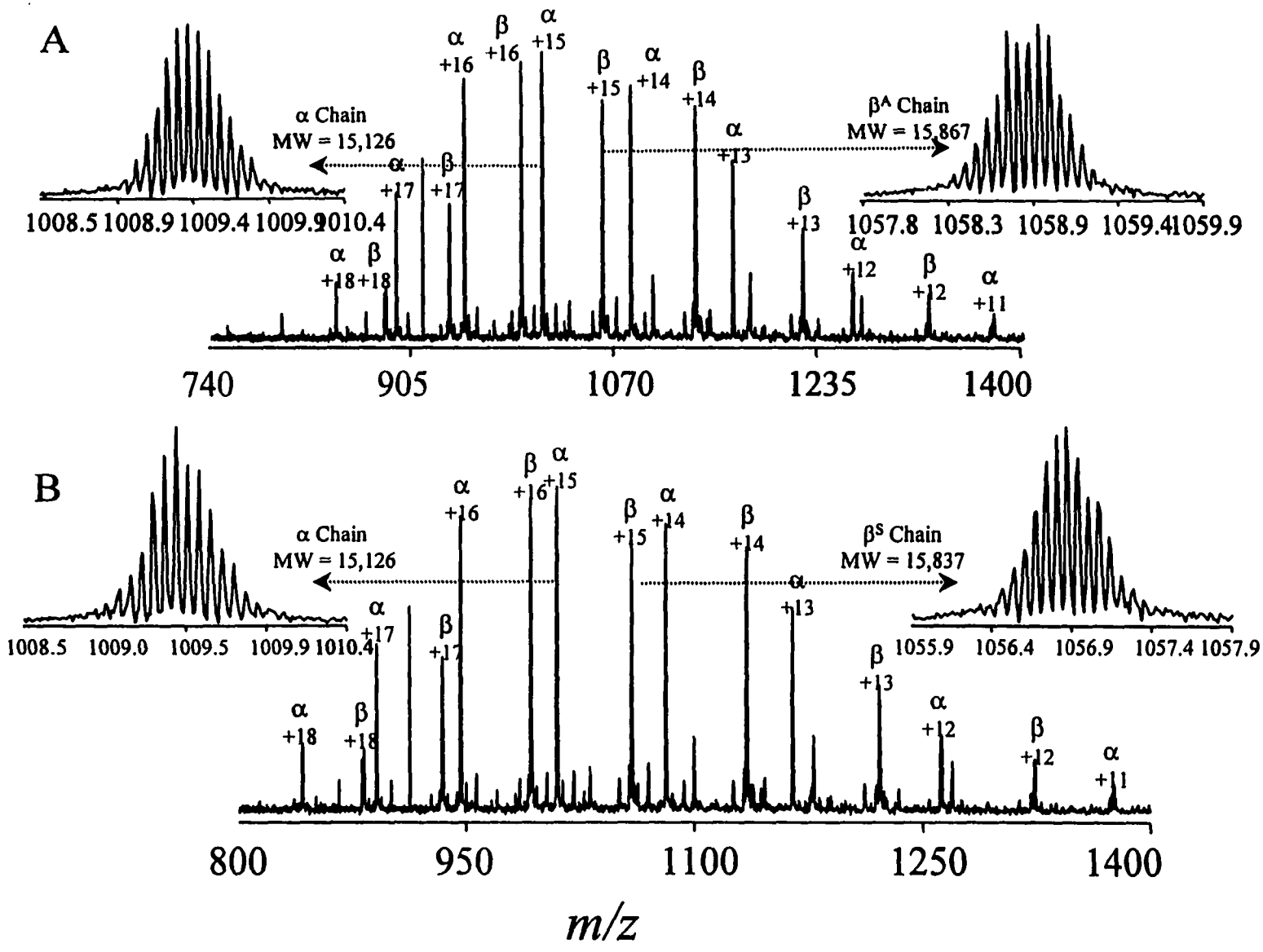
A
α Chain
MW = 15,126
βA Chain
MW = 15,867
1008.5 1008.9 1009.4 1009.9 1010.4
1057.8 1058.3 1058.9 1059.4 1059.9
740
905
1070
1235
1400
B
α Chain
MW = 15,126
βS Chain
MW = 15,837
1008.5 1009.0 1009.5 1009.9 1010.4
1055.9 1056.4 1056.9 1057.4 1057.9
800
950
1100
1250
1400
m/z

Figure 4

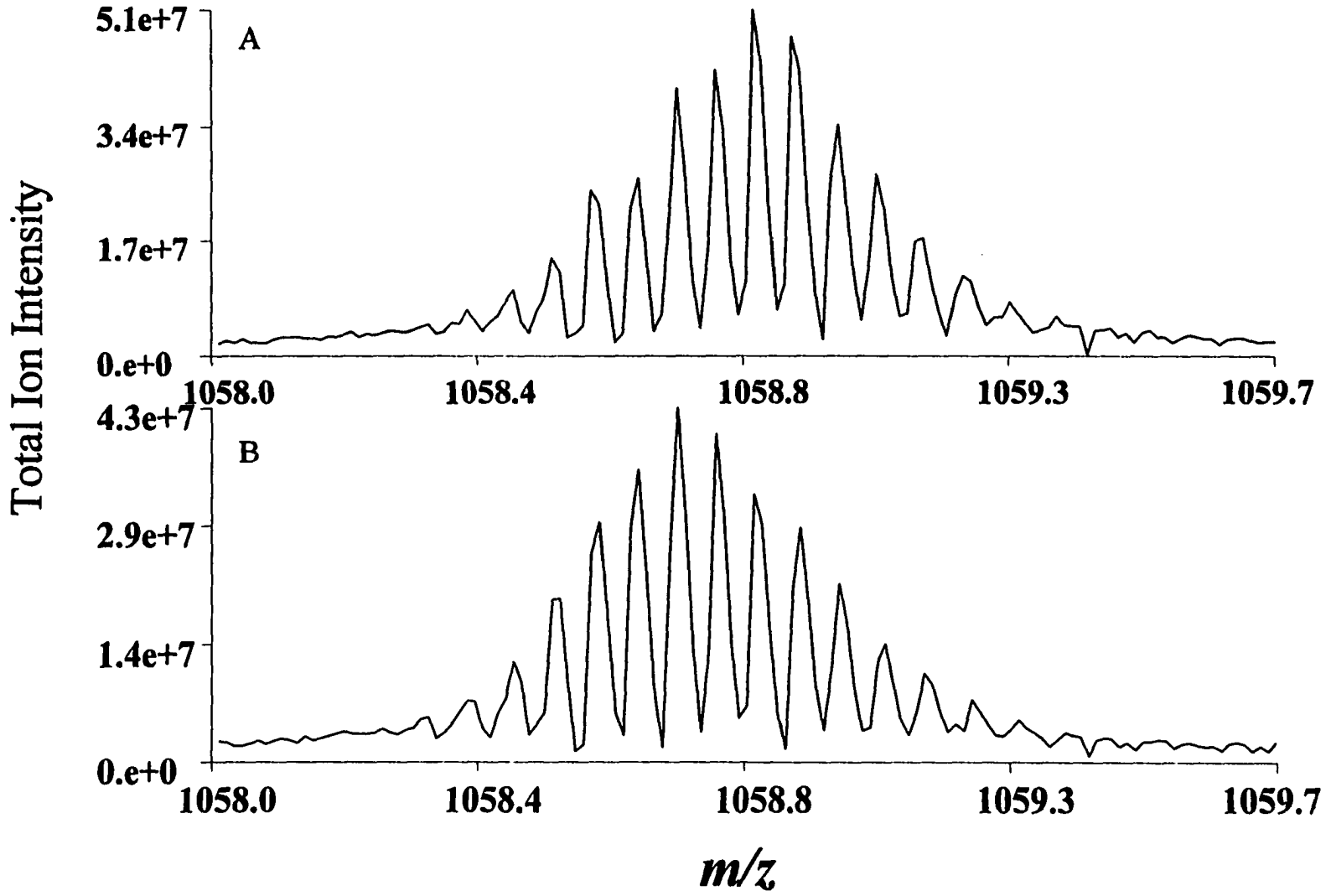
Total Ion Intensity
5.1e+7
3.4e+7
1.7e+7
0.e+0
A
1058.0
1058.4
1058.8
1059.3
1059.7
4.3e+7
2.9e+7
1.4e+7
0.e+0
B
1058.0
1058.4
1058.8
1059.3
1059.7
m/z

Figure 5

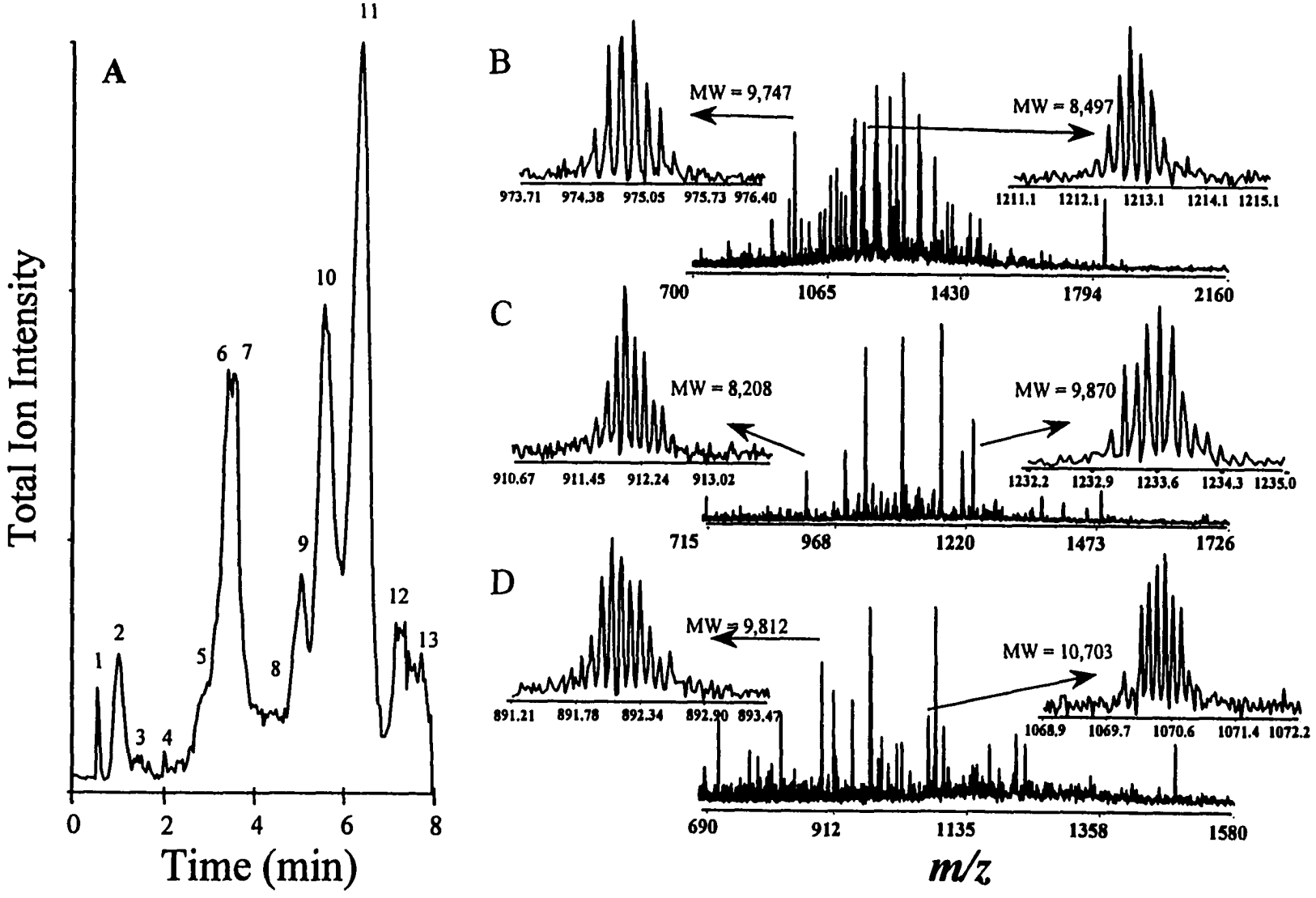
A
Total Ion Intensity
Time (min)
0
2
4
6
8
1
2
3
4
5
6
7
8
9
10
11
12
13
B
MW = 9,747
MW = 8,497
973.71 974.38 975.05 975.73 976.40
1211.1 1212.1 1213.1 1214.1 1215.1
700 1065 1430 1794 2160
C
MW = 8,208
MW = 9,870
910.67 911.45 912.24 913.02
1232.2 1232.9 1233.6 1234.3 1235.0
715 968 1220 1473 1726
D
MW = 9,812
MW = 10,703
891.21 891.78 892.34 892.90 893.47
1068.9 1069.7 1070.6 1071.4 1072.2
690 912 1135 1358 1580
m/z

Figure 6

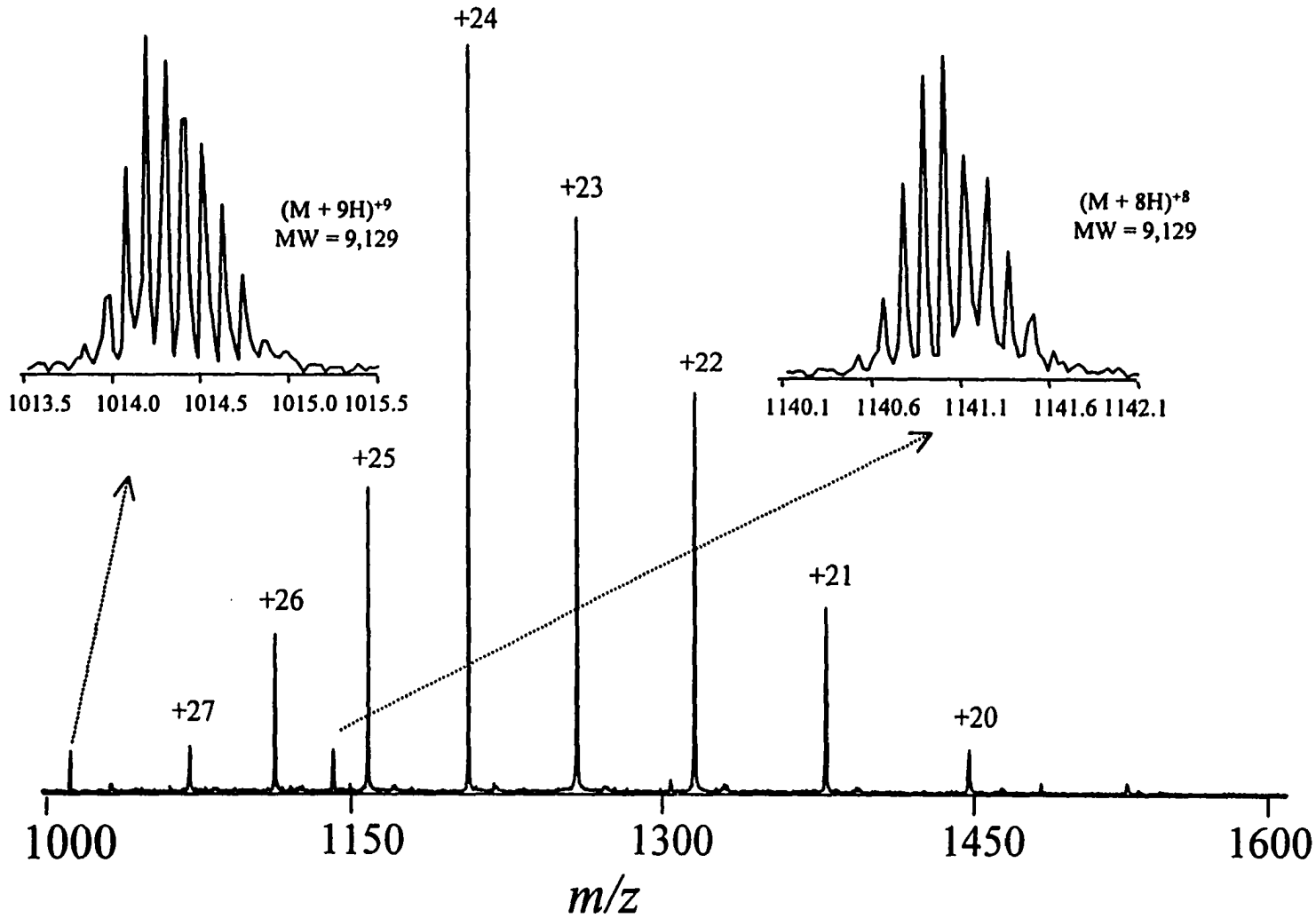
+24
+23
+22
+25
+26
+27
+21
+20
(M + 9H)+9
MW = 9,129
1013.5 1014.0 1014.5 1015.0 1015.5
(M + 8H)+8
MW = 9,129
1140.1 1140.6 1141.1 1141.6 1142.1
1000
1150
1300
1450
1600
m/z

Figure 7

CHARACTERIZATION OF CARBOHYDRATE STRUCTURES IN GLYCOPROTEIN USING EXOGLYCOSIDASE ENZYME ARRAY DIGESTION-LC/MS/MS WITH PARENT ION MONITORING

Liyu Yang, A. Kamel Harrata, and Cheng S. Lee

A paper submitted to J. Chromatogr.

ABSTRACT

An integrated approach, involving the combination of an exoglycosidase enzyme array with LC/MS/MS, for structural characterization of carbohydrates in a glycoprotein is demonstrated using ribonuclease B as a model system. In the exoglycosidase enzyme array, a tryptic digest of a glycoprotein is divided into several aliquots and each aliquot is incubated with a precisely defined mixture of exoglycosidases. The extent of exoglycosidase digestion in each aliquot is monitored using LC/MS/MS for selectively detecting and locating glycopeptides in the reaction mixture. The changes in molecular mass of glycopeptides correspond to the loss of integral numbers of monosaccharide residues. The results of a series of controlled digestions with a specific combination of exoglycosidases in the enzyme array provide the sequence and linkage of individual glycan species attached to glycopeptides and glycoproteins.

1. INTRODUCTION

The growth of the biotechnology industry, and more specifically recombinant DNA derived protein biopharmaceuticals, has placed enormous demands on bioanalytical chemistry for protein characterization. Recent studies implicate glycoproteins in many biological processes including protein targeting, cell-cell recognition, and antigen-antibody reaction [1-3]. The carbohydrate moieties of recombinant glycoproteins of pharmaceutical interest can have direct or indirect influence on the activity of glycoprotein, possible roles in clearance from circulation, and effects on the solubility and stability of protein [4]. The sugar moieties of erythropoietin have been directly linked to the secretion and biological activity of the molecule [5]. An example of the importance of carbohydrates in protein metabolism is the increased clearance of nonsialylated forms of tissue plasminogen activator via the asialoglycoprotein receptor in the liver [6].

The characterization of glycoproteins, however, is time consuming and requires significant amounts of material due to the chemical complexity and diversity of glycoforms present in an individual protein. While the protein amino acid sequence is maintained, glycosylation can occur at a number of sites (macroheterogeneity) and can have a varied and heterogeneous character resulting in a large number of distinct glycoforms (microheterogeneity). To date, most techniques for carbohydrate analysis have involved chemical or enzymatic release of carbohydrate moieties from glycoproteins prior to analysis [7,8]. However, the characterization of glycopeptides, as opposed to analyzing the pool of

released carbohydrates from a glycoprotein, has the advantage that the sequence context of each specific family of glycoforms is preserved.

Several approaches for locating glycopeptide-containing fractions in an LC peptide map of a glycoprotein digest have been developed. Glycopeptides can be selectively isolated from protein digest by appropriate use of a lectin binding agent such as concanavalin A [9-11]. A glycopeptide with more carbohydrate attached tends to elute slightly earlier in reversed-phase separations than the glycopeptide containing less carbohydrate. Although the chromatographic separation is insufficient for UV detection to resolve the peaks, the adjacent mass spectra are quite different [12]. As a result, a diagonal line for the detection of glycopeptides containing the same peptide backbone can be observed after plotting m/z versus retention time in LC/MS [13-15].

The most specific method, requiring a triple quadrupole MS, involves monitoring of sugar oxonium fragment ions during parent ion scan of MS/MS measurement [16-18]. Signals derived from nonglycosylated peptides are virtually eliminated, resulting in a total-ion current trace of only the glycopeptides present in the digest. Together with prior knowledge of the recombinant sequence and of the range of carbohydrate structures previously characterized from the expression cell line used, molecular weight measurements can reveal a relatively detailed picture of the site of glycosylation, the oligosaccharide structural classes present, and their molecular heterogeneity. Alternatively, the approach of in-source collisional-excitation scanning involves fragmentation of glycopeptides to sugar

oxonium fragment ions but does not involve any mass-selection process, permitting the experiment to be performed on a single quadrupole instrument [16-18].

In this study, we describe the combination of an exoglycosidase enzyme array with LC/MS/MS for structural analysis of carbohydrate moieties of glycopeptides from a glycoprotein digest. The enzyme array method involves the division of a glycoprotein digest into aliquots, and the incubation of each aliquot with a precisely defined mixture of exoglycosidases [19]. These exoglycosidases sequentially cleave monosaccharides hydrolytically at the glycosidic linkage from the non-reducing terminal of the oligosaccharides [20,21]. The exoglycosidases and the enzyme array employed in this work are summarized in Table 1 and Fig. 1, respectively.

In the exoglycosidase enzyme array method, the presence of a specific linkage anywhere in the oligosaccharide is determined by the inability of an enzyme mixture lacking a given enzyme to cleave that linkage (a stop point) and the ability of the other enzymes to cleave the linkages up to that point. The use of LC/MS/MS measurements with parent ion monitoring for measuring the extent of enzymatic digestion in each aliquot is based on the separation and identification of remaining uncleaved oligosaccharides attached to glycopeptides. The changes in molecular mass of glycopeptides correspond to the loss of integral numbers of monosaccharide residues. Besides the characterization of carbohydrate moieties in glycoproteins, the "fingerprint" analyses of digestion mixtures in the exoglycosidase enzyme array may have practical utility in the biotechnology industry as the means to demonstrate lot-to-lot consistency in cell culture and purification processes.

2. EXPERIMENTAL

2.1. Materials and Chemicals

Bovine pancreatic ribonuclease B (RNase B), dithiothreitol (DTT), iodoacetamide (IAM), trypsin (sequencing grade), and trifluoroacetic acid (TFA) were obtained from Sigma (St. Louis, MO). Tris(hydroxymethyl)-aminomethane (Tris) and ultrapure urea were acquired from Bio-Rad (Hercules, CA) and ICN (Aurora, OH), respectively. All other chemical reagents, including acetic acid, acetonitrile, ammonium bicarbonate, citric acid, disodium phosphate, and sodium azide, were purchased from Aldrich (Milwaukee, WI) and used without further purification. The PD-10 size exclusion columns and five exoglycosidases (Table 1) were obtained from Pharmacia (Uppsala, Sweden) and Oxford Glycosystems (Rosedale, NY), respectively. Deionized water from a Nanopure II system (Branstead, Dubuque, IA) was further filtered through a 0.2 μm Supor-200 membrane filter (Gelman Science, Ann Arbor, MI) and was used for preparing all buffer and sample solutions.

2.2. Protein Denaturation/Reduction, Alkylation, and Trypsin Digestion

RNase B was completely denatured at a concentration of 5 mg/ml in a solution containing 8 M urea and 0.2 M Tris-HCl (pH 8.0) for approximately 30 min at 37 °C under a nitrogen atmosphere. DTT was then added into the solution with a final concentration of 10 mg/ml. The solution was flushed with nitrogen and incubated at 50 °C for another 30 min.

The reduced RNase B solution was cooled on ice. The alkylation reaction with cysteines was initiated by adding excess IAM reagent (20 mg/ml final concentration) and

allowed to proceed for 15 min at room temperature in the dark. A PD-10 column was employed for buffer exchange and the proteins were eluted in a solution containing 50 mM ammonium bicarbonate at pH 8.0. For trypsin digestion, the reduced and alkylated RNase B was mixed with a 2 mg/ml trypsin solution in 1 mM HCl. The final trypsin to RNase B ratio was 1:50. The reaction mixture was incubated at 37 °C for 18 hr.

2.3. Exoglycosidase Enzyme Array Digestion

After trypsin digestion, the peptide sample was vacuum dried and stored at -20 °C. The sample was divided into seven aliquots and digested with the enzyme array shown in Fig. 1. The exoglycosidases were prepared in 0.1 M citric acid, 0.2 M disodium phosphate, and 0.001% sodium azide at pH 5.3. Incubation was carried out for 48 hr at 37 °C.

2.4. Reversed-Phase LC/MS/MS Analysis of Exoglycosidase Digestion Mixtures

All LC separations were performed using an Applied Biosystem (Fullerton, CA) 140A solvent delivery system at a flow rate of 40 μl/min. Peptide separations were carried out with a 1 mm i.d. x 25 cm Vydac reversed-phase C_{18} column (LC Packings, San Francisco, CA). Approximately 100 pmole of RNase B sample from each exoglycosidase digestion vial was injected for every LC/MS/MS analysis. Solvent A was 0.1% TFA in water; solvent B was 0.1% TFA in acetonitrile/water (90:10, v/v). Separation of the tryptic peptides was effected with a gradient of 5% to 50% B in 30 min. Eluent from the LC column was directed to the mass spectrometer via a 10-cm-long fused-silica tubing with 50 μm i.d. and 192 μm o.d. (Polymicro Technologies, Phoenix, AZ).

The mass spectrometer used in this study was a Finnigan MAT TSQ 700 (San Jose, CA) triple quadrupole equipped with an electrospray ionization source. The mass spectrometer was tuned and the mass range calibrated using an acetic acid solution (methanol/water/acetic acid, 50:49:1 v/v/v) containing myoglobin and a small peptide of methionine-arginine-phenylalanine-alanine. The electrospray voltage was operated at 5 kV and the electron multiplier was set at 1.4 kV with the conversion dynode at -15 kV. Normal LC/MS spectra were acquired by scanning Q1 from m/z 140 to m/z 2400 at a scan rate of 3 sec/scan.. For parent ion tandem MS, the analyzing quadrupole (Q1) was operated at a resolution of about unit m/z, while the mass-selecting quadrupole (Q3) was set to pass a 2-3 dalton window around the ion of interest so as to enhance sensitivity. High purity argon was employed in Q2 as the collision gas with a pressure of 0.2 mtorr. The potentials at the heated capillary, tube lens, and Q2 were set to be 26 V, 86 V, and -35 V, respectively. Detailed conditions of parent ion tandem MS were described and discussed elsewhere [16,17].

3. RESULTS AND DISCUSSION

Concerns about the quality of recombinant glycoproteins arise in connection with the observed macro- and microheterogeneity of glycoforms secreted in the course of a cell culture process. Such variations in glycosylation site occupancy (macroheterogeneity), as well as glycoform antennary structure (microheterogeneity), have been associated with variations in protein properties such as efficacy, clearance rate, antigenicity, and immunogenicity [3,4,22]. Thus, the issue of protein quality is not only one of optimizing

glycoform composition with respect to the above spectrum of glycoprotein properties but also of maintaining glycoform consistency in spite of cellular and process variations.

In this study, the full potential of the exoglycosidase enzyme array in combination with LC/MS/MS for the characterization of carbohydrate moieties in glycoproteins is illustrated using RNase B as a model system. RNase B is a glycoprotein containing a single N-glycosylation site at asparagine (Asn) 34 (Fig. 2). In common with other glycoproteins, it consists of a population of glycosylated variants in which a single amino acid sequence is diversified by the range of oligosaccharides conjugated to it. The high mannose structures contain 5-9 mannose (Man) residues in addition to a N-acetylglucosaminylβ1 - 4 N-acetylglucosamine (GlcNAc) unit linked to Asn.

Proteolytic digestion, such as with trypsin, in combination with reversed-phase LC has been shown to be of importance as a means of characterizing proteins of interest and monitoring for minor alterations in a population of molecules [23]. The integration of electrospray ionization MS with reversed-phase LC was shown to add a new dimension to the usual UV absorbance data and provide mass information to aid in the identification of peptides [13,24,25]. In this study, none of the exoglycosidases were present in aliquot 1 of enzyme array (Fig. 1). Thus, the remaining uncleaved glycopeptides and peptides of RNase B from tryptic digestion were analyzed using LC/MS.

The reconstructed total ion current map observed from separation of a 5-μl injection (100 pmole) of tryptic digest (Fig. 3) correlated well with the UV map (data not shown). Peptide signals were assigned to specific sequence locations with the aid of an interactive

computer program (LC/MS BioToolBox analysis software from Perkin-Elmer, Foster City, CA). The program determined the mass of all of the peptides in the LC/MS data set and matched them, if possible, to the calculated mass of all peptides that would be expected to form based on the reaction conditions and the known sequence (Fig. 2).

In general, the difference between the determined and the calculated mass values of RNase B peptides was less than 0.2 daltons. Only three of the 14 predicted unique tryptic fragments of RNase B were not detected. One of these corresponded to a single lysine (Lys^1). However, this residue was detected in a partial tryptic fragment (Lys^1-Lys^7) formed by incomplete cleavage. The other corresponded to two dipeptides of Ser^{32}-Arg^{33} and Asp^{38}-Arg^{39}. It is often difficult to detect dipeptides by LC/MS since they usually elute in the high-aqueous portion of the chromatogram where buffer salts present in the sample also elute. These excipients tend to suppress peptide-related signals in the electrospray process.

RNase B obtained from Sigma was free of contaminant of RNase A, the nonglycosylated form of the same protein. The peak eluted around 8.75 min (marked with "*" in Fig. 3) contained multiple peptides with molecular masses corresponding to the glycopeptides of RNase B, exhibiting high mannose N-linked oligosaccharides. To selectively detect and locate glycopeptides in the complex digest mixtures, the formation and detection of diagnostic sugar oxonium ions, particularly the N-acetylhexosamine ($HexNAc^+$, m/z 204) fragments, were employed during LC/MS/MS analysis of tryptic digest in aliquot 1 of exoglycosidase enzyme array (Fig. 1). The natural abundance of these low-mass fragment (marker) ions in normal electrospray mass spectra is often quite low, but their abundance can

be significantly enhanced by collision-induced decomposition of the parent ions in Q2 of triple quadrupole mass spectrometer. $HexNAc^+$ is selected as the most universal indicator of glycopeptides because all N- and O-linked carbohydrates are attached to amino acids via HexNAc.

The results of LC/MS/MS with parent ion monitoring of RNase B tryptic digest is shown in Fig. 4A. Parent ion scanning gave a spectrum of all parent ions that dissociate to yield the glycosylation marker ions, the $HexNAc^+$ ions at m/z 204. The selected ion current trace maximized at 7.75 min in the chromatogram, indicating the presence of RNase B glycopeptides. In comparison with the results shown in Fig. 3, the decrease in the elution time of RNase B glycopeptides was attributed to the change in the LC column condition. There were no interferences from nonglycosylated peptide components during LC/MS/MS analysis using parent ion monitoring.

The mass spectrum taken from the average scans under the peak (Fig. 4A) displayed the entire RNase B glycopeptide distribution, indicating the heterogeneity of the glycoforms at one given attachment site (Asn 34). For example, the peaks at m/z 846, 927, 1008, and 1089 all differed by an average of 81 daltons. Because these ions were doubly charged, the true mass difference was 162, which corresponded to the incremental mass of a hexose (e.g., galactose or mannose). In fact, the molecular masses of these glycopeptides displayed a distribution of high mannose oligosaccharide structures from Man_5 to Man_8. The relative percentage of Man_9 glycoform of RNase B was reported to be around 4 - 6% [26]. Besides very small percentage of Man_9 glycoform, the presence of other glycoforms in this study

competed and suppressed the ion intensity of Man_9 glycoform during the electrospray process.

The aliquots 2-7 in the exoglycosidase enzyme array (Fig. 1) were analyzed by LC/MS/MS with parent ion monitoring of $HexNAc^+$ ions at m/z 204. The selected ion current traces for the analyses of aliquots 5 and 6 are illustrated in Fig. 4B-C for comparison. The digestion results are summarized in Table 2. The enzymes needed for the digestion of high mannose N-linked oligosaccharides were jack bean α-mannosidase, helix pomatia β-mannosidase, and jack bean β-N-acetylhexosaminidase. Thus, in any aliquot where all three of these exoglycosidases were present, complete digestion occurred and a glycopeptide of GlcNAc-Asn 34 was observed with a m/z of 340 for doubly charged ions. Aliquots 2 and 7 each showed complete digestion.

Both hexosaminidases were missing from aliquot 3, thus the stop point was the GlcNAcβ1-4GlcNAc linkage, resulting in a glycopeptide of $GlcNAc_2$-Asn 34 with a m/z of 441 for doubly charged ions. Aliquot 4 was missing the α-mannosidase, thus the cleavage from the nonreducing termini of carbohydrate moieties was not initiated and the measured glycopeptides were the same as those in aliquot 1. The β-mannosidase was missing from aliquot 5, therefore the α-mannosidase present in the mixture cleaved until the Manβ1 linkage was reached, resulting in a glycopeptide of Man-$GlcNAc_2$-Asn 34 with a m/z of 521 for doubly charged ions (Fig. 4B). Aliquot 6 was missing jack bean β-N-acetylhexosaminidase, making the stop point the GlcNAcβ1-4GlcNAc linkage (Fig. 4C). There, the measured glycopeptide was identical to that of aliquot 3. By comparing the results shown in Fig. 4A-

C, the removal of carbohydrates from the glycopeptides of RNase B accounted for the increases in hydrophobicity and the elution time in reversed-phase LC.

The selectivity of the parent ion monitoring method is evident for glycopeptide detection of RNase B tryptic digest. The exoglycosidases used in the structural analysis of carbohydrate moieties attached to glycopeptides are very specific for the monosaccharide anomericity (α/β) of the glycosidic linkage, and the absolute stereoisomer (D/L) of the glycan. Their specificities for the ring size (pyranose/furanose), the glycosidic linkage, the branch-points, and the aglycan component are more variable but limited [27]. For example, all of the exoglycosidases used in this study other than b-mannosidase act on a multiplicity of linkages (Table 1). Thus, the removal of a Man residue with α-mannosidase does not provide the exact linkage information. Clearly, the limitation of our integrated approach for structural characterization of glycoproteins arises from the nature of exoglycosidase enzyme array. More sophisticated arrays can be developed than that illustrated in Fig. 1, and there will be a requirement for further introduction of highly pure and highly specific (bond, arm, aglycan) exoglycosidases.

ACKNOWLEDGMENTS

Support for this work by a Carver Trust Grant and the Microanalytical Instrumentation Center of the Institute for Physical Research and Technology at Iowa State University is gratefully acknowledged. C.S.L. is a National Science Foundation Young Investigator (BCS-9258652).

REFERENCES

1. S. Dube, J. W. Fisher, J. S. Powell, *J. Biol. Chem.*, 263 (1988) 17516.
2. A. J. Wittwer, S. C. Howard, *Biochemistry*, 29 (1990) 4175.
3. M. Geisow, *Bio/Technology*, 10 (1992) 277.
4. M. W. Spellman, *Anal. Chem.*, 62 (1990) 1714.
5. E. Delorme, T. Lorenzini, J. Giffin, F. Martin, F. Jacobsen, T. Boone, S. Elliot, *Biochemistry*, 31 (1992) 9871.
6. E. S. Cole, E. H. Nichols, L. Poisson, M. L. Harnois, D. J. Livingston, *Fibrinolysis*, 7 (1993) 15.
7. M. R. Hardy, R. R. Townsend, *Proc. Natl. Acad. Sci.*, 85 (1988) 3289.
8. Y. C. Lee, *Anal. Biochem.*, 189 (1990) 151.
9. M. F. Bean, J. D. Bangs, T. L. Doering, P. T. Englund, R. J. Cotter, *Anal. Chem.*, 61 (1989) 2686.
10. T. Endo, *J. Chromatogr. A*, 720 (1996) 251.
11. A. Apffel, J. A. Chakel, W. S. Hancock, C. Souders, T. M'Timkulu, E. Pungor, *J. Chromatogr. A*, 750 (1996) 35.
12. M. E. Hemling, G. D. Roberts, W. Johnson, S. A. Carr, T. E. Covey, *Biomed. Environ. Mass Spectrom.*, 19 (1990) 677.
13. V. Ling, A. W. Guzzetta, E. Canova-Davis, J. T. Stults, W. S. Hancock, T. R. Covey, B. I. Shushan, *Anal. Chem.*, 63 (1991) 2909.

14. A. W. Guzzetta, L. J. Basa, W. S. Hancock, B. A. Keyt, W. F. Bennett, *Anal. Chem.*, 65 (1993) 2953.

15. D. A. Lewis, A. W. Guzzetta, W. S. Hancock, M. Costello, *Anal. Chem.*, 66 (1994) 585.

16. M. J. Huddleston, M. F. Bean, S. A. Carr, *Anal. Chem.*, 65 (1993) 877.

17. S. A. Carr, M. J. Huddleston, M. F. Bean, *Protein Sci.*, 2 (1993) 183.

18. G. D. Roberts, W. P. Johnson, S. Burman, K. R. Anumula, S. A. Carr, *Anal. Chem.*, 67 (1995) 3613.

19. C. T. Edge, T. W. Rademacher, M. R. Wormald, R. B. Parekh, T. D. Butters, D. R. Wing, R. A. Dwek, *Proc. Natl. Acad. Sci.*, 89 (1992) 6338.

20. A. Kobata, in V. Ginsburg, P. W. Robbins (Eds.), *Biology of Carbohydrates*, Volume 2, John Wiley & Sons, New York, 1984, p. 87.

21. A. Kobata, K. Furukawa, in J. A. Howard, C. K. Edward (Eds.), *Glycoconjugates: Composition, Structure, and Function*, Marcel Dekker, New York, 1992, p. 33.

22. T. W. Rademacher, R. B. Parekh, R. A. Dwek, *Annu. Rev. Biochem.*, 57 (1988) 785.

23. W. S. Hancock, C. A. Bishop, M. T. W. Hearn, *Anal. Biochem.*, 89 (1978) 203.

24. E. C. Huang, J. D. Henion, *J. Am. Soc. Mass Spectrom.* 1 (1990) 158.

25. T. R. Covey, E. C. Huang, J. D. Henion, *Anal. Chem.* 63 (1991) 1193.

26. P. M. Rudd, I. G. Scragg, E. Coghill, R. A. Dwek, *Glycoconjugate J.* 9 (1992) 86.

27. S. Prime, J. Dearnley, A. M. Ventom, R. B. Parekh, C. J. Edge, *J. Chromatogr. A* 720 (1996) 263.

TABLE 1

Activities of Exoglycosidases Used in Enzyme Array

Exoglycosidase	Cleavage Specificity [a]	Activity (units/ml)[b]
Jack bean β-galactosidase	Galβ1 - 6 > 4 >> 3GlcNAc	5.5
Streptococcus pneumoniae β-N-acetylhexosaminidase	GlcNAcβ1 - (2Man or 3, 6Gal)	0.16
Jack bean α-mannosidase	Manα1 - 2, 3, 6 Man	22.0
Helix pomatia β-mannosidase	Manβ1 - 4GlcNAc	1.1
Jack bean β-N-acetylhexosaminidase	GlcNAcβ1 - 2, 3, 4, 6Glycan	5.5

a) Taken from references (20,21).

b) One unit of enzyme activity is defined as the amount of enzyme required to hydrolyze the appropriate 3 mM p-nitrophenylglycoside at a rate of 1 mmol/min at 37 °C.

TABLE 2

The Glycopeptides of RNase B in Each Aliquot of Exoglycosidase Enzyme Array as Measured by LC/MS/MS with Parent Ion Monitoring

Aliquot Number	Doubly Charged Glycopeptide Ions (m/z)	Corresponding Glycoforms
1	846	Man_5-$GlcNAc_2$-Asn 34
	927	Man_6-$GlcNAc_2$-Asn 34
	1008	Man_7-$GlcNAc_2$-Asn 34
	1089	Man_8-$GlcNAc_2$-Asn 34
2	340	GlcNAc-Asn 34
3	441	$GlcNAc_2$-Asn 34
4	846	Man_5-$GlcNAc_2$-Asn 34
	927	Man_6-$GlcNAc_2$-Asn 34
	1008	Man_7-$GlcNAc_2$-Asn 34
	1089	Man_8-$GlcNAc_2$-Asn 34
5	522	Man-$GlcNAc_2$-Asn 34
6	441	$GlcNAc_2$-Asn 34
7	340	GlcNAc-Asn 34

FIGURE CAPTIONS

Fig. 1 Exoglycosidase enzyme array used for the analysis of carbohydrate structures in RNase B. Numbers referred to the separate digestion vials; o, absence of the enzyme; ⊗, presence of the enzyme.

Fig. 2 (A) Amino acid sequence and tryptic peptides of RNase B; (B) high mannose structures of carbohydrate moieties linked to Asn 34.

Fig. 3 On-line LC/MS analysis of a tryptic digest of reduced and alkylated RNase B from aliquot 1 of exoglycosidase enzyme array (Fig. 1). Numbers referred to the peptides summarized in Fig. 2.

Fig. 4 Parent ion LC/MS/MS of $HexNAc^+$ ions at m/z 204 for the analyses of digestion mixtures in (A) aliquot 1, (B) aliquot 5, and (C) aliquot 6 of exoglycosidase enzyme array (Fig. 1). The inset presented the mass spectrum taken from the average scans under the peak.

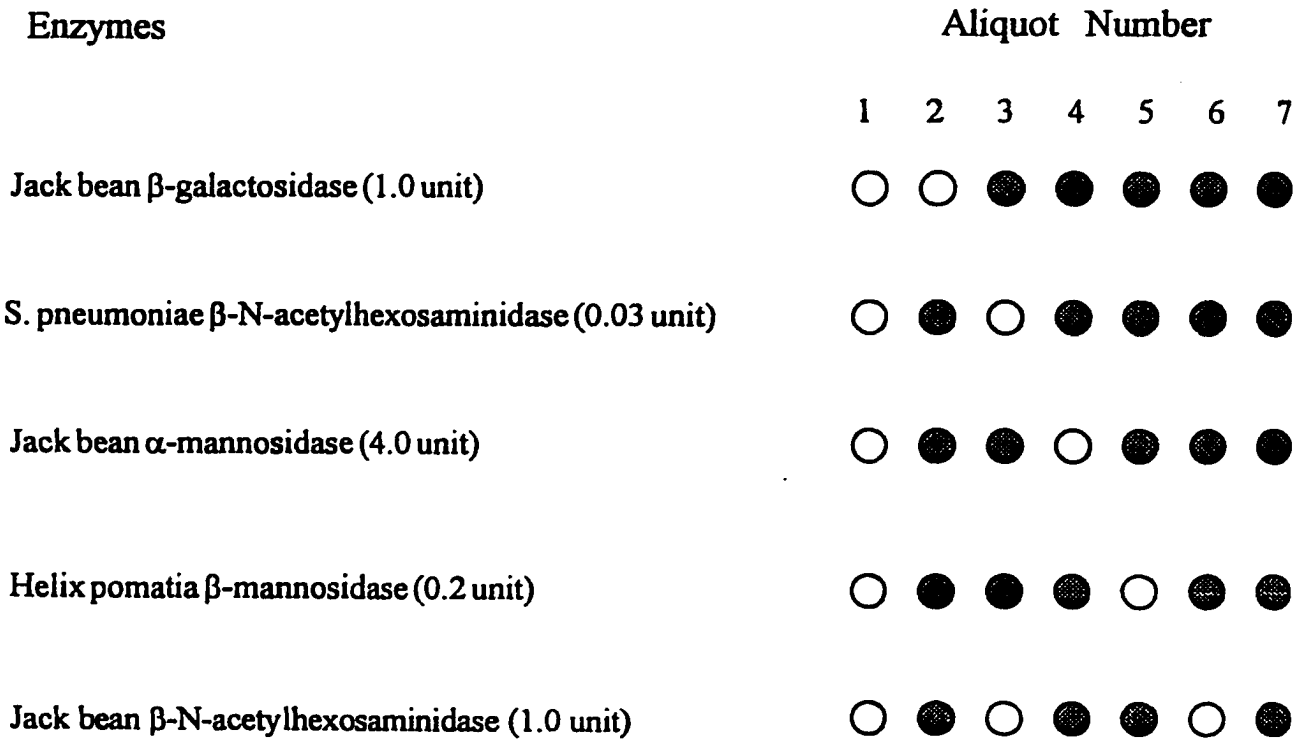
Enzymes
Aliquot Number
1 2 3 4 5 6 7
Jack bean β-galactosidase (1.0 unit)
S. pneumoniae β-N-acetylhexosaminidase (0.03 unit)
Jack bean α-mannosidase (4.0 unit)
Helix pomatia β-mannosidase (0.2 unit)
Jack bean β-N-acetylhexosaminidase (1.0 unit)

Figure 1

A. Tryptic Peptides

No.	Position	Amino Acid Sequence	Average Mass (daltons)
1	1	K	146.2
2	2-7	ETAAAK	589.6
3	8-10	FER	450.5
4	11-31	QHMDSSTSAASSSNYCNQMMK	2307.5
5	32-33	SR	261.3
6	**34-37**	**NLTK**	**474.6 ← Glycosylation site**
7	38-39	DR	289.3
8	40-61	CKPVNTFVHESLADVQAVCSQK	2401.7
9	62-66	NVACK	532.6
10	76-85	NGQTNCYQSYSTMSITDCR	2170.3
11	86-91	ETGSSK	607.6
12	92-98	YPNCAYK	857.0
13	99-104	TTQANK	661.7
14	105-124	HIIVACEGNPYVPVHFDASV	2166.5

B. Glycosylation Microheterogeneity

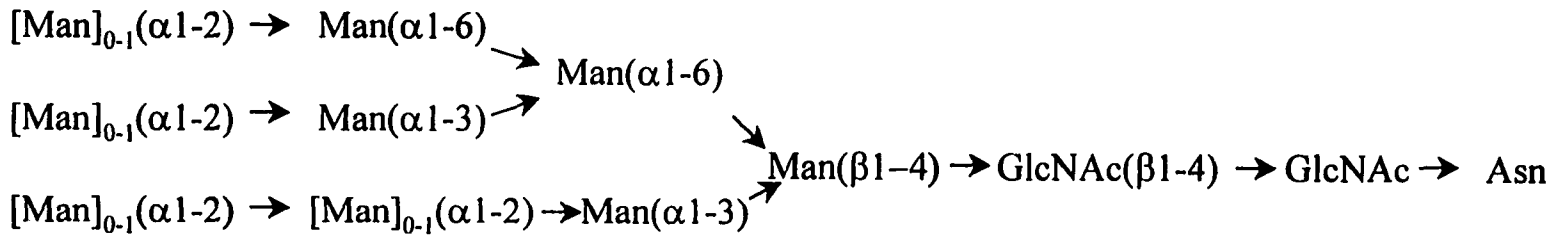

Figure 2

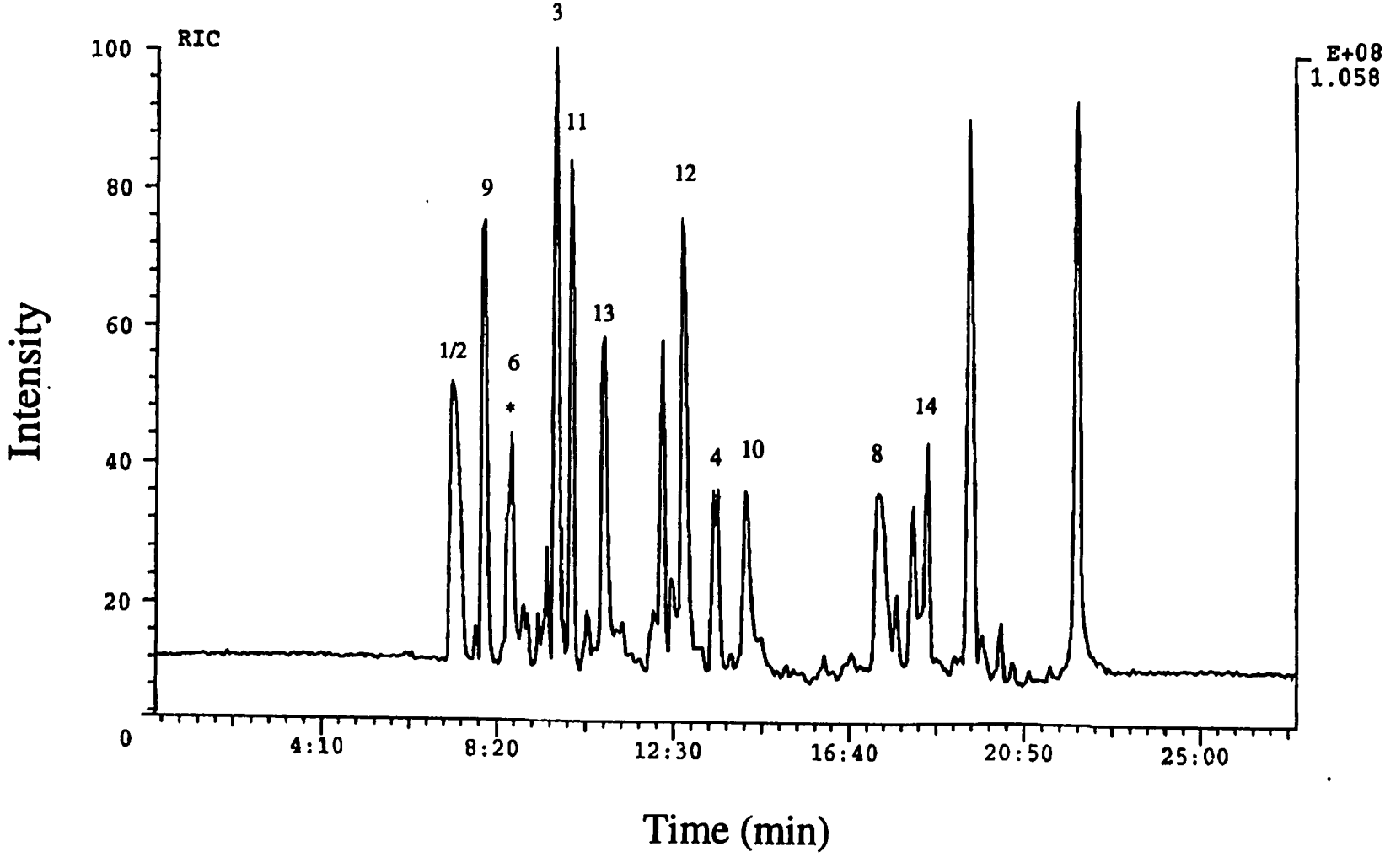
RIC
E+08
1.058
Intensity
100
80
60
40
20
0
1/2
9
6
*
3
11
13
12
4
10
8
14
4:10
8:20
12:30
16:40
20:50
25:00
Time (min)

Figure 3

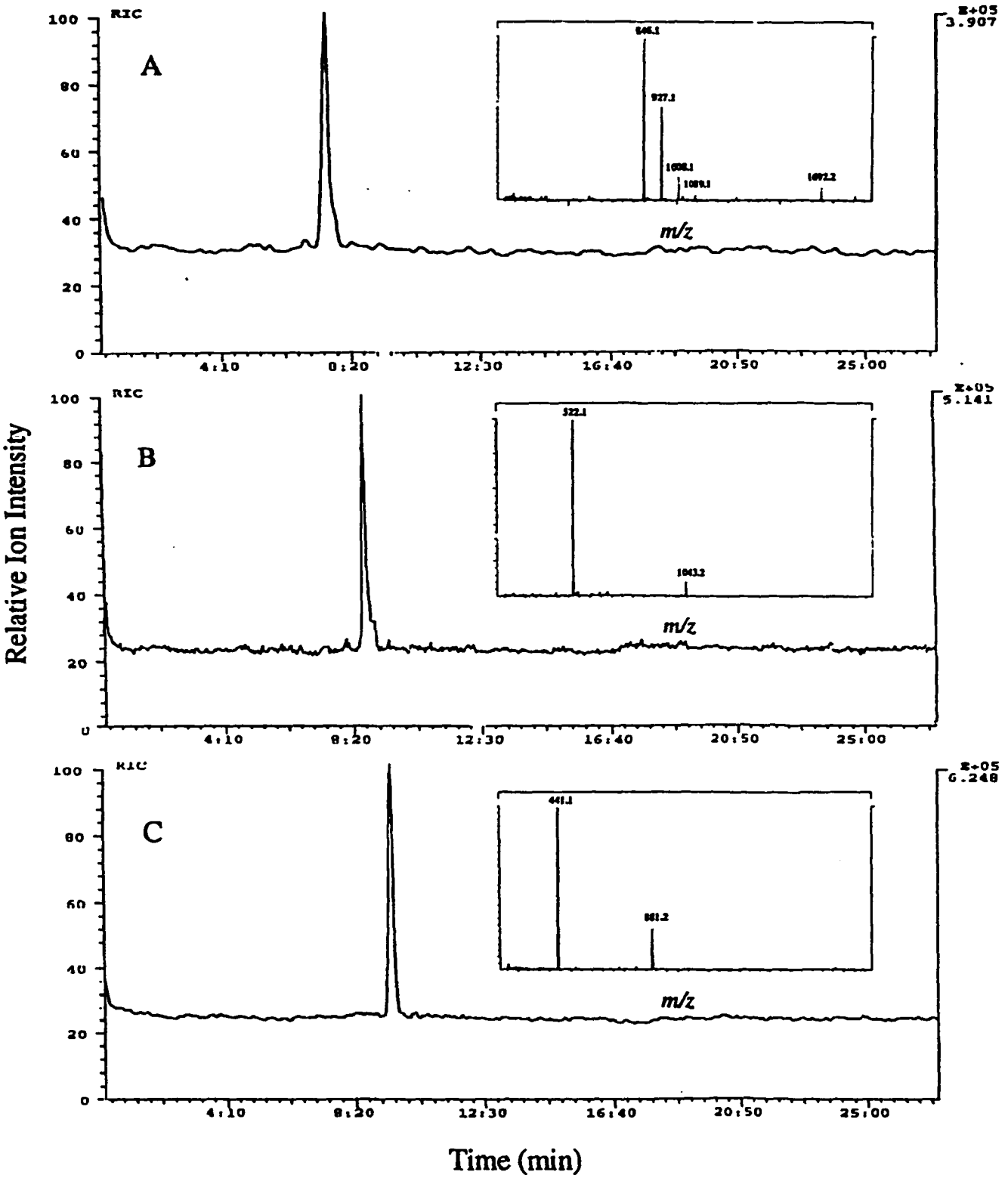
RIC
A
E+05
3.907
927.1
m/z
B
E+05
5.141
522.1
1043.2
m/z
C
E+05
6.248
441.1
881.2
m/z
100
80
60
40
20
0
4:10
8:20
12:30
16:40
20:50
25:00
Relative Ion Intensity
Time (min)

Figure 4

GENERAL SUMMARY

On-line capillary isoelectric focusing (CIEF)-electrospray ionization mass spectrometry (ESIMS) is utilized for protein characterization. Issues such as detection sensitivity and mass resolution are addressed by investigating the use of a microdialysis junction interface and the fourier transform ion cyclotron resonance mass spectrometry (FTICRMS).

A microdialysis junction, based on a microdialysis membrane connecting both a separation capillary and a short, sharply tapered microelectrospray emitter capillary, is demonstrated for on-line CIEF with ESIMS. The microdialysis junction is advantageous over the coaxial liquid sheath interface as evidenced by the simplicity in operation procedures, the enhancement in detection sensitivity, and the linear correlation between protein's migration time and isoelectric point in CIEF-ESIMS.

On-line combination of CIEF with ESI-FTICRMS is demonstrated for high resolution analysis of model proteins, human hemoglobin variants, and *Escherichia coli* proteins. The acquisition of high-resolution mass spectra of hemoglobin β chains allows direct identification of hemoglobin variants A and C, differing in molecular mass by 1 dalton. Direct mass determination of cellular proteins separated in the CIEF capillary is achieved using their isotopic envelopes obtained from ESI-FTICRMS.

An integrated approach, involving the combination of exoglycosidase enzyme array with LC/MS/MS, is demonstrated for structural analysis of carbohydrate moieties of

glycopeptides from a glycoprotein digest. The molecular mass information from a series of controlled digestions together with specific compositions of exoglycosidases in the enzyme array provide the sequence and linkage of individual glycan species attached to glycopeptides and glycoproteins. Besides the characterization of carbohydrate moieties in glycoproteins, the "fingerprint" analyses of digestion mixtures in the exoglycosidase enzyme array using LC/MS/MS may have practical utility as the means to demonstrate lot-to-lot consistency in biopharmaceuticals manufacturing.

REFERENCES

1 J. W. Jorgenson and K. D. Lukacs, *Anal. Chem.*, **53** (1981) 1298.

2 J. W. Jorgenson and K. D. Lukacs, *J. Chromatogr.*, **218** (1981) 209.

3 S. Hjerten, *J. Chromatogr.*, **270** (1983) 1.

4 S. Hjerten and M. D. Zhu, *J. Chromatogr.*, **327** (1985) 157.

5 A. S. Cohen, A. Paulus and B. L. Karger, *Chromatographia*, **24** (1987) 15.

6 B. L. Karger, A. S. Cohen and A. Guttman, *J. Chromatogr.*, **492** (1989) 585.

7 F. M. Everaerts and P. E. M. Verheggen, *New Directions in Electrophoretic Methods*, edited by J. W. Jorgenson and M. Phillips, *Amer. Chem. Soc. Symp.*, Vol. 335, Washington D. C., 1987, Chap. 4.

8 P. Bocek, M. Deml, P. Gebauer and V. Dolnik, *Anal. Isotachophoresis*, VCH Verlagsgesellschaft, Weinhein, 1988.

9 J. H. Knox, *Chromatographia*, **26** (1988) 329.

10 S. Hjerten and M. Zhu, *J. Chromatogr.*, **346** (1985) 265.

11 S. Hjerten, K. Elenbring, F. Kilar, J. L. Liao, J. C. Chen, C. J. Siebert and M. D. Zhu, *J. Chromatogr.*, **403** (1987) 47.

12 S. Hjerten, *J. Chromatogr.*, **347** (1985) 191.

13 S. Hjerten, J. Liao and K. Yao, *J. Chromatogr.*, **387** (1987) 127.

14 J. R. Mazzeo and I. S. Krull, *Bio/Techniques*, **10** (1991) 638.

15 S. Terabe, K. Otsuka and T. Ando, *Anal. Chem.*, **57** (1985) 834.

16 B. A. Bidlingmeyer, *Practical HPLC Methodology and Applications*, John Wiley & Sons, New York, 1992.

17 C. F. Poole and S. A. Schuette, *Contemporary Practice of Chromatography*, Elsevier, Amsterdam, 1984.

18 S. G. Perry and P. O. Brewer, *Practical Liquid Chromatography*, Plenum Press, New York, 1972.

19 L. R. Snyder, *Principles of Adsorption Chromatography*, Plenum Press, New York, 1968.

20 T. M. Phipplips, *The Use of HPLC in Receptor Biochemistry*, Alan R. Liss, New York, 1989.

21 C. R. Lowe et al., *J. Chromatogr.*, **215** (1981) 303.

22 J. Porath and B. Olin, *Immobilized Metal Ion Affinity Adsorption and Affinity Chromatography of Biomaterials, Biochemistry*, **22** (1983) 1621.

23 J. Turkova., *J. Chromatogr.*, **376** (1986) 315.

24 J. R. Sportsman and G. S. Wilson, *Anal. Chem.*, **52** (1980) 2013.

25 T. Halicioglu, and O. Sinanoglu, *Ann. N. Y. Acad. Sci.*, **158** (1969) 308.

26 C. Horvath, W. Melander, and I. Molnar, *Anal. Chem.*, **49** (1977) 142.

27 F. P. B. van der Maeden, *J. Chromatogr.*, **149** (1978) 539.

28 V. Ling, *Anal. Chem.*, **63** (1991) 2909.

29 B. J. Harmon, X. Gu, and D. I. C. Wang, *Anal. Chem.*, **68** (1996) 1465.

30 M. Dole, L. L. Mach, R. L. Hines, R. C. Mobley, L. P. Ferguson and M. B. Alice, *J. Chem. Phys.*, **49** (1968) 2240.

31 M. Yamashita and J. B. Fenn, *Phys. Chem.*, **88** (1984) 4451.

32 M. Yamashita and J. B. Fenn, *Phys. Chem.*, **88** (1984) 4671.

33 G. I. Taylor, *Proc. R. Soc. London A*, **280** (1964) 383.

34 L. Rayleigh, *Philos. Mag.* **14** (1882) 184.

35 J. V. Iribarne and B. A. Thomson, *J. Chem. Phys.*, **64** (1976) 2287.

36 B. A. Thomson and J. V. Iribarne, *J. Chem. Phys.*, **71** (1979) 4451.

37 P. Kebarle and L. Tang, *Anal. Chem.*, **65** (1993) 972 A.

38 T. Nohmi and J. B. Fenn, *J. Am. Chem. Soc.*, **114** (1992) 3245.

39 J. B. Fenn, *J. Am. Soc. Mass Spectrom.*, **4** (1993) 524.

40 M. Wilm, and M. Mann, *Int. J. Mass. Spectrom. Ion Processes.*, **136** (1994) 167.

41 P. Thibault, C. Paris and S. Pleasance, *J. Rapid Commun. Mass Spectrom.*, **5** (1991) 484.

42 R. Feng, Y. Konishi and A. W. Bell, *J. Am. Soc. Mass Spectrom.*, **2** (1991) 387.

43 R. D. Smith, J. A. Loo, C. G. Edmonds, C. J. Barinaga and H. R. Udseth, *Anal. Chem.*, **62** (1990) 882.

44 V. Katta and B. T. Chait, *J. Am. Chem. Soc.*, **113** (1991) 8534.

45 M. Baca and S. B. H. Kent, *J. Am. Chem. Soc.*, **114** (1992) 3392.

46 K. J. Wahl, *J. Am. Chem. Soc.*, **115** (1993) 803.

47 K. J. Wahl, B. L. Schwatz and R. D. Smith, *J. Am. Chem. Soc.*, **116** (1994) 5271.

48 H. K. Lim, Y. L. Hsieh, B. Ganem and J. Henion, *J. Am. Soc. Mass Spectrom.*, **30** (1995) 708.

49 Y. L. Hsieh, J. Cai, Y. T. Li and J. D. Henion, *J. Am. Soc. Mass Spectrom.*, **6** (1995) 85.

50 P. E. Miller and M. B. Denton, *J. Chem. Education*, **63** (1986) 617.

51 C. N. McEwen and B. S. Larsen, *Electrospray Ionization on Quadrupole and Magnetic-Sector Mass Spectrometers* in *Electrospray Ionization Mass Spectrometry-Fundamentals, Instrumentation, and Applications*, edited by R. B. Cole, Wiley, New York, 1997, pp. 177.

52 A. G. Marshall, M. B. Comisarow and G. Parisod, *J. Chem. Phys.*, **71** (1979) 4434.

53 M. L. Gross and D. Rempel, *Science*, **226** (1984) 261.

54 A. G. Marshall and P. B. Grosshans, *Anal. Chem.*, **63** (1991) 215A.

55 A. G. Marshall and L. Schweikhard, *Int. J. Mass Spectrom. and Ion Processes*, **118** (1992) 37.

56 I. J. Amster, *J. Mass Spectrom.* **31** (1996) 1325.

57 K. D. Henry and F. W. McLafferty, *Org. Mass Spectrom.*, **25** (1990) 490.

58 B. E. Winger, S. A. Hofstadler, J. E. Bruce, H. R. Udseth, and R. D. Smith, *J. Am. Soc. Mass Spectrom.*, **4** (1993) 566.

59 P. Kofel, M. Alleman, H. P. Kellerhals, and K. P. Wanczek, *Int. J. Mass Spectrom. Ion Processes*, **65** (1985) 97.

60 B. E. Winger, R. E. Hein, B. L. Becker, and J. E. Campana, *J. Rapid Commun. Mass Spectrom.*, **8** (1994) 495.

61 M. B. Comisarow, *J. Chem. Phys.*, **69** (1978) 4097.

62 K. D. Henry, E. R. Williams, B. H. Wang, F. W. McLafferty, J. Shabanowitz, and D. F. Hunt, *Proc. Natl. Acad. Sci.*, **86** (1989), 9075.

63 S. A. Hofstadler and D. A. Laude, *Anal. Chem.*, **64** (1992) 572.

64 J. A. Olivares, N. T. Nguyen, C. R. Yonker and R. D. Smith, *Anal. Chem.*, **59** (1987) 1230.

65 R. D. Smith, J.A. Olivares, N. T. Nguyen and H R. Udseth, *Anal. Chem.*, **60** (1988) 436.

66 R. D. Smith, C. Barinaga and H. R. Udseth, *Anal. Chem.*, **60** (1988) 1948.

67 E. D. Lee, W. Miick, J. D. Henion and T. R. Covey, *Biomedical and Environmental Mass Spectrom.*, **18** (1989) 844.

68 S. Pleasance, P. Thibault and J. Kelly, *J. Chromatogr.*, **591** (1992) 325.

69 D. C. Cale and R. D. Smith, *J. Rapid Commun. Mass Spectrom.*, 7 (1993) 1017.

70 K. Tsuji, L. Baczynskyj and G.E. Bronson, *Anal. Chem.*, **64** (1992) 1864.

71 J. Zhou and S. M. Lunte, *Anal. Chem.*, **67** (1995) 13.

72 J. C. Severs, A. C. Harms, and R. D. Smith, *J. Rapid Commun. Mass Spectrom.*, **10** (1996) 1175-1178.

73 J. C. Severs and R. D. Smith, *Anal. Chem.*, **69** (1997) 2154.

74 D. R. Goodlett, J. H. Wahl, H. R. Udseth and R. D. Smith, *J. Microcol. Sep.*, **5** (1993) 57.

75 J. H. Wahl, D. R. Goodlett, H. R. Udseth and R. D. Smith, *Anal. Chem.*, **64** (1992) 3194.

76 T. J. Thompson, F. Foret, P. Vouros and B. L. Karger, *Anal. Chem.*, **65** (1993) 900.

77 F. Foret, T. J. Thompson, P. Vouros and B. L. Karger, *Anal. Chem.*, **66** (1994) 4450.

78 A. E. Ashcroft, H. J. Major, S. Lowes and I. D. Wilson, *Anal. Proceedings Including Anal. Communications*, **32** (1995) 459.

79 A. J. Tomlinson, L. M. Benson and S. Naylor, *Electrophoresis*, **15** (1994) 62.

80 A. J. Tomlinson, L. M. Benson and S. Naylor, *Electrophoresis*, **17** (1994) 175.

81 F. Garcia and J. Henion, *J. Chromatogr.*, **606** (1992) 237.

82 E. D. Lee, W. Muck, J. D. Henion and T. R. Covey, *Biomed. Environ. Mass Spectrom.*, **18** (1989) 253.

83 M. H. Lamoree, N. J. Reinhoud and U. R. Tjaden, *Biol. Mass Spectrom.*, **23** (1994) 175.

84 T. G. Huggins and J. D. Henion, *Electrophoresis*, **14** (1993) 531.

85 S. A. Hofstadler, J. H. Wahl, J. E. Bruce, and R. D. Smith, *J. Am. Chem. Soc.*, **115** (1993) 6983.

86 J. H. Wahl, S. A. Hofstadler, and R. D. Smith, *Anal. Chem.*, **67** (1995) 462.

87 S. A. Hofstadler, J. H. Wahl, R. Bakhtiar, G. A. Anderson, J. E. Bruce, and R. D. Smith, *J. Am. Soc. Mass Spectrom.*, **5** (1994) 894.

88 S. A. Hofstadler, F. D. Swanek, D. C. Gale, A. G. Ewing, and R. D. Smith, *Anal. Chem.*, **67** (1995) 1477.

89 C. P. Tsai, A. Sahil, J. M. McGuire, B. L. Karger and P. Vouros, *Anal. Chem.*, **59** (1986) 2.

90 B. L. Karger, D. P. Kirby, P. Vouros, R. L. Foltz and B. Hidy, *Anal. Chem.*, **61** (1989) 2324.

91 P. O. Edlund, L. Bowers and J. D. Henion, *J. Chromatogr.*, **487** (1989) 341.

92 A. Walhagen et al., *J. Chromatogr.*, **474** (1989) 257.

93 W. M. A. Niessen, *J. Rapid Commun. Mass Spectrom.*, **6** (1992) 474.

94 E. Gelpi, *J. Chromatogr.*, **703** (1995) 59.

95 W. M. A. Niessen, and A. P. Tinke, *J. Chromatogr.*, **703** (1995) 37.

96 P. J. Arpino, *Mass Spectrom. Rev.*, **8** (1989) 35.

97 A. L. Yergey, C. G. Edmonds, I. A. S. Lewis and M. Vestal, *Liquid Chromatography/Mass Spectrometry-Techniques and Applications*, Plenum Press, New York, 1990, pp. 31-86.

98 R. M. Caprioli, *Continuous-flow Fast Atom Bombardment Mass Spectrometry*, Wiley, New York, 1990.

99 R. C. Willoughby and R. F. Browner, *Anal. Chem.*, **56** (1984) 2626.

100 The API Book, PE Sciex, Thornhill, Ontario, 1989.

101 C. M. Whitehouse, R. N. Dreyer, M, Yamashita, J. B. Fenn, *Anal. Chem.*, **57** (1985) 675.

102 J. B. Fenn, M. Mann, C. K. Meng, S. F. Wong and C. M. Whitehouse, *Mass Spectrom. Rev.*, **9** (1990) 37.

103 A. P. Bruins, T. R. Covey and J. D. Henion, *Anal. Chem.*, **59** (1987) 2642.

104 *Electrospray Ionization Mass Spectrometry-Fundamentals, Instrumentation, and Applications*, edited by R. B. Cole, Wiley, New York, 1997.

105 M. J. Huddleston, M. F. Bean, and S. A. Carr, *Anal. Chem.*, **65** (1993) 877.

106 J. Crowther, V. Adusumall, T. Mukherjee, K. Jordan, P. Abuaf, N. Corkum, G. Goldstein, and J. Tolan, *Anal. Chem.*, **66** (1994) 2356.

107 P. J. Jackson, R. D. Brownsill, A. R. Taylor and B. Walther, *J. Mass Spectrom.*, **30** (1995) 446.

108 L. O. G. Weidolf, E. D. Lee and J. D. Henion, *Biomed. Environ. Mass Spectrom.*, **15** (1988) 283.

ACKNOWLEDGMENTS

First, I would like to give my heartfelt appreciation to Dr. Cheng S. Lee, for his supporting and encouraging me throughout my graduate study. I cannot thank him enough for his patient and expert guidance which made this work possible; I cannot thank him enough for challenging me whenever possible which kept my mind working and made the research enjoyable and exciting; I cannot thank him enough for his enthusiasm and eternally optimistic attitude from which I learned gradually the way to become a successful chemist.

I am also very grateful to Dr. Robert S. Houk for his advise. He is a great guy with a lot of sense of humor which made the lecture room a pleasant place to study. I learned a lot of analytical spectroscopy instrumentation and theory, especially mass spectrometry from him. He is one of the best teachers I ever had.

Drs. Donald J. Graves, Nenad M. Kostic, Patricia A. Thiel, and Marc D. Porter, honored me by investing time and showing interest in my project. I would like to express my appreciation to them.

I thank Dr. A. Kamel Harrata for his friendship and many interesting discussions concerning mass spectrometry. I thank all Lee research group members, both past and present. In particular, I would like to thank Jing Wei, Pam Jensen, Meng Sun, Yun Jiang and Yan Cao for their friendship and support while I was working away from the group at the Pacific Northwest National Laboratory (PNNL).

Special thanks to Dr. Richard D. Smith at PNNL and each of his group members, especially Drs. steven A. Hofstadler and Ljiljana P. Tolic. You have made my five months at PNNL a fruitful and enjoyable experience.

Last but certainly not least, I am eternally indebted to my parents, Wenlong Yang and Dihua Lu. Their love and care are always the greatest motivation for me to do my best under any circumstance. They are the greatest parents in the whole world.

This work is supported by an EPA Grant (R823292-01), the National Institutes of Health (R01 GM 53231), the Carver Trust Fund and the Microanalytical Instrumentation Center of the Institute for Physical Research and Technology at Iowa State University.

IMAGE EVALUATION TEST TARGET (QA-3)

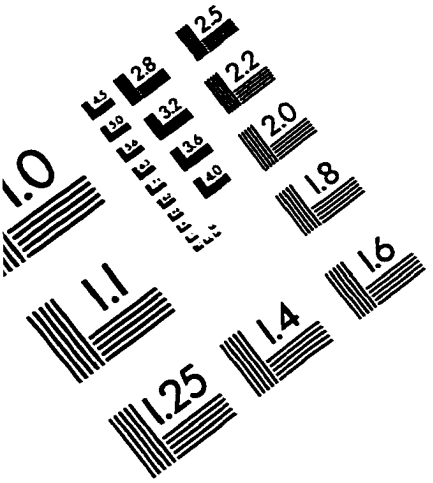

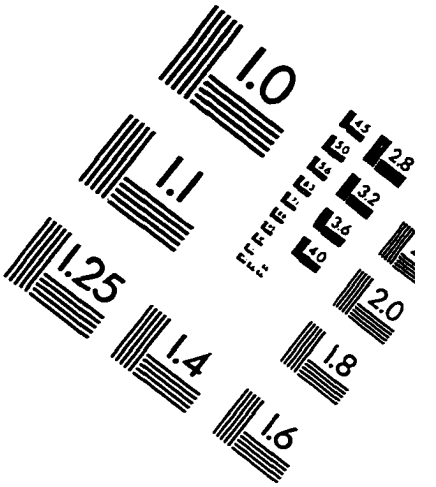

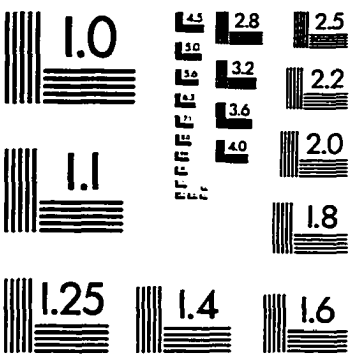

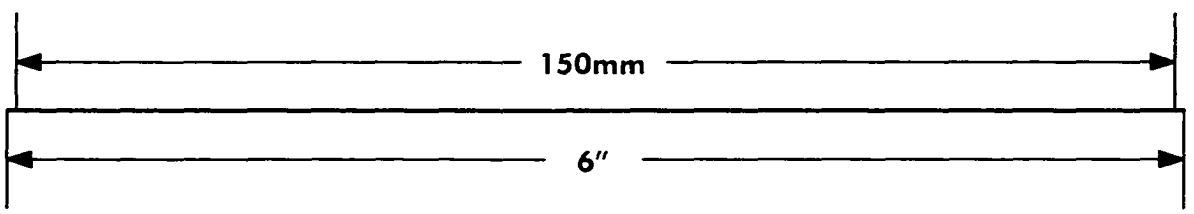

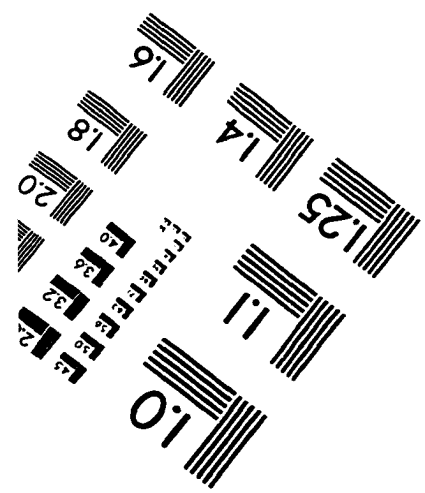

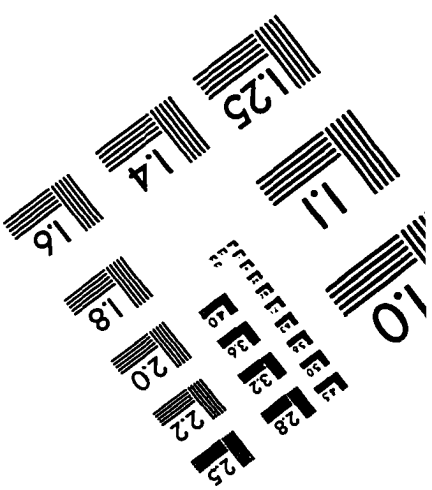

APPLIED IMAGE, Inc
1653 East Main Street
Rochester, NY 14609 USA
Phone: 716/482-0300
Fax: 716/288-5989